What Makes Us Anxious:

A Cross-Species Multi-omics Approach to the Biological Basis of Anxiety Disorders

Zuzanna Misiewicz

Molecular and Integrative Biosciences Research Programme
Faculty of Biological and Environmental Sciences
University of Helsinki

and

Doctoral Programme Brain & Mind
University of Helsinki

DOCTORAL DISSERTATION

To be presented for public examination with the permission of the Faculty of Biological and Environmental Sciences of the University of Helsinki, in lecture room 1041, Biocenter 2, on the 3rd of April 2019, at 12 noon.

Helsinki, Finland 2019

Supervised by

Professor Iiris Hovatta, PhD
Molecular and Integrative Biosciences Research Programme
University of Helsinki
Helsinki, Finland

Department of Psychology and Logopedics
University of Helsinki
Helsinki, Finland

Advisory committee

Professor Samuli Ripatti, PhD
Hjelt Institute, Faculty of Medicine,

Institute for Molecular Medicine Finland (FIMM)
University of Helsinki
Helsinki, Finland

Wellcome Trust Sanger Institute
Cambridge, United Kingdom

Professor Eero Castrén, MD, PhD
Neuroscience Center
University of Helsinki
Helsinki, Finland

Reviewed by

Adjunct Professor Eleanor Coffey
Turku Centre for Biotechnology
Åbo Akademi University and University of Turku
Turku, Finland

Professor Mikko Hiltunen
Institute of Biomedicine University of Eastern Finland
Kuopio, Finland

Opponent Professor John F. Cryan
University College Cork
Cork, Ireland

The Faculty of Biological and Environmental Sciences, University of Helsinki, uses the Urkund system (plagiarism recognition) to examine all doctoral dissertations.

Cover layout by Anita Tienhaara
ISBN 978-951-51-5083-7 (paperback)
ISBN 978-951-51-5084-4 (PDF, http://ethesis.helsinki.fi)
ISSN 2342-3161 (paperback)
ISSN 2342-317X (PDF, http://ethesis.helsinki.fi)
Press: Unigrafia Oy, Helsinki 2019

“Forty-two,” said Deep Thought, with infinite majesty and calm.

“Forty-two!” yelled Loonquawl. “Is that all you've got to show for seven and a half million years' work?”

“I checked it very thoroughly,” said the computer, “and that quite definitely is the answer.”

Douglas Adams, The Hitchhiker's Guide to the Galaxy

Table of contents

List of original publications

This thesis is based on the original articles listed below, which are referred to in the text by their Roman numerals. Article I is reproduced with the kind permission of its copyright holders. Article III is reproduced under the Creative Commons Attribution 4.0 International (CC BY 4.0) license. In addition, some unpublished data are presented.

I **Misiewicz Z**, Hiekkalinna T, Paunio T, Varilo T, Terwilliger JD, Partonen T, Hovatta I. A genome-wide screen for acrophobia susceptibility loci in a Finnish isolate. *Scientific Reports* 2016; 6: 39345.

II **Misiewicz Z**, Iurato S, Kulesskaya K, Salminen L, Rodrigues L, Maccarrone G, Martins J, Czamara D, Laine MA, Sokolowska E, Trontti K, Rewerts C, Novak B, Volk N, Park DI, Jokitalo E, Paulin L, Auvinen P, Voikar V, Chen A, Erhardt A, Turck CW, Hovatta I. Multi-omics analysis identifies mitochondrial pathways associated with anxiety-related behavior in mice and panic disorder patients. Submitted.

III Laine MA*, Trontti K*, **Misiewicz Z***, Sokolowska E*, Kulesskaya N, Heikkinen A, Saarnio S, Balcells I, Ameslon P, Greco D, Mattila P, Ellonen P, Paulin L, Auvinen P, Jokitalo E, Hovatta I. Genetic Control of Myelin Plasticity after Chronic Psychosocial Stress. *eNeuro* 2018; 0166-18

* These authors contributed equally to the respective article.

Author's contribution to the studies included in this thesis:

Article I: The author: 1) planned and conducted parametric, nonparametric, joint linkage and linkage disequilibrium analyses; 2) produced all figures and tables and wrote the manuscript.

Article II: The author: 1) planned and conducted animal behavioral experiments and collected and prepared tissue samples from those experiments; 2) performed statistical and bioinformatic analyses of mouse transcriptome and proteome data and gene set enrichment analyses (GSEA) of gene expression data from blood cells of panic disorder patients, followed by integrated analyses of all data sets; 3) performed part of the image acquisition for transmission electron microscopy (TEM) samples; 4) produced all figures and tables and wrote the manuscript.

Article III: The author: 1) participated in planning, conducting, and analyzing animal behavioral experiments and collecting and extracting tissue samples from those experiments; 2) conducted statistical and bioinformatic analyses for bed nucleus of the stria terminals (BNST) data and GSEA of all data sets; 3) performed part of the image acquisition and all of the image quantification and data analysis for BNST TEM samples; 4) produced Fig. 2E and Extended Data Fig. 2-1, 2-3C, 2-4, 5-2D, and assembled and edited Fig. 2 and Extended Data Fig. 2-3; 5) wrote parts of the manuscript concerning animal experiments, RNA-Seq and GSEA, and analysis of the BNST samples.

Abstract

Anxiety disorders manifest themselves as a prolonged or exaggerated response to a threatening situation, which can be either real or perceived. Their high prevalence (14%) places them as one of the most common mental disorders within the European Union. This conveys an important message about the necessity of finding new clinically relevant drug targets leading to the development of novel personalized treatment practices. To facilitate this process, efforts should be focused on gaining a deeper understanding of the complex molecular, biochemical, and system-level mechanisms behind the neurobiology of stress, and the role of stress as one of the main etiological factors in anxiety-related psychiatric disorders. The phenotypic heterogeneity of human populations and high variability of external environmental factors, along with limited access to brain tissue samples, presents some of the main challenges to studying anxiety disorders in humans. As these aspects can be controlled for in animals, animal models are often used to administer specific stressors in a uniform manner and to obtain brain tissue at a precisely chosen time point. Thereby, within the scope of this thesis, we take advantage of the fact that anxiety is an evolutionarily conserved response and address the integration of both human and mouse data obtained from a variety of approaches, including genomic, transcriptomic, and proteomic methods.

First, to identify genetic loci predisposing to a specific phobia, the fear of heights, we conducted a genome-wide parametric and non-parametric linkage scan, followed by joint linkage and association analysis in a small population isolate with reduced genetic and environmental heterogeneity. Our results implicated three regions with suggestive evidence for linkage, including region 8q24.2-q24.3 (LOD = 2.09), which encompasses 49 genes, containing several candidate genes for psychiatric disorders.

Second, we identified molecules and biological pathways affected by chronic social defeat stress (CSDS), a mouse model of chronic psychosocial stress, in the following three brain regions: medial prefrontal cortex (PFC_M), ventral hippocampus (HIP_V), and bed nucleus of the stria terminalis (BNST). We used two inbred mouse strains with different basal anxiety levels, the innately non-anxious C57BL/6NCrl (B6) and innately anxious DBA/2NCrl (D2). Following analysis of RNA sequencing results, we discovered that differentially expressed (DE) oligodendrocyte-related genes were over-represented in gene set enrichment analysis (GSEA) of all studied brain regions. As oligodendrocytes are known for their function in axon myelination, we followed the

results from transcriptomic analyses with transmission electron microscopy (TEM) and established that B6 stress-susceptible mice had thicker myelin in BNST axons compared to controls.

Third, using the CSDS model, we further investigated the role of the BNST through additional studies of gene regulatory networks (GRN) of mRNAs and miRNAs and protein-protein interaction networks. Subsequently, we followed with an integration analysis of the results from both transcriptomic (mRNA sequencing, as well as AGO2-immunoprecipitation miRNA and mRNA sequencing) and proteomic (liquid chromatography–tandem mass spectrometry) experiments. Furthermore, to translate our results to human anxiety disorders, we performed transcriptome profiling in blood cells of CSDS-subjected mice and compared it with gene expression patterns from blood cells of panic disorder patients who underwent exposure-induced panic attacks. We then followed with integrative gene set enrichment analysis of mouse and human data, which showed systemic genetic background-specific enrichment of mitochondria-related gene sets. Importantly, our results showed downregulation of the oxidative phosphorylation pathway in the CSDS-subjected D2 strain and panic disorder patients after a panic attack.

To conclude, our results suggest (1) brain-region and mouse strain-specific differences in myelination in susceptibility and resilience to stress and (2) dysregulation of mitochondrial pathways associated with anxiety-related behavior in both mice and humans. Taken together, our results provide further insight into the complex genetic architecture of anxiety disorders and support the suitability of cross-species approaches to studying biological mechanisms underlying anxiety disorders.

Keywords: anxiety disorders, chronic social defeat stress (CSDS), panic disorder, acrophobia, linkage analysis, gene expression, protein abundance, multi-omics studies

Abbreviations

129	129S2/SvPasCrl
5HT	Serotonin
ABCA1	ATP-binding cassette transporter
ACC	Anterior cingulate cortex
ACTH	Adrenocorticotropin hormone
AMYG	Amygdala
ATM	Ataxia-telangiectasia mutated serine/threonine kinase
ATP	Adenosine triphosphate
AVP	Arginine-vasopressin
B6	C57BL/6NCrl
BALB	BALB/cAnNCrl
BNST	Bed nucleus of the stria terminalis
BRCA1	Breast cancer, DNA repair associated
cAMP	Cyclic adenosine monophosphate
CDK5	Cell division protein kinase 5
CG	Guanine-cytosine content
CHECK2	Checkpoint kinase 2
cM	Centimorgan
Con (C)	Control
CRH	Corticotropin releasing factor
Crhr2	Corticotropin releasing hormone receptor 2
CSDS	Chronic social defeat stress
D2	DBA/2NCrl
DA	Dopamine
DARPP-32	Dopamine-and cAMP-regulated phosphoprotein
DE	Differentially expressed
DMTF1	Cyclin D binding Myb-like transcription factor 1
DNA	Deoxyribonucleic acid
DSM	Diagnostic and Statistical Manual
EPM	Elevated plus maze
ESR1	Estrogen receptor 1 alpha
EZM	Elevated zero maze
FC	Fold change
FOXP3	Forkhead box P3
FST	Forced swim test
GABA	γ- aminobutyric acid
GAD	Generalized anxiety disorder
GO	Gene ontology
GSEA	Gene set enrichment analysis
GWAS	Genome-wide association studies
HIP	Hippocampus
HIP_A	Anterior hippocampus
HIP_V	Ventral hippocampus
HPA	Hypothalamic-pituitary-adrenal
ICD	International statistical classification of diseases and related health problems
IGF2	Insulin-like growth factor 1
INS	Insular cortex
IPA	Ingenuity pathway analysis
IRS1	Insulin receptor substrate 1
JAG1	Jagged1
L/D	Light-dark box
LC-MS/MS	Liquid chromatography-tandem mass spectrometry
LD	Linkage disequilibrium
LOD	Logarithm of odds
MAPK1	Mitogen-activated protein kinase 1
Mb	Megabase
MC	Medium concentrate
miRNA	MicroRNA
mRNA	Messenger RNA
Mt	Mitochondrial
mtDNA	Mitochondrial DNA
mTOR	Mammalian target of rapamycin
NACC	Nucleus accumbens
NAD	Nicotinamide adenine dinucleotide

nDNA	Nuclear linear DNA
NE	Norepinephrine
NGS	Next-generation sequencing
NIPP1	Nuclear inhibitor of protein phosphatase-1
No.	Number
NPY	Neuropeptide Y
OCD	Obsessive-compulsive disorder
OF	Open field
OFC_M	Orbital frontal cortex
OLG	Oligodendrocyte
OPC	Oligodendrocyte progenitor cell
P	*P*-value
PACAP	Pituitary adenylate-cyclase activating polypeptide
PAG	Periaqueductal grey
PAR	Parietal cortex
PCC	Pearson correlation coefficient
PCR	Polymerase chain reaction
PD	Panic disorder
PFC	Prefrontal cortex
PFC_{DM}	Dorsal medial prefrontal cortex
PFC_L	Lateral prefrontal cortex
PFC_M	Medial prefrontal cortex
PFC_{VM}	Ventral medial prefrontal cortex
PFD_R	*P*-value corrected for multiple testing
PGC	Peroxisome proliferator-activated receptor gamma coactivator 1-alpha, see also **PPARGC1A**
PPARGC1A	Peroxisome proliferator-activated receptor gamma coactivator 1-alpha, see also **PGC**
PTSD	Post-traumatic stress disorder
RDoc	Research Domain Criteria
Res (R)	Resilient
RFLPI	Restriction fragment length polymorphisms identification
RICTOR	Rapamycin-insensitive companion of mTOR
RNA	Ribonucleic acid
RNA-seq	RNA sequencing
rRNA	Ribosomal RNA
SA	Social avoidance
SAD	Social anxiety disorder
SNP	Single-nucleotide polymorphism
SSTR2	Somatostatin receptor 2
STR	Dorsal striatum
STRs	Short tandem repeats
Sus (S)	Susceptible
SV	Structural variation
TCA	Tricarboxylic acid
TEM	Transmission electron microscope
TOP2A	Topoisomerase II alpha
tRNA	transfer RNA
vHPC	Ventral hippocampus
VOXPHOS	Oxidative phosphorylation genes

The list includes abbreviations appearing in the text more than twice.

1 Introduction

Anxiety disorders, including generalized anxiety disorder (GAD), social anxiety disorder (SAD), panic disorder (PD), and specific phobias, are the most common family of neuropsychiatric disorders (Shackman and Fox, 2016) and affect one in seven Europeans annually (Wittchen et al., 2011; Craske et al., 2017). They describe the state of disproportional or maladaptive anxiety or fear (or both) (American Psychiatric Association, 2013) in response to or in anticipation of a potential threat, either real or perceived (LeDoux, 2015). Although a distinction between anxiety and fear is present both in clinical and preclinical literature and states that while we are *anxious* in an anticipation of potential threat, we *fear* a specific immediate danger, the two are frequently used interchangeably, often defining one in the terms of other (Perusini and Fanselow, 2015). For example, in the Diagnostic and Statistical Manual of Mental Disorders (DSM-5) (American Psychiatric Association, 2013), a specific phobia is described *as a persistent fear of clearly discernible, circumscribed objects or situations,* while exposure to the phobic stimulus is said to *invariably provoke an immediate anxiety response.* The ambiguity further persists in clinical classification of preclinical laboratory models (Bouton, 2002). Somatically, threats, whether anticipated (anxiety) or present (fear), imagined or real, trigger a behavioral reaction known as *freeze-fight-flight response* caused by an activation of the sympathetic nervous system (LeDoux, 2015; Roelofs, 2017). A model by Michael Fanselow proposed to assess these elements (*freeze, fight and flight*) of defensive behavior in relation to the momentary imminence of threat and further depicted anxiety and fear as a part of a continuum (Fig. 1a). This instrumental idea is known as the predatory (threat) imminence theory (Perusini and Fanselow, 2015). In the modern world, although we do not have much to fear from predators, we still are *prey* to the daily stress of life.

Anxiety and fear are both symptoms of an individual experience of stress, which is commonly viewed as the brain's response to a challenging or demanding situation. Some elements of the stress response, such as *individual variability, timing, predictability, and controllability* (Hartley et al., 2014; Lucas et al., 2014; Maier et al., 2015) of the stressor (Fig. 1b), are determinant of the shift from *a healthy* to *a stressed* brain and the development, as well as maintenance, of the pathological anxiety and fear (Sousa, 2016). The interplay of these elements, which can be conventionally classified as either genetic or environmental risk factors (Sapolsky, 2015), is what leads to anxiety disorder.

The modest genetic heritability of anxiety disorders (up to 40%) (Hettema et al., 2001; Erhardt and Spoormaker, 2013), the high variability of environmental influence (Provencal and Binder, 2015), and the complexity of their clinical phenotypes (Peltonen et al., 2000) constitute some of the major challenges hindering the investigation of molecular and cellular mechanisms behind these disorders. Consequently, many researchers have resorted to studying disorders of pathological fear and anxiety in human genetic isolates with reduced genetic and environmental heterogeneity (Peltonen et al., 2000) and animal models, thus allowing for control over both genetic and environmental risk factors (Laine et al., 2017). Further integration of these studies is possible as the molecular and anatomical response to stress in animals is evolutionarily conserved (Soliman et al., 2010; Sokolowska and Hovatta, 2013). Such cross-species studies, especially involving high-throughput unbiased -omics approaches, may reveal specific biological mechanisms underlying anxiety disorders and aid in the identification of much-needed targets for future therapeutic intervention (Sokolowska and Hovatta, 2013).

The recent shift from conventional molecular biology approaches into the rapidly advancing field of comprehensive high-throughput -omics technologies (Hasin et al., 2017), including RNA sequencing (Wang et al., 2009) and liquid chromatography-tandem mass spectrometry (Shushan, 2010; Filiou et al., 2011; Martins-de-Souza, 2014), enable us to simultaneously survey thousands of molecules (e.g., gene transcripts and proteins) (Fig. 1c). However, as many cellular mechanisms are determined by networks of connections across several -omics layers, integrative multi-omics approaches offer the insight into the flow of information that captures the dynamic nature of disease-related alterations (Yugi et al., 2016; Hasin et al., 2017).

The main aim of this study was to identify the genes and proteins associated with anxiety disorders and establish the main biological pathways underlying stress-induced anxiety with the assistance of integrated cross-species multi-omics analyses. The following review of the literature describes the comparison of human and mouse genetic variation and their implications in studying fear and anxiety disorders using cross-species approaches. The high-throughput -omics approaches performed in this work are briefly described followed by an overview of the psychopathology of anxiety disorders, with a special emphasis on PD and specific phobias and the role of animal models in studying the underlying specific biological mechanisms.

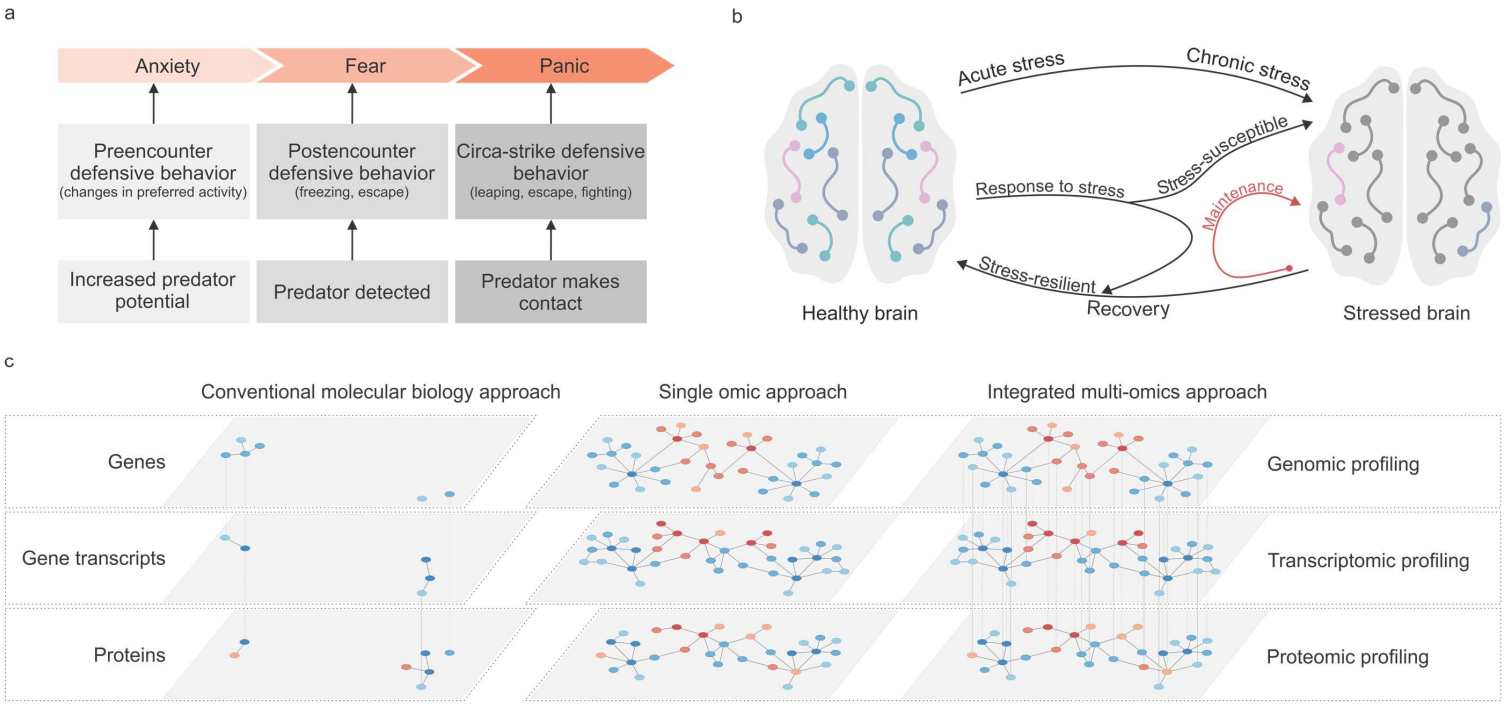

Figure 1. An integrated multi-omics approach to studying anxiety, fear, and chronic stress. (a) Fanselow's Predatory Imminence Theory of prey's defensive behavior. The defensive behavior of the prey in subdivided into three stages (pre-encounter, post-encounter, and circa-strike) and depends on the spatial and temporal distance to the threat (predator potential, predator detected, predator makes contact), depicting anxiety and fear as a part of a continuum. Based on an idea by Perusini and Fanselow (2015) and LeDoux (2015). **(b)** Sousa's model of dynamic stress neuromatrix between healthy and stressed brain. Four interacting steps are distinguished in this model: 1) Response to stress, 2) development of susceptibility to stress 3) transition from acute to chronic stress, and 4) maintenance of the *stressed* brain (a red dot represents a *point of no return* where changes to the stressed brain become irreversible). Based on idea by Sousa (2016). **(c)** Integrated multi-omics network across multiple -omics platforms. In the past, a network was identified by accumulation of research on specific molecules. Currently, we observe a transition from research based on single -omic analyses to trans-omics (integrated multi-omics) analyses. Trans-omics analyses reconstruct global biochemical networks across multi-omics measurements with the assistance of computational data integration. Based on idea from Yugi et al. (2015) and Hasin et al. (2017).

2 Review of the literature

2.1 Comparison of mouse and human genomes, transcriptomes, and proteomes

As the name suggests, all eukaryotic organisms store their genetic information in the base sequence of linear double-stranded deoxyribonucleic acid (DNA), separated in an internal compartment of the cell (the nucleus) and organized into chromosomes. In addition to nuclear linear DNA (nDNA), almost all eukaryotes carry mitochondria, *the powerhouse of the cell* (Karnkowska et al., 2016). Mitochondria have their own genome consisting of mitochondrial DNA (mtDNA) organized in the form of a circular molecule (Alberts, 2015). Like all other animal species, humans and mice are created by eukaryotic cells. Their genomes, which diverged an estimated 65–110 million years ago, are very similar, not only in structure but also in the sequence of their nuclear and mitochondrial DNA (Emes et al., 2004). The extensive similarity between the human genome and the genomes of many model organisms utilized in preclinical studies (such as mice) is a cornerstone of modern biology.

2.1.1 Similarities and differences between mouse and human genomes

The human genome consists of 22 autosomal chromosomes and two sex-determining chromosomes, X and Y. In general, an individual with two X chromosomes is a female and an individual with one X and one Y chromosome is a male (Jung et al., 2017). Although sex in the mouse is determined in the same manner (X and Y chromosomes), the mouse genome contains only 19 autosomes. Additionally, in both organisms, while the autosomal and sex chromosomes are inherited from both parents, ordinarily mtDNA comes solely from the mother (Sato and Sato, 2013).

The human and mouse sequencing projects (Lander et al., 2001; Venter et al., 2001; Mouse Genome Sequencing et al., 2002) performed almost two decades ago, and the subsequent comparative analyses of both genomes, created one of the most powerful approaches to link the laboratory notebooks of preclinical and clinical researchers and advance the knowledge of mammalian biology and human disease (Mouse Genome Sequencing et al., 2002). We now know that both genomes are of similar length, namely 3 billion base pairs (bp) (Table 1) (The Genome Reference Consortium, assemblies CRCh38.p12 and CRCm38.p6) (The Genome Reference

Consortium, 2017). There are approximately 20 000 protein-coding genes in both mice and humans, with the majority of them shared between the two species (International Human Genome Sequencing, 2004; Yue et al., 2014). While an equal number of non-coding evolutionarily conserved genes representing regions of functional importance is also present in humans and mice (Dermitzakis et al., 2005), the role of a portion of the remaining sequence is largely unknown and currently under investigation (Rands et al., 2014; Roadmap Epigenomics Consortium et al., 2015). Furthermore, along with nDNAs, mouse and human mtDNAs have also shown high levels of homology, both in the structure as well as the overall sequence (Bibb et al., 1981) (Table 1).

2.1.2 Mouse and human brain transcriptomes

The DNA in both mouse and human genomes is copied into RNA in a process called *transcription*. If the part of the transcribed DNA contains information on a protein-encoding gene, the transcription produces messenger RNA (mRNA) (Alberts, 2015). This process is known as gene expression. In contrast, transcription of a non-coding RNA (ncRNA), such as ribosomal RNA (rRNA), transfer RNA (tRNA), long ncRNA, and microRNA (miRNA) (Lee et al., 2004), produces an RNA molecule that is not subsequently translated into protein. MicroRNAs constitute a family of non-coding RNAs found in viruses, plants, and animals (Bartel, 2004; Pfeffer et al., 2004) whose role is to regulate gene expression by translational repression, mRNA cleavage, or both (Lee et al., 2004). The expression pattern of mRNAs and miRNAs is both tissue and time dependent (Sonawane et al., 2017). Additionally, all RNAs vary in their inherent half-lives (the time during which their level decreases by half). In most non-dividing cells, the half-life of most mRNAs ranges from 30 minutes to several hours, while the average miRNA decays approximately 10 times slower (Gantier et al., 2011).

Comparative analyses of regional and cellular gene expression in healthy mice and humans revealed a significant level of similarity between them (correlation coefficient [r] = 0.75 - 0.86, depending on the brain region). The similarity was especially high for evolutionarily conserved genes, as they have shown parallel patterns of region-specific expression across both organisms (Strand et al., 2007). Furthermore, recent studies of miRNA expression revealed a high level of conservation at the transcriptome level, even between distantly related species (Warnefors et al., 2014).

Table 1. Comparison of mouse and human genomes. Information included in the table is in accordance with The Genome Reference Consortium, assemblies CRCH37.p7 and CRCm38.p6 (2017), for *Homo sapiens* (human) and *Mus musculus* (house mouse) respectively, and GENCODE (2017).

Species and common name	Genome	No. of autosomal chromosomes	No. of sex chromosomes	Estimated total size (Mb)	Median GC (%)	Estimated number						
						Genes	Protein-coding genes	lnRNA genes	snRNA genes	tRNA	rRNA	Pseudogenes
Homo sapiens (human)	Nuclear	22	2	3257.32	42.1	58721	19940	16066	7577	414	29	14729
	Mt	-	-	0.02	44.4	37	13	-	-	22	2	-
Mus musculus (mouse)	Nuclear	19	2	2818.97	41.9	54446	21969	12840	6108	403	33	13033
	Mt	-	-	0.02	36.7	37	13	-	-	22	2	-

GC: guanine-cytosine content, Mb: megabase; Mt: mitochondrial; No.: number; rRNA: ribosomal RNA; tRNA: transfer RNA.

2.1.3 Mouse and human brain proteomes

Translation is the second major step in gene expression. During translation the mRNA is *read* according to the genetic code template and a protein is formed. On average, only 30% to 40% of variance in protein abundance can be explained by mRNA expression due to, between others, protein degradation mechanisms and post-transcriptional and post-translational processing (Vogel and Marcotte, 2012; Sharma et al., 2015).

Although little is known about the similarities and differences in mouse and human protein expression, the most recent integrative analyses of mouse and human brain protein abundance have shown a significant positive correlation in a brain region-specific pattern of protein expression (Carlyle et al., 2017).

2.2 The genetic basis of complex disorders

2.2.1 Genetic variation and effect size

In April 2003, more than 15 years ago, scientists announced that they had finalized the Human Genome Project; the sequence of a first hypothetical (i.e., coming from several individuals) (Kolata, 2013) reference genome was thus known (National Human Genome Research Institute, 2003). However, the idea behind the project was much larger than what was achieved. The researchers aimed to develop a cost-effective resource that would allow us to access the DNA sequence of any two individuals and establish what makes them different (Schwarze et al., 2018). This became possible with the introduction of modern sequencing technologies (see also Introduction and section 2.3.3), known as massively parallel sequencing, high-throughput, or next-generation sequencing (NGS). We now know that genomes of any two individuals are estimated to be 99.5% identical (Levy et al., 2007), which means that they differ in approximately 15 million bases. These differences in a specific region of the DNA sequence are known as sequence variants, while different versions of the same variant are called alleles (Manolio et al., 2009; MacArthur et al., 2014). Humans, similar to mice, have two alleles at each genetic locus (a fixed position on a chromosome), with one allele typically inherited from the mother and the other from the father. In addition to the variation in sequence (e.g., in a single nucleotide, or single-nucleotide polymorphism [SNP] or in short tandem repeats [STRs], such as microsatellites; see also section 2.3.2), the DNA sequence can also vary in structure. Structural variation (SV) is

defined as a genetic variation of a DNA region, 1 kb or larger, with different types of rearrangements (Ye et al., 2018).

Although most genetic variation is benign (i.e., it does not negatively affect our health), some variants are pathogenic (i.e., associated with a disease). It is important to note that not all variants are created equal. The magnitude of the effect of a pathogenic genetic variant on phenotype is called effect size (Hindorff et al., 2011). Furthermore, genetic variants differ in their frequency in the human population. Low-frequency variants are present in 1% to 5% of the population while rare variants account for less than 1%. Very rare variants with large effect sizes (Fig. 2, upper left corner) are most frequently known to cause monogenic diseases (see section 2.2.2) and are often identified in family-based genome-wide linkage studies (see section 2.3.2). On the other hand, common genetic variants with small effect sizes (Fig. 2, lower right corner) are thought to be the cause behind many complex disorders and are investigated with the assistance of genome-wide association studies (GWAS).

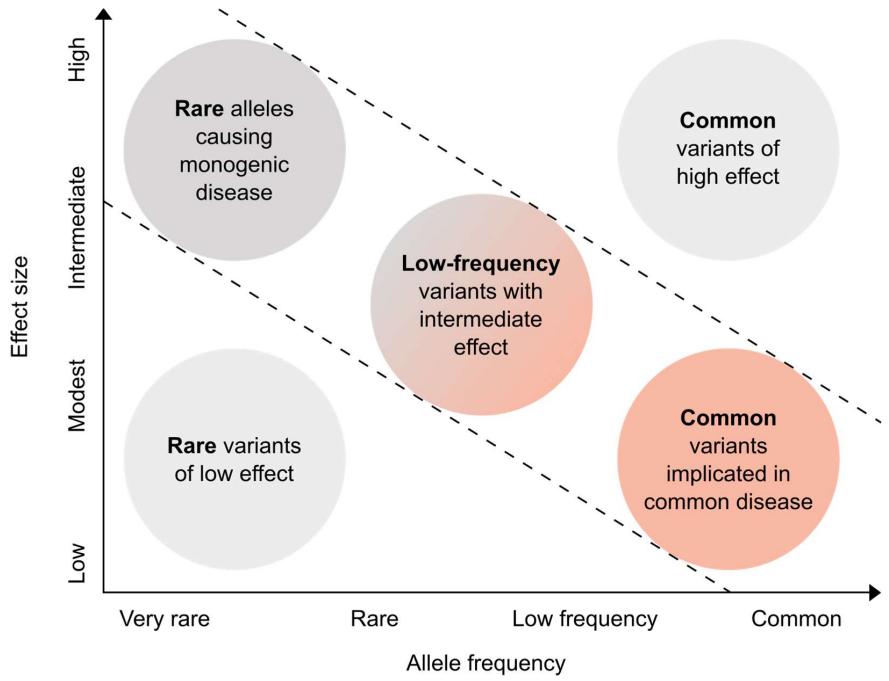

Figure 2. Models of genetic etiology behind monogenic and complex diseases. Risk variance is grouped according to allele frequencies (y axis) and their effect sizes (x axis). Based on idea from McCarthy et al. (2008) and Manolio et al. (2009).

2.2.2 Monogenic traits and disorders

Monogenic traits and diseases, also called Mendelian traits and diseases, are caused by alterations in a single gene. If such an alteration is present in both copies of the gene, one from each parent, the disease is known as recessive. If it is present only in one copy, it is dominant. Furthermore, monogenic diseases can be either autosomal, linked to a sex chromosome (X or Y), or mitochondrial. While Y-linked monogenic diseases can be passed only from father to son (Mau Kai et al., 2008), generally mitochondrial monogenic diseases can be passed to sons and daughters only by their mothers (Koopman et al., 2012) (see section 2.1.1). Many neurological diseases, or conditions with neurological features, are caused by defects in single genes. Examples of such diseases are Huntington's disease, neurofibromatosis, and homocystinuria (Larner, 2008).

2.2.3 Complex traits and disorders

Far more common than monogenic disorders are complex (multifactorial) diseases. Unlike Mendelian diseases, multifactorial diseases are not caused by a single gene but by an interplay of multiple genes and various environmental factors (see also Introduction). Furthermore, although complex diseases are largely heritable, they do not obey the Mendelian patterns of inheritance (see section 2.2.2). Instead, the complexity of the human genome and human physiology is suggested to be caused by a number of specific phenomena (e.g., non-Mendelian familial aggregation, gene-gene interactions, polygenes, genetic modifiers, and locus heterogeneity) (Buchanan et al., 2006). Most commonly, the rules of polygenic inheritance state that multiple genetic factors, each contributing to the continuous trait and segregating in families according to Mendel's law, are proposed to describe the inheritance of complex disease (Fisher, 1918; Buchanan et al., 2006).

Although the clinical disease phenotypes of complex diseases, including many neuropsychiatric diseases (American Psychiatric Association, 2013), are most often discrete, nature almost always operates based on continuums (Gleick, 2008). The liability-threshold model assumes that each human has a continuous liability comprised of latent genetic variants and environmental factors. Thus, if the liability threshold is exceeded, the individual will acquire the binary trait (i.e., the disease). This makes it difficult to determine the risk and inheritance of developing a complex disorder and passing it to the offspring (Benchek and Morris, 2013). Another more recent

approach launched by the National Institute of Mental Health, called the Research Domain Criteria (RDoC), proposes to classify complex (mental) diseases based on their continuous variables (i.e., dimensions of detectable behavior and neurological measures) (Iacono, 2016). Neuropsychiatric disorders, such as anxiety disorders and autism spectrum disorders, are presumed to be complex in nature (Veenstra-Vanderweele et al., 2004; Smoller et al., 2009).

2.3 Molecular biology approaches to studying complex traits

To discover the genetic variants within genes contributing to the studied disorder, it is necessary to localize the genomic loci harboring them. The primary principle of this process, known as genetic mapping, is to identify the association between a recognized polymorphic variant (i.e., a genetic marker) with a known chromosomal location and the phenotype (i.e., disease or lack thereof) (Kheirallah et al., 2016). Two different types of analyses with different underlying assumptions (see section 2.3.2) are employed to study this correlation (see Fig. 5), namely linkage and association analyses (Ott, 1999; Hiekkalinna, 2012).

2.3.1 Genotyping and sequencing of genetic markers

Genetic variants, used both in linkage and association analyses, can be identified with both genotyping and sequencing (see also section 2.2.1). While sequencing determines the exact sequence of a chosen DNA fragment or the whole genome, genotyping examines specific pre-selected genetic variants. To explain the difference between those techniques, an analogy to a book is frequently used, in which genotyping is represented by searching for a few words scattered across several pages, while sequencing is compared to analyzing whole paragraphs or chapters. Genotyping can be performed with a variety of biological assays, such as polymerase chain reaction (PCR), restriction fragment length polymorphisms identification (RFLPI), and hybridization reactions with a DNA microarray composed of various probes containing SNPs. The advantages and disadvantages of both massively parallel sequencing and microarrays are extensively discussed in the literature. For example, while microarrays focus mostly on relatively common variants (see Fig. 2), they are also less prone to design bias (Bumgarner, 2013).

2.3.2 Linkage analysis and linkage disequilibrium

Linkage analysis

Linkage analysis takes advantage of genetic linkage. This is a physical phenomenon where large fragments of a DNA sequence located closely together on a chromosome are inherited intact during meiosis, only sporadically disrupted by crossovers. A chromosomal crossover is an exchange of a part of two homologous chromosomes resulting in recombinant chromosomes (Hiekkalinna, 2012) (Fig. 3a).

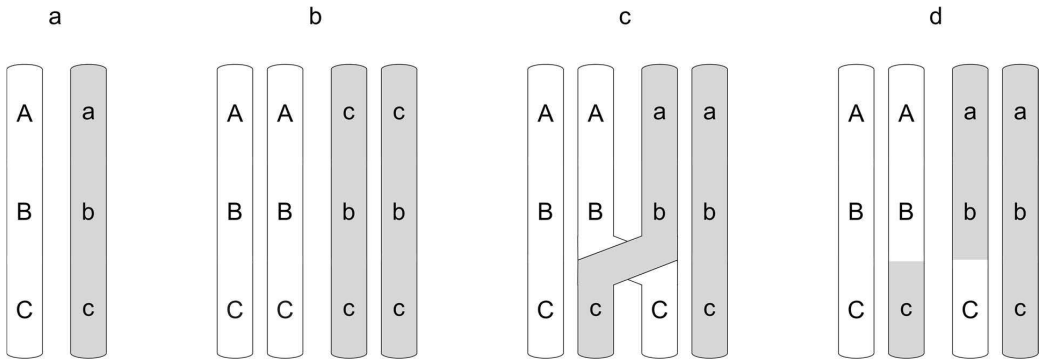

Figure 3. Chromosomal crossover in meiosis. (a) Aligned homologous chromosomes, one derived from each parent, each of them with three loci (ABC and abc). **(b)** Chromosome duplication. **(c)** Crossing-over between the chromosomes creates variation **(d)** resulting in recombinant chromosomes (Abc and abC). Figure adapted from Hiekkalinna (2012).

The probability that two loci are transmitted together in meiosis is linked to the genetic distance between them (i.e., two loci located on opposite ends of a chromosome are less likely to be transmitted together) (Sham, 1998). The recombination fraction (θ), which in humans ranges from 0 to 0.5, is the probability of recombination in a given meiosis. A recombination fraction of θ = 0.5 means that the two loci are unlinked or non-syntenic (e.g., located on different chromosomes). The objective of linkage analysis is to estimate the recombination fraction and subsequently test the null hypothesis that θ = 0.5. In other words, the analysis aims to identify a genetic marker that co-segregates with the gene of interest, and therefore, the disease phenotype (Fig. 4 and Fig. 5) (Wright et al., 1983). This information is the foundation of the linkage test statistic, *the-logarithm-of-odds* (LOD) score. Traditionally, a LOD score above three corresponds to a pointwise *P*-value (*P*) equal to 0.0001 and is considered significant. However, in genome-wide linkage scans, when the marker map is infinitely dense (i.e., covers the whole

genome) a more appropriate LOD score of 3.3 has been shown to correspond to a P_{FDR} (P-value corrected for multiple testing) of 0.05 (Lander and Kruglyak, 1995).

Linkage analysis can be subdivided into parametric and nonparametric analyses. While parametric analysis requires the estimation of allele frequency and penetrance (see Fig. 2), nonparametric analysis does not (Ott et al., 2015). Additionally, both can be further subdivided into two-point analysis (also known as single-point analysis) and multipoint analysis, examining the linkage of a putative disease locus to a single or multiple marker loci at a time, respectively (Szymczak et al., 2014).

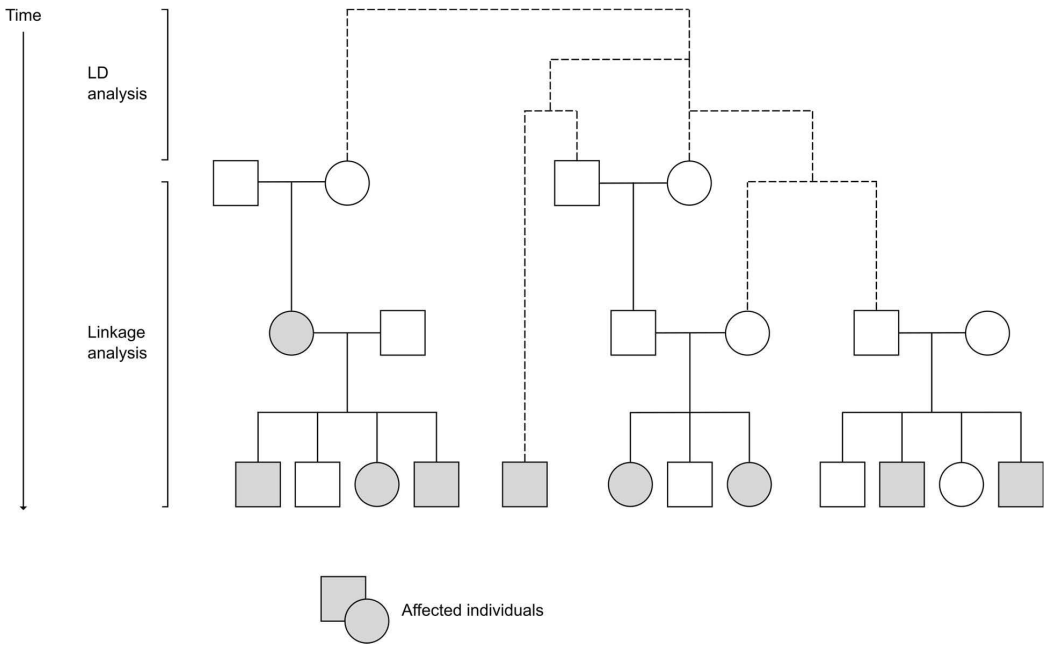

Figure 4. Comparison of linkage analysis and linkage disequilibrium analysis (LD). Linkage analysis can be performed only in families, as the relationship status (solid lines) between two individuals is required for the analysis. LD uses a case-control design, where the relationship between the individuals is unknown. Figure adapted from Hiekkalinna (2012).

Linkage disequilibrium (LD)

When a new change in the DNA base sequence is introduced, it is only found in one of the inherited chromosomes (haplotype). With the passage of time, as the allele segregates through the population, the length of the haplotype decreases due to recombination (Terwilliger and Goring, 2000). Eventually, only variants located in direct proximity to the mutation are still inherited together (Fig. 4). Two measures are used to quantify linkage disequilibrium (LD). The

first one is Lewontin's *D'* (Lewontin, 1964), which is calculated by dividing the gametic LD coefficient (the difference between the observed frequency of a two-locus haplotype) and its expected frequency assuming random segregation of the alleles. The absolute value of Lewontin's *D'* ranges from 0 to 1, where *D'* = 1 describes complete LD. The second measurement, the squared correlation coefficient (r^2), calculates how well the alleles of either locus can be predicted from the other (Gabriel et al., 2002). It ranges from 0 to 1, with 1 obtained in the case of no recombination between the loci and equal allele frequencies.

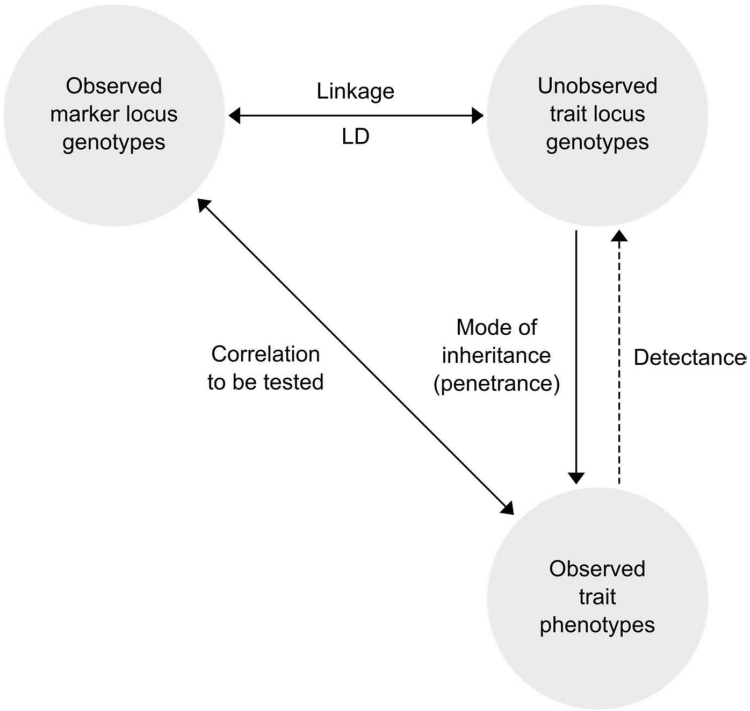

Figure 5. The objective behind linkage analysis and linkage disequilibrium analysis. In addition to the linkage, LD, or both described in the text, the power of the study depends on *detectance*, namely the predictive value of the observed phenotype on the unobserved disease locus genotype**.** Figure adapted from Hiekkalinna (2012) and Terwilliger and Göring (2000).

2.3.3 From genomic to transcriptomic and proteomic analyses

In molecular biology, *omics* refers to a global and comprehensive assessment, or a qualitative characterization and quantification of a set of molecules (e.g., genes, miRNAs, and proteins). Genomics, the study of the entire genomes (see Fig. 1 and section 2.3.1), was the first -omics discipline to be established (Hasin et al., 2017).

The technological advances in the field of genomics (e.g., the development of cost-efficient, high-throughput sequencing methodologies) (see section 2.2.1) has largely driven the progress in other omics disciplines, such as transcriptomics, which focuses on the genome-wide examination of different RNA types, such as mRNA and miRNA (Hasin et al., 2017). With the entrance of next-generation sequencing, it was revealed that although only a small part of the genome encodes proteins, as much as 80% of it is transcribed (ENCODE Project Consortium, 2012). However, the most important contribution in the field of transcriptomics was made with the discovery of different subclasses of non-coding RNA (Uszczynska-Ratajczak et al., 2018), including miRNAs, which are implicated in many neuropsychiatric disorders (Hunsberger et al., 2009; Issler and Chen, 2015). miRNAs are single-stranded RNA molecules of approximately 21 to 26 nucleotide length that regulate gene expression through inhibition of target mRNAs and by subsequently initiating mRNA target degradation (Fig. 6, see also section 2.1.1) (Valencia-Sanchez et al., 2006). Nevertheless, changes in miRNA expression levels are not directly indicative of their immediate activity (i.e., degradation of mRNA). They are active and associate with their target mRNAs only at the moment of incorporation of miRNA into the RNA-induced silencing complex (RISC) in the presence of a catalytic protein, Argonaute 2 (AGO2) (Volk et al., 2014; Catalanotto et al., 2016). Therefore, to detect active miRNAs and their mRNA targets, the AGO2 protein can be immunoprecipitated with the miRNA-mRNA pairs attached before sequencing them. In -omics studies, the integration of information on mRNA and miRNA expression is possible with the help of bioinformatic tools (Chen et al., 2018).

Proteomics, or the study of the proteome, is employed to quantify abundance, interaction, and modification of peptides. The field of proteomics has been revolutionized by advances in methods based on the analytical technique mass spectrometry (MS), which have been recently adapted for high-throughput analyses that enable simultaneous assessment of thousands of proteins within cells or body fluids (Hasin et al., 2017). MS measures the mass-to-charge ratio of ionized chemical species (Glish and Vachet, 2003).

2.3.4 Differential gene expression and protein abundance profiling analyses

In the fields of quantitative transcriptomics and proteomics, statistical analyses of gene expression and protein abundance (also sometimes referred to as protein expression) are performed to measure the changes in levels between different experimental groups. For

example, Student's t-test (Tsai et al., 2003) is performed to measure the change in read counts of a certain gene between two samples and to determine if the observed difference is greater than expected by chance. Most commonly, genes or proteins are considered differentially expressed (DE) if the obtained *P*-value is smaller than 0.05. Due to a large number of genes and proteins in typical RNA sequencing and liquid chromatography tandem mass spectrometry (LC-MS/MS) experiments, correction for multiple testing is usually applied (Diz et al., 2011; Li et al., 2012). In addition to the *P*-value, fold change (FC), calculated as a change in quantity between the two experimental groups, is defined. In the field of genomics and proteomics, FC log ratios are often used for analysis and visualization (Zhou et al., 2018).

Many pathway analysis methods, a phrase used here in a broad sense (Khatri et al., 2012), aimed at interpreting the gene and protein expression data have been developed in recent years. The most common ones are knowledge-based (i.e., aimed at describing the data in the context of known biological processes, components, or structures) and differ in their statistical approaches. The methods used in this work are further described in section 4.5.

2.4 Psychopathology of anxiety disorders

2.4.1 Clinical features of common anxiety disorders

When anxiety and fear become maladaptive, or excessive in duration, intensity, or frequency and cause considerable disability and distress, they *become* anxiety disorders (Table 2).

Table 2. The difference between everyday and pathological anxiety. Based on LeDoux (2015) and https://adaa.org/understanding-anxiety.

Everyday anxiety	Anxiety disorders
Worry about paying bills, finding a job, or other important life events	Constant and unsubstantiated worry causing significant distress and interfering with daily life
Embarrassment or self-consciousness in an uncomfortable situation or socially awkward moment	Avoiding social situations for fear of being judged, embarrassed, or humiliated
A case of sweating or heart palpitations before an important exam, presentation, public performance or other significant event	Seeming out-of-the-blue panic attacks and the preoccupation with the fear of having another one
Worry about an actual dangerous object, place or situation	Irrational worry about and avoidance of an object, place or situation that poses little or no threat of danger

Pathological fear and anxiety are subclassified based on their disorder-specific features including the anxiety and/or fear-associated behavior, as well as the course and the onset of the disorder. A well-known classification of anxiety disorders is based on the *Diagnostic and Statistical Manual* (DSM) of the American Psychiatric Association (American Psychiatric Association, 2013). The current DSM (DSM-5) recognizes the following anxiety disorders: separation anxiety disorder, selective mutism, specific phobia, social anxiety disorder (SAD, until recently known as social phobia), PD, agoraphobia, and GAD. The diagnostic criteria for the most common anxiety disorders are described in Table 3. Another standard set of criteria used to classify anxiety disorders is known as International Statistical Classification of Diseases and Related Health problems (ICD). The current version of ICD (ICD-10) groups anxiety disorders under *neurotic, stress-related,* and *somatoform disorders*.

Table 3. Diagnostic criteria for most common anxiety disorders according to DSM-5. See *pages 28-30.* Adapted from American Psychiatric Association (2013).

Panic Disorder

A. Recurrent unexpected panic attacks. A panic attack is an abrupt surge of intense fear or intense discomfort that reaches a peak within minutes, and during which time four (or more) of the following symptoms occur;

Note: The abrupt surge can occur from a calm state or an anxious state.

1. Palpitations, pounding heart, or accelerated heart rate.
2. Sweating.
3. Trembling or shaking.
4. Sensations of shortness of breath or smothering.
5. Feelings of choking.
6. Chest pain or discomfort.
7. Nausea or abdominal distress.
8. Feeling dizzy, unsteady, light-headed, or faint.
9. Chills or heat sensations.
10. Paresthesia (numbness or tingling sensations).
11. Derealization (feelings of unreality) or depersonalization (being detached from oneself).
12. Fear of losing control or "going crazy."
13. Fear of dying.

Note: Culture-specific symptoms (e.g., tinnitus, neck soreness, headache, uncontrollable screaming or crying) may be seen. Such symptoms should not count as one of the four required symptoms.

B. At least one of the attacks has been followed by 1 month (or more) of one or both of the following:

1. Persistent concern or worry about additional panic attacks or their consequences (e.g., losing control, having a heart attack, "going crazy").
2. A significant maladaptive change in behavior related to the attacks (e.g., behaviors designed to avoid having panic attacks, such as avoidance of exercise or unfamiliar situations).

C. The disturbance is not attributable to the physiological effects of a substance (e.g., a drug of abuse, a medication) or another medical condition (e.g., hyperthyroidism, cardiopulmonary disorders).

D. The disturbance is not better explained by another mental disorder (e.g., the panic attacks do not occur only in response to feared social situations, as in social anxiety disorder; in response to circumscribed phobic objects or situations, as in specific phobia; in response to obsessions, as in obsessive-compulsive disorder: in response to reminders of traumatic events, as in posttraumatic stress disorder: or in response to separation from attachment figures, as in separation anxiety disorder).

Generalized Anxiety Disorder

A. Excessive anxiety and worry (apprehensive expectation), occurring more days than not for at least 6 months, about a number of events or activities (such as work or school performance).

B. The individual finds it difficult to control the worry.

C. The anxiety and worry are associated with three (or more) of the following six symptoms (with at least some symptoms having been present for more days than not for the past 6 months):

Note: Only one item is required in children.

1. Restlessness or feeling keyed up or on edge.
2. Being easily fatigued.
3. Difficulty concentrating or mind going blank.
4. Irritability.
5. Muscle tension.
6. Sleep disturbance (difficulty falling or staying asleep, or restless, unsatisfying sleep).

D. The anxiety, worry, or physical symptoms cause clinically significant distress or impairment in social, occupational, or other important areas of functioning.

E. The disturbance is not attributable to the physiological effects of a substance (e.g., a drug of abuse, a medication) or another medical condition (e.g., hyperthyroidism).

F. The disturbance is not better explained by another mental disorder (e.g., anxiety or worry about having panic attacks in panic disorder, negative evaluation in social anxiety disorder [social phobia], contamination or other obsessions in obsessive-compulsive disorder, separation from attachment figures in separation anxiety disorder, reminders of traumatic events in posttraumatic stress disorder, gaining weight in anorexia nervosa, physical complaints in somatic symptom disorder, perceived appearance flaws in body dysmorphic disorder, having a serious illness in illness anxiety disorder, or the content of delusional beliefs in schizophrenia or delusional disorder).

Agoraphobia

A. Marked fear or anxiety about two (or more) of the following five situations:
   1. Using public transportation (e.g., automobiles, buses, trains, ships, planes).
   2. Being in open spaces (e.g., parking lots, marketplaces, bridges).
   3. Being in enclosed places (e.g., shops, theaters, cinemas).
   4. Standing in line or being in a crowd.
   5. Being outside of the home alone.

B. The individual fears or avoids these situations because of thoughts that escape might be difficult or help might not be available in the event of developing panic-like symptoms or other incapacitating or embarrassing symptoms (e.g., fear of falling in the elderly; fear of incontinence).

C. The agoraphobic situations almost always provoke fear or anxiety.

D. The agoraphobic situations are actively avoided, require the presence of a companion, or are endured with intense fear

E. The fear or anxiety is out of proportion to the actual danger posed by the agoraphobic situations and to the

F. The fear, anxiety, or avoidance is persistent, typically lasting for 6 months or more.

G. The fear, anxiety, or avoidance causes clinically significant distress or impairment in social, occupational, or other important areas of functioning.

H. If another medical condition (e.g., inflammatory bowel disease, Parkinson's disease) is present, the fear, anxiety, or avoidance is clearly excessive.

I. The fear, anxiety, or avoidance is not better explained by the symptoms of another mental disorder—for example, the symptoms are not confined to specific phobia, situational type; do not involve only social situations (as in social anxiety disorder); and are not related exclusively to obsessions (as in obsessive-compulsive disorder), perceived defects or flaws in physical appearance (as in body dysmorphic disorder), reminders of traumatic events (as in posttraumatic stress disorder), or fear of separation (as in separation anxiety disorder).

Note: Agoraphobia is diagnosed irrespective of the presence of panic disorder. If an individual's presentation meets criteria for panic disorder and agoraphobia, both diagnoses should be assigned.

Social Phobia

A. Marked fear or anxiety about one or more social situations in which the individual is exposed to possible scrutiny by others. Examples include social interactions (e.g., having a conversation, meeting unfamiliar people), being observed (e.g., eating or drinking), and performing in front of others (e.g., giving a speech). **Note**: In children, the anxiety must occur in peer settings and not just during interactions with adults.

B. The individual fears that he or she will act in a way or show anxiety symptoms that will be negatively evaluated (i.e., will be humiliating or embarrassing: will lead to rejection or offend others).

C. The social situations almost always provoke fear or anxiety.
   Note: In children, the fear or anxiety may be expressed by crying, tantrums, freezing, clinging, shrinking, or failing to speak in social situations.

D. The social situations are avoided or endured with intense fear or anxiety.

E. The fear or anxiety is out of proportion to the actual threat posed by the social situation and to the sociocultural

F. The fear, anxiety, or avoidance is persistent, typically lasting for 6 months or more.

G. The fear, anxiety, or avoidance causes clinically significant distress or impairment in social, occupational, or other important areas of functioning.

H. The fear, anxiety, or avoidance is not attributable to the physiological effects of a substance (e.g., a drug of abuse, a medication) or another medical condition.

I. The fear, anxiety, or avoidance is not better explained by the symptoms of another mental disorder, such as panic disorder, body dysmorphic disorder, or autism spectrum disorder.

J. If another medical condition (e.g., Parkinson's disease, obesity, disfigurement from burns or injury) is present, the fear, anxiety, or avoidance is clearly unrelated or is excessive.

Specify if :
Performance only: If the fear is restricted to speaking or performing in public.

Specific Phobia
A. Marked fear or anxiety about a specific object or situation (e.g., flying, heights, animals, receiving an injection, seeing blood).
Note: In children, the fear or anxiety may be expressed by crying, tantrums, freezing, or clinging.
B. The phobic object or situation almost always provokes immediate fear or anxiety.
C. The phobic object or situation is actively avoided or endured with intense fear or anxiety.
D. The fear or anxiety is out of proportion to the actual danger posed by the specific object or situation and to the sociocultural context.
E. The fear, anxiety, or avoidance is persistent, typically lasting for 6 months or more.
F. The fear, anxiety, or avoidance causes clinically significant distress or impairment in social, occupational, or other important areas of functioning.
G. The disturbance is not better explained by the symptoms of another mental disorder, including fear, anxiety, and avoidance of situations associated with panic-like symptoms or other incapacitating symptoms (as in agoraphobia): objects or situations related to obsessions (as in obsessive-compulsive disorder); reminders of traumatic events (as in posttraumatic stress disorder); separation from home or attachment figures (as in separation anxiety disorder); or social situations (as in social anxiety disorder).
Coding note: When more than one phobic stimulus is present, code all ICD-10-CM codes that apply (e.g., for fear of snakes and flying, F40.218 specific phobia, animal, and F40.248 specific phobia, situational).

2.4.2 Clinical and genetic epidemiology of anxiety disorders

Prevalence

The prevalence of a disease is a statistical concept referring to the number of individuals suffering from the disease in a particular population at a given time. (Bandelow and Michaelis, 2015). The data on prevalence of a disease might provide valuable information to health services and researchers conducting clinical and preclinical studies and impact future allocation of economic resources.

The reported prevalence of anxiety disorders shows large variability across studies due to differences in diagnostic criteria and instruments, response rates, and sample sizes of the epidemiological surveys (Somers et al., 2006; Bandelow and Michaelis, 2015). While the estimated lifetime prevalence for all anxiety disorders varies from 13% to 14% (Wittchen and Jacobi, 2005; Wittchen et al., 2011) to 34% (Kessler et al., 2012), it has been shown that anxiety disorders are the most common type of mental health disorder (Kessler et al., 2012). Among them, specific phobia is the most prevalent, with an estimated lifetime rate of between 8% (Wittchen and Jacobi, 2005) and 14% (Kessler et al., 2012). The second and third most common subtypes of anxiety disorders are SAD and generalized anxiety disorder, respectively (Table 4). The large variation in prevalence between the Wittchen and Jacobi (2005), Wittchen et al. (2011), and Kessler et al. (2012) studies are most likely a result of differences in data selection and statistical methodologies. Importantly, while the first two studies used meta-analytic

techniques to review and appraise 27 population-based European studies, the third one is an original study based on a face-to-face household survey of adults conducted in the USA.
In addition to the studies described above, numerous other epidemiological surveys and meta-analyses have been conducted (Hettema et al., 2001; Pirkola et al., 2005; Somers et al., 2006; Alonso et al., 2007; Kessler et al., 2009; Smoller et al., 2009).

Table 4. Lifetime and 12-month prevalence rates of anxiety disorders in various epidemiological surveys. Estimates based on Kessler et al. (2012), Wittchen et al. (2011) and Wittchen and Jacobi (2005).

Anxiety disorder	Wittchen and Jacobi study (2005)	Wittchen et al. study (2011)	Kessler et al. study (2012)	
	12-month P (%)	12-month P (%)	12-month P (%)	Lifetime P (%)
Panic disorder	1.8 (0.7 – 3.1)	1.8	3.1	5.2
General anxiety disorder	1.7 (0.8 – 2.2)	1.7 – 3.4	2.9	6.2
Social anxiety disorder	2.3 (1.1 – 4.8)	2.3	8.0	13.0
Agoraphobia	1.3 (0.7 – 2.0)	2.0	1.7	2.6
Specific phobia	6.4 (3.4 – 7.6)	6.4	10.1	13.8
All anxiety disorders[a]	11.1-13.0	14.0	21.3	33.7

[a] The studies were conducted before the introduction of DSM-5, when obsessive-compulsive disorder (OCD) and post-traumatic stress disorders (PTSD) were still a part of the anxiety disorders category.
P: Prevalence.

Comorbidity

Comorbidity is the presence of one or more additional diseases. Anxiety disorders show a high degree of overlap not only with each other, but also with other mental disorders (Pirkola et al., 2005). The highest correlation within anxiety disorders was observed between SAD and agoraphobia and agoraphobia and PD (r = 0.68 and r = 0.62, respectively). The highest overlap with other psychiatric disorders was measured between generalized anxiety disorder and major depression (r = 0.62) (Kessler et al., 2005). Additionally, numerous studies have shown that 40% to 70% of people suffering from major depressive disorder simultaneously meet the criteria for one or more anxiety disorders (Kessler et al., 2007; Lamers et al., 2011; Wu and Fang, 2014). However, it is important to note that the detected correlation is most probably higher than that found in a representative population, as individuals suffering from two or more concomitant disorders are usually more likely to seek treatment. This phenomenon is known as Berkson's Paradox (Merikangas and Kalaydjian, 2007).

Heritability and genetic factors

Heritability (h^2) is a term describing how well the additive genetic variation accounts for the differences in given individual's trait. For example, a $h^2 = 0.4$ means that 40% of the variability in the studied trait in a population is due to genetic differences among people (Tenesa and Haley, 2013). The heritability estimates for anxiety disorders obtained through twin studies is between 30% and 50% (Hettema et al., 2001; Shimada-Sugimoto et al., 2015).

As reported in several genetic association studies, multiple putative susceptibility genes are thought to contribute to anxiety disorders. Those genes include *5-HT1A and 5-HT2A* (5-hydroxytryptamine serotonin receptor 1A and 2A) (Rothe et al., 2004; Choi et al., 2010; Albert et al., 2014), *MAO-A* (monoamine oxidase A) (Deckert et al., 1999; Tadic et al., 2003; Ziegler et al., 2016), *COMT* (catechol-O-methyltransferase) (Rothe et al., 2006; Pooley et al., 2007; Lee and Prescott, 2014)*, ADORA2A* (adenosine A2a receptor) (Deckert et al., 1998; Lam et al., 2005; Hohoff et al., 2010)*,* and *CRHR1* (corticotropin releasing hormone receptor 1) (Reul and Holsboer, 2002; Schartner et al., 2017; Savarese and Lasek, 2018). Many of the listed genes, some of which are a part of common biological pathways, have been shown to interact with environmental factors (see below) and contribute to an overall risk score in complex genetic models of anxiety disorders (Domschke and Maron, 2013). Furthermore, the information on variants within some of those genes can be further utilized in clinical practice to partially predict a patient's response to anxiolytic drugs (Tiwari et al., 2009).

Gender differences

On average, the prevalence rates of anxiety disorders are about 1.7 to 2.0 times higher in females than in males. Genetic and neurobiological factors, along with psychosocial contributors (see Stressful life events below) are thought to contribute to the observed differences between genders. Table 5 shows the 12-month (Wittchen and Jacobi, 2005) and lifetime (Kessler et al., 2012) prevalence women-to-men ratios for all anxiety disorders.

Age of onset

While the median age of onset (i.e., age at which an individual first develops a disorder) for anxiety disorders is 11 years (Goodwin et al., 2005; Kessler et al., 2005), their different subclasses show significant variability. For example, the median age of onset for specific phobia and generalized anxiety disorder are 7 and 31 years, respectively. Furthermore, epidemiological

studies of anxiety disorders suggest their chronic nature (i.e., many patients suffer from the disorders throughout life) (Kessler et al., 2009; Kessler et al., 2012).

Table 5. Prevalence rates for anxiety disorders in women vs men. The numbers represent women-to-men ratios. Table adapted from Bandelow (2015).

Anxiety disorder	Wittchen and Jacobi study (2005)	Kessler et al. study (2012)
	12-month P (%)	Lifetime P (%)
Panic disorder	1.8	2.1
General anxiety disorder	2.1	1.7
Social anxiety disorder	2.0	1.2
Agoraphobia	3.1	1.6
Specific phobia	2.4	1.8
All anxiety disorders[a]	2.1	1.5

[a] The studies were conducted before the introduction of DSM-5, when obsessive-compulsive disorder (OCD) and post-traumatic stress disorders were still a part of the anxiety disorders category.

Stressful life events

The risk of onset and relapse of anxiety disorders is also associated with environmental factors, such as stressful life events (Pirkola et al., 2005; Moffitt et al., 2007; Francis et al., 2012). Over 50 years ago, Holmes and Rahe (1967) developed the initial stress scale that assessed the incidence of 43 life events that were positive, adverse, or ambiguous to the respondent's life (Holmes and Rahe, 1967; Miloyan et al., 2018). Since then, adverse (i.e., stressful) life events have been established as a well-known risk for mental disorders, particularly during childhood, which is a sensitive developmental period (Brydges et al., 2014). A study by Pirkola et al. (2005) has shown that of the 60% of adults who reported at least five childhood adversities (e.g., being bullied at school), as much as 10% suffered from anxiety disorders. Interestingly, more adversities had a stronger association with anxiety disorders in females than in males, with the exception of being bullied at school.

2.4.3 Neurobiological basis of anxiety disorders

Brain regions involved in anxiety disorders

Due to their essential role in survival of mammals, the brain mechanisms underlying the processing of defensive responses to threats (see Fig. 1a), in both normal and pathological fear

and anxiety, are similar between humans and mice (see section 2.4.5). Some of the core brain structures involved in this process, historically referred to as the limbic system, include the hippocampus (HIP), amygdala (AMYG), and cingulate gyrus. These three phylogenetically ancient structures, present in all mammals, were the core of the limbic system theory proposed by Paul MacLean (1949). The theory stated that our reptilian ancestors were ruled by instincts and reflexes generated within these three structures and that the emotions they produced were only weakly regulated by the neocortex (MacLean, 1949; Roxo et al., 2011). Although we now know that the evolutionary preconceptions of the limbic brain theory are largely untrue (Grupe and Nitschke, 2013; LeDoux, 2015), the idea behind it is still frequently discussed in scientific articles and lay conversations.

The circuits currently thought to be responsible in normal and pathological anxiety include the AMYG, nucleus accumbens (NA_{CC}), bed nucleus of the stria terminalis (BNST), HIP, periaqueductal grey (PAG), and many areas within the prefrontal cortex (PFC). These areas, and the connections between them, are altered in people suffering from anxiety disorders (Fig. 6). The medial prefrontal cortex (PFC_M), anterior hippocampus (HIP_A, equivalent to ventral HIP, HIP_V, in rodents), and the BNST are of particular interest to many researchers. While the PFC_M is involved in visceral response to emotions and reward processing, HIP_A is associated with sustained anxiety and required for avoidance behavior (Berkowitz et al., 2007; Oler et al., 2010). The direct monosynaptic projection from the HIP_V to the PFC_M is thought to be a crucial component of a circuit responsible for innate forms of anxiety-like behavior in mice (Padilla-Coreano et al., 2016). The BNST is a sexually dimorphic brain region and a central element of the circuit responsible for sustained fear states (Fig 6). It processes information related to response to threats from a vast connectivity network, including PFC_M and HIP (Lebow and Chen, 2016). All brain regions involved in regulation of normal and pathological anxiety communicate through neurotransmitters and neuropeptides, which transmit impulses from one neuron to another via the synapse. Neurotransmitters and neuropeptides differ in size, with the first group being relatively smaller (Purves, 2018). The four main neurotransmitters implicated in anxiety disorders are γ-aminobutyric acid (GABA) (Nuss, 2015), serotonin (5HT) (Gordon and Hen, 2004), norepinephrine (NE) (Montoya et al., 2016), and dopamine (DA) (Russo and Nestler, 2013). The main neuropeptides are corticotropin releasing factor (CRH), arginine-vasopressin (AVP), neuropeptide Y (NPY), pituitary adenylate-cyclase activating polypeptide (PACAP), neuropeptide S (NPS), and oxytocin (Donner et al., 2010; Gottschalk and Domschke, 2018). Neurotransmitters

and neuropeptides are frequently co-released within the central nervous system where they play a central role in regulating stress and emotion circuitry (e.g., by increasing attention and vigilance). Furthermore, they also mediate the peripheral response to stress via increased blood pressure and heart rate and visceral organ activation (Landgraf, 2005; Garakani et al., 2009).

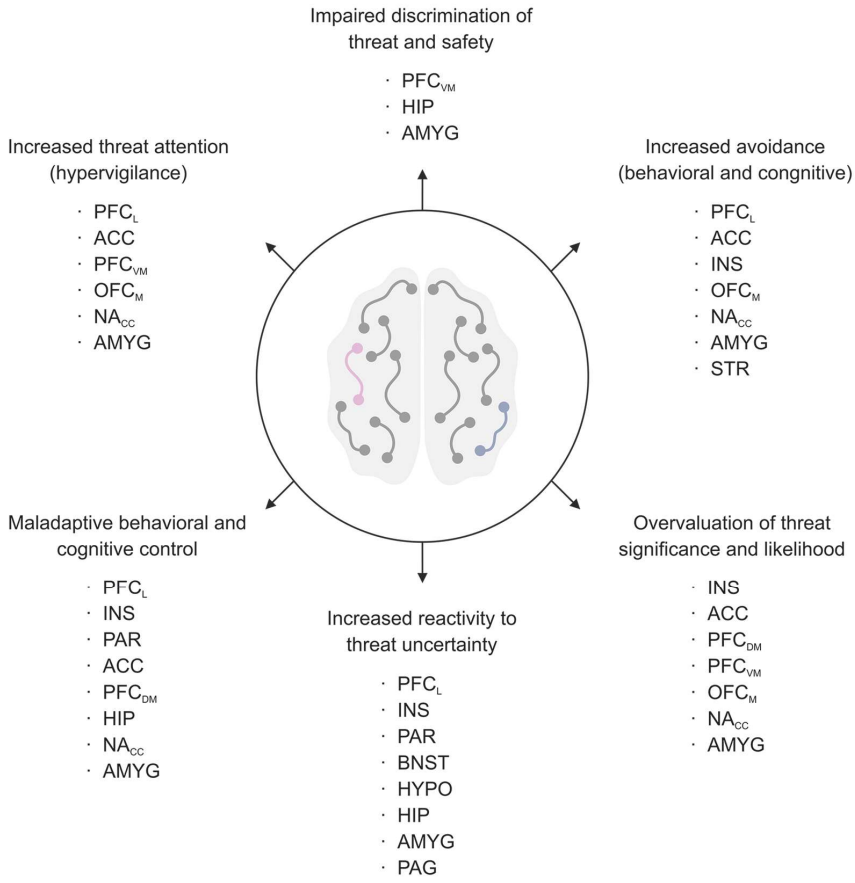

Figure 6. Brain regions involved in anxiety disorders. Six main processes altered in the brains of people suffering from anxiety disorders, as proposed by Grupe and Nitschke (2013). ACC: anterior cingulate cortex, AMYG: amygdala, BNST: bed nucleus of the stria terminalis, INS: insular cortex, HIP: hippocampus, NA_{CC}: Nucleus Accumbens, PAG: periaqueductal grey, PAR: parietal cortex, PFC_{DM}: dorsal medial prefrontal cortex, PFC_{L}: lateral prefrontal cortex, PFC_{VM}: ventral medial prefrontal cortex, OFC_{M}: orbital frontal cortex, STR: dorsal striatum. Figure adapted from LeDoux (2015) and Grupe and Nitschke (2013).

Hypothalamic-pituitary-adrenal (HPA) axis

The brain circuits involved in normal and pathological anxiety (Fig. 6) overlap and interact with that of the stress response (Fig. 1a). Perhaps the best-known aspect of the stress response in mammals is the activation of the hypothalamic-pituitary-adrenal (HPA) axis. This complex

process involves a feedback loop including the hypothalamus, anterior pituitary, and the adrenal gland and inputs from multiple other brain regions implicated in anxiety (e.g., BNST) (Lebow and Chen, 2016) and the HIP (Stephens and Wand, 2012).

During the activation of the HPA axis, the hypothalamus secretes two hormones, AVP and CRH, into the blood vessels, known as hypophysial portal blood, leading to activation of the pituitary gland, which releases adrenocorticotropin hormone (ACTH). ACTH is then transported in the blood to the adrenal cortex, where it binds to the receptors of adrenocortical cells, stimulating the production and release of glucocorticoids, including the stress hormone, cortisol. In mice, a similar hormone, known as corticosterone, is released. Glucocorticoids are important for energy metabolism and for immune and inflammatory responses. The loop is completed by negative feedback to the pituitary gland, hypothalamus, and other brain regions (Fig. 7) (Tsigos and Chrousos, 2002; Faravelli et al., 2012). Dysregulation of the HPA axis (i.e., either hyper- or hyposensitivity) has been shown to be important in different anxiety disorders (Varghese and Brown, 2001; Tanoue et al., 2004).

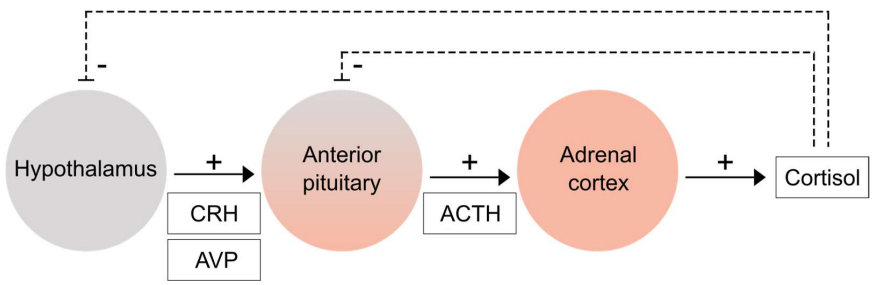

Figure 7. Hypothalamic-pituitary-adrenal (HPA) axis. CRH: corticotropin releasing factor, AVP: arginine-vasopressin, ACTH: adrenocorticotropin hormone. Based on information from Tanoue et al. (2004) and Faravelli et al. (2012).

2.4.4 Behavioral animal models of anxiety disorders

An animal model is a non-human animal employed to investigate the biological bases of human diseases and disorders or basic mechanisms involved in human behavior. Animal models of anxiety disorders take advantage of the fact that anxiety is an evolutionarily conserved response (see section 2.4.3) and enable us to circumvent some of the challenges connected to studying stress and pathological anxiety in humans (see Introduction). It is important to note that

although response to stress has largely been shown to involve the same brain circuits and to evoke similar behavioral responses in both mice and humans (e.g., increase in vigilance and blood pressure, hypoactivity and/or freezing, and hypophagia), their anthropomorphic projection to human traits may sometimes lead to overinterpretation (Cryan and Holmes, 2005). For example, we often describe mice that avoid well-lit areas (see Light-dark box test in Table 7) as being *anxious* rather than expressing *anxiety-like* behavior (Lezak et al., 2017).

Different types of approaches have been established for animal models, including pharmacological, genetic, and behavioral models (Steimer, 2011; Campos et al., 2013). The vast number of behavioral paradigms that have been developed to induce (Table 6) and measure (Table 7) anxiety-like behavior in rodents differs in their predictive (animal performance in the test predicts performance in the condition it is being modeled after), face (phenomenological similarity), and construct (theoretical rationale) validities. Although both acute and chronic stress-inducing paradigms exist, the latter paradigms are more suitable to study anxiety from the perspective of several validities (Cryan and Holmes, 2005; Nestler and Hyman, 2010). In particular, the CSDS model, a model of chronic psychosocial stress (see section 2.4.2 subsection *Stressful life events*), has been successfully used to produce a significant amount of knowledge on the biological basis of anxiety-like behavior (Krishnan et al., 2007; Kovalenko et al., 2014; Volk et al., 2014; Volk et al., 2016; Laine et al., 2017). The CSDS model involves repeated daily interactions of an experimental animal with a conspecific aggressor, without the possibility of escaping the situation (see section 4.3) (Golden et al. 2011). Lastly, with the recent introduction of RDoc (see section 2.2.3), which focuses on symptoms of disorders rather than the disorders themselves, more animal models concentrate on the observation of simple behavioral and physiological measures that can be straightforwardly extrapolated to humans (Lezak et al., 2017; Toyoda, 2017).

Table 6. Overview of the most common models to induce anxiety-like behavior in mice. See Materials and methods for extended description of the chronic social defeat (CSDS) paradigm. Adapted from Toyoda (2017).

Stress type	Behavioral model	Reference(s)
Chronic, physical and emotional	Chronic social defeat stress (CSDS)	Golden et al., 2011
	Subchronic social defeat	Goto et al., 2014
	Unpredictable chronic stress (UCS)	Mineur et al., 2006; Monteiro et al., 2015
	Chronic restraint stress (CRS)	Kvetnansky and Mikulaj, 1970
Chronic and emotional	Witness stress	Sial et al., 2016

Table 7. Overview of the most common tests to assess anxiety-like behavior in mice. See Materials and methods for extended description of the social avoidance (SA) test. FST is most often considered a model of *despair*, not *anxiety-like* behavior. However, it can also be used to induce acute physical and emotional stress (Porsolt et al., 1977; Allsop et al., 2014). Adapted from Allsop et al. (2014), Golden et al. (2011), Kumar et al., (2013) and Blanchard, Griebel and Blanchard (2001).

Behavioral test	Brief description
Elevated plus maze (EPM)	An elevated, plus-shaped apparatus composed of 2 enclosed arms opposed by 2 open arms (Pellow et al., 1985)
Elevated zero maze (EZM)	An elevated, circular runway that alternates open, brightly lit areas with enclosed, dark areas (Shepherd et al., 1994)
Open field (OF)	Novel, relatively lit square or circular arena divided into peripheral and central units (Hall and Ballachey, 1932)
Light-dark box (L/D)	Box with 2 different compartments: protected (dark) and unprotected (lit) (Lorenzini et al., 1984)
Social avoidance (SA)	An animal is placed in the center of an open arena and allowed to explore it during two sessions, with and without an unfamiliar aggressor placed in perforated container; time in the interaction zone (IZ) around the container is measured (Golden et al., 2011)
Novelty suppressed feeding (NSF)	Food-deprived animals are exposed to a box with a sawdust-covered floor, a central platform holding a single pellet of chow or liquid, and focused lighting (Dulawa and Hen, 2005; Deacon, 2011)
Forced swim test (FST)	An animal is placed in a container filled with water from which it cannot escape. Time to immobility is measured (Kumar et al., 2013)

3 Aims of the study

The aim of this thesis was to improve the understanding of the molecular etiology behind vulnerability and resiliency to pathological anxiety in mammals.

The following specific objectives were addressed in the studies of this thesis:

1. To identify genetic loci that predispose to a specific phobia, fear of heights, in an isolated Finnish population with a reduced genetic heterogeneity using a microsatellite marker panel (study I).

2. To identify converging gene regulatory networks (GRN) of mRNAs and miRNAs and protein-protein interaction networks in the bed nucleus of the stria terminalis (BNST) affected by exposure to chronic social defeat stress (CSDS), a well-established mouse model of chronic psychosocial stress. To examine major biological pathways and molecules associated with the anxiety-related phenotype through comparative analyses of BNST and whole-blood transcriptome of CSDS-exposed mice and blood cell gene expression profiling of samples from panic disorder (PD) patients after exposure-induced panic attacks (study II).

3. To establish common biological pathways affected by CSDS in the BNST and two other brain regions, the medial prefrontal cortex (PFC_M) and ventral hippocampus (HIP_V), through comprehensive transcriptome analysis (study III).

4 Materials and methods

All methods presented in this work are described in detail in the original publications (studies I and III) or the manuscript (study II). A brief description of the study samples and an overview of all methods used by the author (Tables 8-11) are presented below. Additionally, an overview of all data sets used in studies II and III is shown in Figure 8. Only the main methods, essential to the understanding of the results and discussion, are further explained in the following sections.

4.1 Ethics statements (studies I, II, and III)

All animal procedures were approved by the Regional State Administration Agency for Southern Finland (ESAVI-3801-041003-2011 and ESAVI/2766/04.10.07/2014) and performed in accordance with directive 2010/63/EU of the European Parliament and of the Council and the Finnish Act on the Protection of Animals Used for Science or Educational Purposes (497/2013). All human procedures were approved by the ethical review board of the National Institute for Health and Welfare (THL), formerly the National Public Health Institute of Finland (KTL) (study II), or the Ethics Committee of the Ludwig Maximilian University of Munich, Germany (study I) and are in accordance with the Declaration of Helsinki.

4.2 Study samples (studies I, II, and III)

The following three main samples were used as a part of this work: two human samples including individuals suffering from acrophobia (the fear of heights, study I) and panic disorder (study II) and one animal sample of mice from four inbred strains subjected to CSDS, a mouse model of chronic psychosocial stress (studies II and III). The samples are briefly described in the following section and their use is detailed in Tables 8 to 11 and in Figure 9.

Human acrophobia study sample (study I)

The sample included 57 mostly large multigenerational pedigrees with multiple affected individuals and at least one parent born in a Finnish genetic isolate. This sample consisted of 642 people, 42 of which are affected with pure acrophobia (6.5%) and 75 with acrophobia with comorbid schizophrenia (11.7%). All pedigrees are part of a Finnish severe mental disorders' family collection of the National Institute for Health and Welfare (Varilo et al., 1996; Hovatta et

al., 1999; Arajarvi et al., 2006; Wedenoja et al., 2008; Paunio et al., 2009). Blood samples were collected and analyzed for 575 autosomal microsatellite markers across the genome. For information about sample collection and genotyping, which was not a part of this study, please refer to Arajärvi et al. (2006) and the original publication.

Human Panic Disorder (PD) study sample (study II)

The sample was composed of 21 non-medicated PD patients, including 6 males (age 29.33 ± 8.48 years) and 15 females (age 32.60 ± 9.61 years) recruited in the anxiety disorder outpatient unit at the Max Planck Institute of Psychiatry, Munich, Germany. PD with (n = 18; 85.7%) or without (n = 3; 14.3%) comorbid agoraphobia was given as the primary diagnosis, while mild secondary depression was allowed (n = 2; 9.5%). As a part of behavioral therapy, patients underwent exposure therapy, which depended on the feared situation (e.g., subway, supermarket, tower) and specific concern (e.g., fainting, asphyxiation, losing control). Blood samples were collected at three timepoints: baseline, 1-hour post-exposure and 24-hour post-exposure. Blood cell RNA was extracted and gene expression was performed using Illumina HumanHT-12 v4 Expression BeadChips (Illumina, CA, USA).

Mice chronic social defeat study sample (studies II and III)

Male 5-week-old mice from two (study II) or four (study III) inbred mouse strains (see below) and 13 to 26-week-old outbred Clr-CD1 (CD-1) mice (Charles River Laboratories, Sulzfeld, Germany) were housed in a pathogen-free, humidity- (50 ± 15%) and temperature-controlled (22 ± 2 °C) animal facility at the University of Helsinki on a 12-hour light-dark cycle (lights on at 6 A.M. to 6 P.M.) and with ad libitum access to Teklad 2916 rodent chow (Envigo, Huntingdon, United Kingdom) and water. Before the beginning of the behavioral experiments, all inbred mice were acclimatized for 10 days in group housing. CD-1 mice were acclimatized for 7 days in single individually ventilated cages (IVC) (Tecniplast, Buguggiate, Italy) prior to CD-1 aggressor screening (see Table 8). Behavioral experiments were conducted on four inbred strains 129S2/SvPasCrl (129), BALB/cAnNCrl (BALB) DBA/2NCrl (D2) and C57BL/6NCrl (B6), of which the two latter strains were only included in study III.

4.3 Behavioral experiments in mice (studies II and III)

Chronic social defeat stress (CSDS)

B6, D2, 129, and BALB male mice were subjected to 10 days of CSDS (Fig. 8) (Berton et al., 2006; Golden et al., 2011). Briefly, each intruder mouse (B6, D2, 129 or BALB) was placed into a cage of a resident (CD-1) (Fig. 8) for a maximum of 10 minutes. Following the defeat session, both mice remained in the same cage until the next day, separated by a perforated clear plexiglass divider to allow sensory contact. The defeat sessions were repeated for 10 consecutive days, each day with a new unfamiliar CD-1 resident. During the 10-day protocol, the control mice were housed in identical cages, on two sides of a clear plexiglass divider. While the control mice were handled and switched cagemates every day, similarly to the defeated mice, they were not in a direct physical contact with other mice at any time.

Social avoidance (SA) test

All mice underwent a SA test (Berton et al., 2006) 24 hours after the last social defeat session to assess the effects of CSDS and divide them into stress-resilient and stress-susceptible groups. Briefly, the SA test consisted of two trials, the first without a CD-1 aggressor (target absent) and second with aggressor (target present), each lasting 150 seconds. During both trials, the test mouse was placed in the middle of an open field (OF) arena with a clear circular perforated plexiglass cylinder located adjacent to one of the walls (Fig. 8). The test mouse was allowed to freely explore the arena while its movements were tracked using a camera connected to a computer running EthoVision XT10 video tracking software (Noldus Information Technology, Wageningen, Netherlands). The time the mouse spent in the interaction zone (IZ), a semicircle around the cylinder, during both trials was measured and a social interaction (SI) ratio was calculated by dividing the IZ time of the second trial by the IZ time of the first trial. To separate the mice into stress-susceptible and stress-resilient phenotypes, we calculated the mean and median SI ratio. Subsequently, we log-transformed the values to obtain normal distribution and removed outliers (SI > 3 IQRs from the median). We next divided the defeated mice into stress-resilient and -susceptible phenotypes based on the SI ratio, with the border determined as the controls' mean SI score minus one SD. SI ratio border values for each strain were the following: 129 = 62.68, BALB = 81.76, B6 = 76.49, D2 = 105.99. Of all B6 mice subjected to a SA test, 9% of

the susceptible, 20% of the resilient, and 35% of the control mice were included in both study II and III.

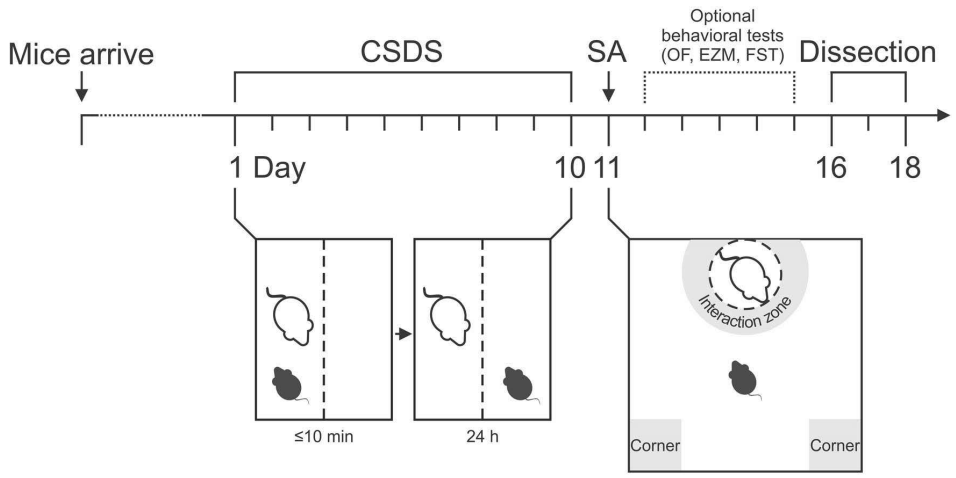

Figure 8. Overview of the timeline of behavioral experiments including schemes of the chronic social defeat stress (CSDS) and social avoidance (SA) test. CSDS: chronic social defeat stress, EZM: Elevated zero maze, FST: Forced swim test, OF: Open field, SA: Social avoidance. For description of the OF, EZM and FST, please see section 2.4.4.

4.4 Overview of the analyzed data sets (studies II and III)

Studies II and III included a large number of data sets from various brain structures (PFC_M, HIP_V, and BNST) and species (*Homo sapiens* and *Mus musculus*; see also section 4.2) used for experiments conducted across different -omics platforms and other approaches. For simplification, the data sets are thereafter also referred to by their letter equivalents (Fig. 9). For details regarding the methods listed in Figure 9, see Tables 8 to 11 and section 4.5.

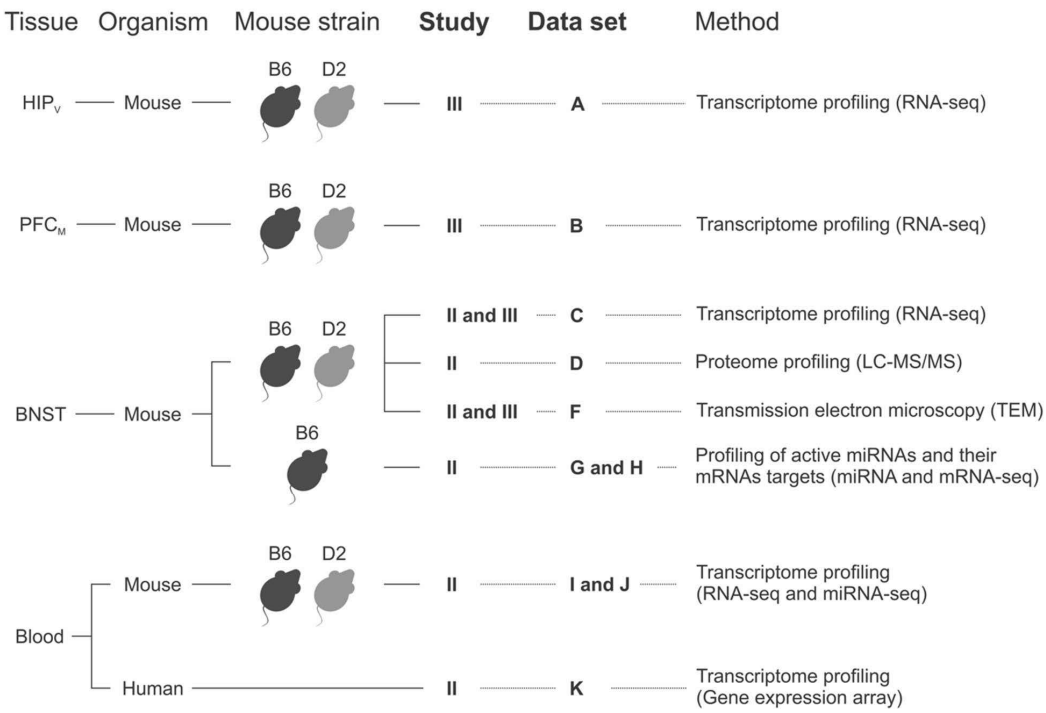

Figure 9. An overview of all data sets used in studies II and III. All data sets are organized by their tissue, organism (common name), study, and method. B6: C57BL/6NCrl strain; D2: DBA/2NCrl strain, LC-MS/MS: Liquid chromatography-tandem mass spectrometry; RNA-seq: RNA sequencing; TEM: Transmission electron microscopy.

4.5 Overview of methods (studies I, II and III)

The section below presents an overview of all methods used in studies I, II, and III. Table 8 shows the methods used in behavioral experiments in mice, animal tissue collection, and RNA extraction. Table 9 discusses methods related to RNA sequencing (RNA-seq), miRNA sequencing (miRNA-seq), transmission electron microscopy (TEM), and Western blot experiments. Tables 10 to 11 include statistical methods used in all studies. Additionally, a short description of gene set enrichment analysis and pathway analysis (the main methods applied in studies II and II) is presented. Lastly, Figure 10 includes a guide for reading Figures 15, 16, 19 and 20, which are a part of section 5.2.

Table 8. Overview of the methods used in behavioral experiments in mice, animal tissue collection, and RNA extraction (studies II and III).

Category	Brief description and/or method	Reference	Study
I. Behavioral experiments in mice			
CD-1 aggressor screening	Aggression levels of CD-1 mice were checked on 3 consecutive days by introducing an unfamiliar screener mouse into their home cage	Golden et al., 2011	II, III
CSDS	See section 4.3	Golden et al., 2011; Berton et al., 2006	II, III
SA test	See section 4.3	Berton et al., 2006	II, III
Body weight	Recorded for all defeated and control mice on days 1, 4, 6, 8, 10 of CSDS	-	II, III
FST	See section 2.4.4 and Figure 8	Kumar et al., 2011	II, III
OF test	See section 2.4.4 and Figure 8	Can et al., 2012	II, III
EZM	See section 2.4.4 and Figure 8	Shepherd et al., 1994	II, III
II. Animal tissue collection			
Brain tissue collection	Mice sacrificed by cervical dislocation 6-8 days after CSDS, at which point all brain regions were collected	Lebow et al., 2012	II, III
Blood samples	Trunk blood was collected at the moment of decapitation	Parasurman et al., 2010	II, III
III. RNA extraction and related experiments			
RNA extraction from brain tissue	Extracted with TriReagent (Molecular Research Center Inc., OH, USA)	-	II, III
RNA extraction from blood	TRIzol LS reagent (Thermo Fisher Scientific, MA, USA)	Winn et al., 2010	II
Immunoprecipitation of AGO2 protein	Immunoprecipitation of AGO2-bound miRNAs and their target mRNAs was performed on pools of 3 BNST collected from all phenotypic groups; RNA was isolated using the RNeasy plus kit (Qiagen, Hilden, Germany)	Volk et al., 2014	II

AGO2: Argonaute-2; BNST: Bed nucleus of the stria terminalis; CSDS: chronic social defeat stress; EZM: Elevated zero maze; FST: Forced swim test; OF: Open field; SA: Social avoidance.

Table 9. Overview of the methods related to RNA sequencing (RNA-seq), miRNA sequencing (miRNA-seq), transmission electron microscopy (TEM) and Western blot experiments (studies II and III).

Category	Brief description and/or method	Study
I. RNA-seq (data sets A, B, C, H and I)		
rRNA depletion	Ribo-Zero Gold rRNA Removal kit (Illumina Inc, CA, USA; data sets A and B), Insert Dependent Adaptor Cleavage primers (data set C) or Ribozero Globin depletion Kit (Illumina; data set I)	II, III
RNA fragmentation	S2 ultrasonicator (Covaris Inc., MA, USA)	II, III
Library preparation	Nextera (Illumina; data set A), ScriptSeq v2 (Epicentre, WI, USA; data set B), Ovation Universal RNA-Seq System (NuGEN, CA, USA; data set C), TruSeq Stranded mRNA Library Prep (Illumina; data set H) or TruSeq Stranded Total RNA (Illumina; data set I) library preparation kits	II, III
Library size selection	Pippin Prep (Sage Science, MA, USA)	II, III
Sequencing	HighSeq 2000 (Illumina; data set A; paired-end) or NextSeq 500 platforms (Illumina; data sets B, C, H and I; single-end)	II, III
II. miRNA-seq (data sets G and J)		
Library preparation	TruSeq Small RNA Library Prep Kit (Illumina; data set D) or NEXTflex Small RNA-Seq Kit v3 (Bioo Scientific, TX, USA; data set J) library preparation kits	II
Library size selection	Pippin Prep (Sage Science)	II
Sequencing	NextSeq 500 platform (Illumina, single-end)	II
III. Other experimental methods		
Transmission electron microscopy	See the original publication and manuscript for sample preparation, imaging, image analysis and quantification; for statistical analyses, see below	II, III
IV. Primary antibodies		
Mouse monoclonal anti-Cytochrome	Diluted 1:500, (Santa Cruz Biotechnology, TX, USA; #sc13156)	II
Mouse monoclonal anti-DARPP-32	Diluted 1:200, (Santa Cruz Biotechnology; #sc-271111)	II

All materials and instruments are identified by the supplier's name and location. However, the location is given only the first time the supplier is mentioned. DARPP-32: Dopamine-and cAMP-regulated phosphoprotein; rRNA: Ribosomal RNA.

Table 10. Overview of statistical methods used in studies I, II, and III.

Category	Brief description and/or method	Reference	Study
I. Linkage and LD analyses			
PedCheck	Genotypes were checked for Mendelian inconsistencies	O'Connell and Weeks, 1998	I
FASTLINK 4.1 P implemented in AUTOGSCAN	Parametric two-point recessive and dominant linkage analysis (penetrance: 0.001% and 90%, disease allele frequency: 0.00001 and 0.01, and phenocopy rates: 0 and 0.01, respectively)	Hiekkalinna et al., 2005	I
SimWalk2	Parametric and nonparametric multipoint linkage analysis	Sobel et al., 2001	I
Mega2	Preparation of files for SimWalk2 software	Baron et al., 2014	I
PSEUDOMARKER	Linkage disequilibrium conditional on linkage analysis	Gertz et al., 2014; Hiekkalinna et al., 2011	I
SLINK	Power simulation	Weeks et al., 1990	I
II. Analysis of mice behavioral experiments			
SPSS Statistics	For applied tests, see Table 11 and 12 in section 5.2.1 (IBM, NY, USA)	-	II, III
III. Initial RNA-seq analysis			
FastQC	Quality assessment of the data	http://www.bioinformatics.babraham.ac.uk	II, III
SortMeRna tool	Quality assessment (data set I)	Kopylova et al., 2012	III
Cutadapt	Adapters trimming	Martin, 2011	II, III
FastX toolkit	Adapters trimming	Gordon and Hannon, 2010	II, III
PRINSEQ	Quality assessment of the data; Removal of PCR duplicates	Schmieder and Edwards, 2011	II, III
STAR	Reads were aligned to mouse genome GRCm38	Dobin et al., 2013	II, III
HTSeq	Genome annotation using GTF release 86 (update 2016-10)	Anders et al., 2015	II, III
IV. Initial miRNA-seq analysis			
FastX toolkit	Adapters trimming	Gordon and Hannon, 2010	II
PRINSEQ	Adapters trimming (data set J)	Schmieder and Edwards, 2011	II
STAR	Reads were aligned to mouse genome GRCm38	Dobin et al., 2013	II
miRDeep2	Genome annotation (miRBase v21) and quantification	Friedländer et al., 2008	II
Bowtie	Genome annotation using GTF release 86 (update 2016-10)	Anders et al., 2015	II

Table 11. Overview of statistical methods used in studies II and III.

Category	Brief description and/or method	Reference	Study
V. Initial LC-MS/MS data analysis			
ProteinScape Software Platform	Raw data were searched against SwissProt *Mus musculus* database (Matrix Science, London, UK)	Chamrad et al., 2007	III
VI. Differential expression (DE)			
Rcpp[a]	Direct interchange of rich R objects between R and C++ languages	Eddelbuettel and Balamuta, 2018	II, III
edgeR[a]	Data normalization and filtering of RNA-seq data	Robinson et al., 2010	II, III
Perseus	Data normalization, quality assessment and filtering	Tyanova et al., 2016; Cox and Mann, 2012	II
PVCA[a]	Quality assessment of the data; principal variance component analysis (PVCA)	Bushel, 2018	II
sva[a]	Quality assessment of the data; surrogate variable analysis (sva)	Leek et al., 2018	II, III
ComBat[a]	Batch adjustments of RNA-seq data	Johnson et al., 2007	II, III
DanteR[a]	Normalization of systematic biases in LC-MS/MS data	Taverner et al., 2012	II
limma eBayes[a]	DE analysis of RNA-seq and LC-MS/MS data	Phipson et al., 2016; Ritchie et al., 2015	II, III
VII. GSEA, IPA and GO term enrichment			
GSEA Desktop	Gene set enrichment analysis (GSEA); see below	Subramanian et al., 2005; Mootha et al., 2003	II, III
IPA	Ingenuity Pathway Analysis (IPA); see below	https://www.qiagenbioinformatics.com/	II, III
topGO[a]	Enrichment Analysis for Gene Ontology; see below	Alexa et al., 2006	II, III
VIII. Transmission electron microscopy			
SPSS Statistics	See below (IBM)	Hanley et al., 2003	II, III

[a] R package

DE: Differential expression; GO: Gene ontology; GSEA: gene set enrichment analysis; IPA: Ingenuity pathway analysis; LC-MS/MS: LC-MS/MS: liquid chromatography-tandem mass spectrometry; PVCA: Principal variance component analysis; RNA-seq: RNA sequencing; sva: Surrogate variable analysis

Gene set enrichment analysis (GSEA) (studies II and III)

We performed gene set enrichment analysis (GSEA) on data sets A to D, I, and K using the GSEA Preranked tool implemented in GSEA Desktop v3.0 and the curated gene sets (C2) of the Molecular Signature Database (MSigDB) v6.0 provided by the Broad Institute (Mootha et al., 2003; Subramanian et al., 2005). In study II, we further selected the top significantly dysregulated gene set present in at least 50% of the respective comparisons (Fig. 13b, data sets C and D; Fig. 17 data sets C, I, and K) for visualization. Due to the large number of data sets and differences in -omics platforms, a recommended exploratory false discovery rate (FDR) of 25% (Mootha et al., 2003) was applied. The DE genes, common among the B6 and D2 stress-susceptible mice in comparison to controls (data sets C and I) were further investigated by hypergeometric distribution implemented in the MSigDB v6.0. In study III, we selected the top five gene sets with the highest positive and lowest negative enrichment scores (NES; $P_{FDR} < 0.05$) within each strain (i.e., B6 and D2) and comparison (i.e., stress-susceptible, stress-resilient, and control) for further analysis. From the selected gene sets, all present in at least two brain regions and two comparisons were visualized (Fig. 11). The top enriched gene sets were further investigated for overlapping genes with hypergeometric test implemented in the MsigDB v6.0. All gene sets in Figures 17, 21b, and 25 are organized by frequency of gene sets with $P < 0.05$ and then alphabetically.

Ingenuity Pathway Analysis (IPA) (study II)

The core and comparison network analyses were performed with IPA v.483681M (QIAGEN Inc., 2018) for all genes (data set C) and proteins (data set D) with nominal $P < 0.05$ and absolute fold change ($|FC|$) ≥ 1.2. Figure 21a shows the top significantly dysregulated pathways present in at least 30% of all comparisons. All pathways in Figure 21a are organized by frequency of canonical pathways with $P < 0.05$ and then alphabetically.

Gene Ontology (GO) term enrichment analysis

We performed GO term enrichment analysis on DE genes ($P < 0.05$ and $|FC| \geq 1.2$) overlapping between the B6 and D2 stress-susceptible vs control comparisons (data set C). The analysis was performed using the topGO R package (Alexa et al., 2006) with standard parameters. For data set K, we performed classical enrichment analysis by testing over-representation of GO terms

with the group of DE genes ($P < 0.05$). As background in the analysis, we used all annotated genes and probes.

Transmission electron microscopy (TEM) statistical analysis (studies II and III)

Mitochondria (study II)

We measured the maximum (length) and minimum (width) diameter of all mitochondrial cross-sections entirely within the microscope field using Microscopy Image Browser software (Belevich et al., 2016). Following identification of synaptic densities, we counted the number of mitochondrial cross-sections localized in the pre- or post-synaptic compartment. Study II included 60 to 80 individual axons from three to four animals per group.

Myelinated axons (study III)

We measured axon diameter, myelin thickness, and g ratio (ratio of the inner axonal diameter to the outer axonal diameter) with ImageJ software (Schneider et al., 2012). The diameter was measured by taking the circumference of the whole fiber and the circumference of the axon. The g ratio was calculated by dividing the diameter of the axon with the diameter of the whole fiber. Study III included 32 to 69 individual images from three to five animals per group.

Group differences in TEM data (studies II and III) were assessed using generalized estimating equations (GEEs) to control for within-subject dependencies of individual axons measured from the same animal, which violated the ANOVA assumption of the independence of observation (see Hanley et al., 2003). Pair-wise contrasts were computed with Fisher's LSD and significance determined with the Bonferroni method using SPSS Statistics v25 (IBM, NY, USA).

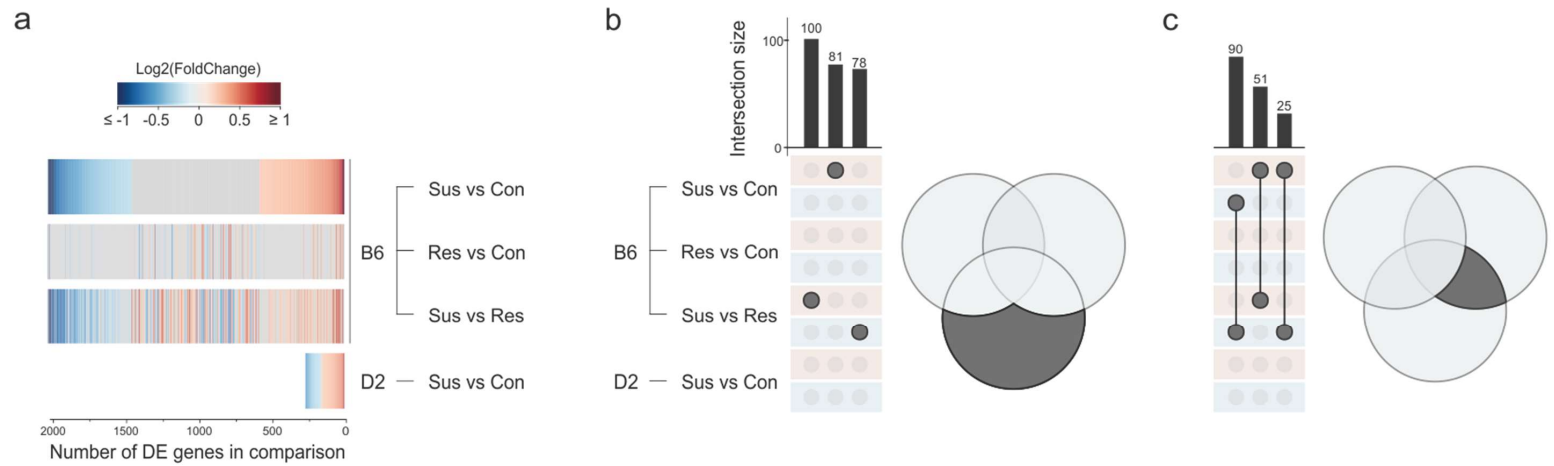

Figure 10. A guide to reading the union heatmap plots and the UpSet plots. (a) Union heatmaps showing the number of differentially expressed (DE) ($P < 0.05$, $|FC| > 1.2$) genes for all available comparisons within each mouse strain. The genes are rank-ordered by the FCs in the susceptible vs control comparison, separately for each strain and data set. In the example, a higher number of red and blue lines representing the DE genes is observed, with positive and negative FC, respectively, in the susceptible (Sus) vs control (Con) comparison than in the resilient (Res) vs control (Con) comparison within the B6 strain (Bagot et al. 2016). **(b)** UpSet R package (Conway et al., 2017) plots the intersections between the comparisons. In this panel, each row represents a part of the comparison including either *upregulated* (red background) or *downregulated* (blue background) DE genes. In the example, we selected three comparisons marked with dark gray dots, i.e., *upregulated* DE genes in the B6 Sus vs Con and Sus vs Res comparisons and *downregulated* DE genes in the B6 Sus vs Res comparison. The light gray dots indicate that this comparison is not a part of that intersection. As shown in panel b, none of the DE genes are overlapping between the selected comparisons. The same information is shown on the Venn diagram on the right. **(c)** The comparisons share a number of common DE genes. For example, 90 of the DE genes are *downregulated* in both B6 Sus vs Con and B6 Sus vs Res, while 51 DE genes are *upregulated* and shared between the same comparisons. A number of DE genes shared between two comparisons is also represented by the shaded area on the Venn diagram (right). B6: C57BL/6NCrl strain; Con: Control; D2: DBA/2NCrl strain; Res: Resilient; Sus: Susceptible.

5 Results

5.1 Genetic predisposition to acrophobia is likely to have a complex genetic architecture (study I)

We aimed to identify genetic risk variants for acrophobia, an abnormal fear of heights, through a genome-wide linkage scan using a panel of 570 microsatellite markers. The microsatellite marker panel had been genotyped as part of earlier schizophrenia linkage-based gene mapping studies (Hovatta et al., 1999; Wedenoja et al., 2008). Our analyses were performed in large multigenerational pedigrees belonging to an isolated homogenous population from a northeastern part of Finland. The cohort consisted of 642 people, of which 42 were affected only with acrophobia (6.5%) and 75 with acrophobia comorbid with schizophrenia (11.7%). As the inheritance pattern of acrophobia is unknown, due to their different strengths and weaknesses in detecting linkage, we applied a wide range of analytical methods and models (Ott, 1999; Sham et al., 2000; Goode et al., 2005) and accordingly divided our study into three stages. Stage I of the study consisted of parametric two-point (IA) and multipoint (IB) analyses and stage II of nonparametric multipoint analysis. Unlike nonparametric analysis, parametric linkage analysis requires the estimation of allele frequency and penetrance (Ott et al., 2015). Furthermore, while two-point analysis (also referred to as single-point analysis) examines linkage of a putative disease locus to a single marker locus at a time, significantly reducing computational load and enabling parallel processing, multipoint analysis evaluates linkage to multiple markers simultaneously (Szymczak et al., 2014). Lastly, in stage III of the study, we conducted joint linkage and LD analysis. Due to a significant number of individuals suffering from acrophobia with comorbid schizophrenia (44.0%), the three-stage analysis was conducted both for acrophobia with and without comorbid schizophrenia, thereafter also referred to as the pure acrophobia sample. An overview of the results of all performed analyses with both sub-samples is presented in Table 12.

Table 12. Summary of suggestive results from parametric, nonparametric, and joint linkage and linkage disequilibrium analyses.

Stage	Software (reference)	Analysis	Statistical criterion for selection	Model or method	Marker	Chromosome	Genetic locus (cM)	LOD score or P-value[a]	
								Acrophobia without comorbid psychiatric diagnosis	Acrophobia with comorbid schizophrenia
I(A)	FASTLINK 4.1P implemented in AUTOGSCAN (Hiekkalinna et al. 2011)	Parametric two-point linkage	LOD > 1.6 in any of the models	Dominant	D5S2115	5	147.47	0.58	**2.16**
				Recessive	D13S173	13	87.49	0.99	**1.89**
					D1S1728	1	97.17	1.20	**1.62**
					D8S373	8	163.74	**2.09**	0.51
					D21S1441	21	7.80	**1.61**	0.47
I(B)	SimWalk2 (Sobel and Lange 1996; Sobel, Sengul and Weeks 2001; Lange and Lange 2004)	Parametric multipoint linkage	LOD > 2.0 in parametric two-point linkage analysis [Stage I(A)]		D5S2115	5	147.47	-	0.054[b]
					D8S373	8	163.74	0.533[c]	-
II	SimWalk2 (Sobel and Lange 1996; Sobel, Sengul and Weeks 2001; Lange and Lange 2004)	Nonparametric linkage	LOD > 2.0 in any of the models	NPL_{all}	D13S173	13	87.49	**2.11**	**2.91**
					D1S2817	1	198.45	0.59	**2.33**
					D5S490	5	137.60	1.34	**2.05**
					D13S162	13	52.51	**2.22**	1.55
					D4S2394	4	116.99	**2.12**	0.42
				NPL_{pair}	D13S173	13	87.49	1.73	**2.45**
					D1S2817	1	198.45	0.47	**2.52**
					D5S490	5	137.60	1.48	**2.41**
					D13S162	13	52.51	**2.11**	0.97
					D4S2394	4	116.99	**2.17**	0.52
III	PSEUDOMARKER (Hiekkalinna et al. 2011; Gertz et al. 2014)	Joint linkage and linkage disequilibrium	Two most significant results in each phenotype and any of the models.	Recessive	D4S2431	4	160.98	0.1704	**0.0003**
				Dominant	D14S267	14	115.49	0.0244	**0.0019**
				Dominant	D17S2196	17	43.99	**0.0054**	0.3898
				Recessive	D1S235	1	236.19	**0.0054**	0.2910

[a] LOD scores are given for analyses performed at stage I and II, while *P*-values are specified for joint linkage and linkage disequilibrium analysis (stage III).
[b] At $\alpha = 0.15$. α = overall proportion of linked pedigrees, e.g., $\alpha = 1.00$ implies no locus heterogeneity (Bhat et al., 1999).
[c] At $\alpha = 1.00$ (Also see b).
All markers exceeding the statistical criterion for selection (see column four) for at least one for either acrophobia with or without comorbid diagnosis are written in bold. LOD: Logarithm (base 10) of odds; cM: Centimorgan.

5.1.1 Parametric two-point and multipoint analyses (stage I)

The strongest evidence for linkage was detected for marker D5S2115 (LOD = 2.16, dominant model) when the analysis was performed with the acrophobia with comorbid schizophrenia sample and marker D8S373 (LOD = 2.09, recessive model) for the pure acrophobia sample. In acrophobia with comorbid schizophrenia, marker D8S373 obtained a LOD score of only 0.51 (recessive model) and in the pure schizophrenia sample a LOD score of 0.00 (recessive model) (Fig. 11).

Chromosomes 5 and 8, for which we obtained a LOD score of >2 with either the recessive or dominant inheritance model, were further examined using parametric multipoint linkage analysis. We obtained a maximum multipoint LOD score (MLOD) of 0.054 (α = 0.15, dominant model) for marker D5S2115 in the acrophobia sample with comorbid schizophrenia. In the pure schizophrenia sample, marker D8S373 yielded the maximum MLOD score of 0.533 (α = 1.00 recessive model), the highest LOD score on chromosome 8.

5.1.2 Nonparametric multipoint analysis (stage II)

In stage II of the study, we conducted a multipoint nonparametric genome-wide linkage analysis with both an empirical, NPL_{all} and NPL_{pair} methods. While NPL_{all} allows us to calculate if founder alleles are overrepresented in individuals affected with acrophobia, and NPL_{pair} estimates the sum of conditional kinship coefficients for all affected pairs.

The NPL_{all} method yielded the highest LOD score of 2.91 for marker D13S173 in the acrophobia with comorbid schizophrenia sample, while the maximum score of 2.22 in the pure acrophobia sample was obtained for marker D13S162 (Fig. 11). Both markers are located on chromosome 13, 37.8 cM apart. The distance between markers suggest that they are not strongly linked.

The NPL_{pair} approach gave the highest LOD score of 2.52 for marker D1S2817 in the acrophobia with comorbid schizophrenia sample and the maximum LOD score of 2.17 for marker D4S2394 in the pure acrophobia sample (Fig. 11). It is likely that the signal detected for marker D4S2394 comes from the acrophobia phenotype as the same marker in the acrophobia with comorbid schizophrenia yielded a LOD score of only 0.52.

Two-point nonparametric analysis was not performed as a part of this study as multiple pedigrees sizes, without being divided, exceeded the limits for the currently available software (Dudbridge, 2003).

5.1.3 Joint linkage and linkage disequilibrium analysis (stage III)

Genetic isolates, such as the one presented in this study, are characterized by reduced genetic heterogeneity that can result in the majority of affected individuals carrying the same predisposing variant, detectable as LD (Hiekkalinna et al., 2011). Marker D4S231 showed the strongest evidence for association with acrophobia including the samples with comorbid schizophrenia (*P* = 0.0003, recessive model), while in the acrophobia sample without comorbid psychiatric diagnosis the strongest association was obtained by both markers D1S235 and D17S2196 (*P* = 0.0054 for both markers).

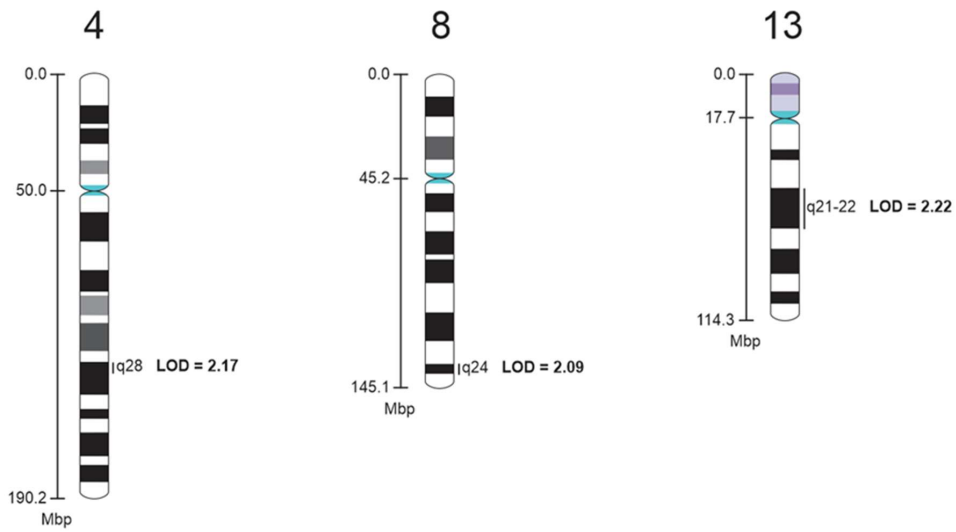

Figure 11. A summary of the most significant chromosomal regions implicated in a genome-wide linkage scan for acrophobia without comorbid schizophrenia. Chromosome numbers are indicated above the ideograms. Blue: Centromere; Light purple: variable region; dark purple: stalk. LOD: Logarithm (base 10) of odds.

5.1.4 Estimation of statistical power

To estimate the power of the analyzed sample to detect linkage, we performed a PSEUDOMARKER simulation with SLINK software package (Ott, 1989; Cottingham et al., 1993;

Hiekkalinna et al., 2011)). According to this analysis, average maximum LOD scores of 5.77 and 5.03 were obtained with the dominant and recessive models, respectively. Furthermore, a conventional LOD score of 3.0 was reached by 31% and 12% of replicates in the recessive and dominant models (allele frequency of 0.00001 and 0.01 and phenocopy rates of 0 and 0.01, respectively) with the assumption of complete linkage ($\theta = 0.0$), respectively. We therefore concluded that our sample has adequate power to detect significant evidence for linkage.

5.2 Trans-omics cross-species approach to identify molecular pathways associated with anxiety-related behavior (studies II and III)

In study II and III, we aimed to establish the major molecular mechanisms underlying anxiety-related behavior in mice and humans. We used CSDS to study resilience and susceptibility to chronic psychosocial stress in mice. In humans, we used samples from PD patients who underwent exposure-induced panic attacks.

In study II, we investigated gene and protein expression in the BNST and blood cells of mice subjected to CSDS. We further followed our analyses with integrative pathway analyses and comparison of mouse and human blood cell gene expression data. Information on BNST gene expression was further used in study III (see Fig. 9).

In study III, following CSDS, we analyzed gene expression data from three brain regions, specifically the PFC_M, the HIP_V, and the BNST, followed by GSEA and data integration of all three structures. To compare and contrast the results obtained from different -omics platforms in studies II and III, different criteria to define DE genes were selected than in the original article (III) (i.e., $P < 0.05$ and $|FC| \geq 1.2$ instead of the top 300 genes). However, as both criteria are relative, not simultaneously exclusive, and lead to the same conclusions, only the former are presented below. In addition to comparing stress-resilient and stress-susceptible mice to the same-strain controls (included in study III), this work also presents the DE profiles for the stress-susceptible vs stress-resilient comparisons.

For clarity, the data sets are also thereafter referred to by their letters (see Fig. 9).

5.2.1 The effect of genetic background on behavioral response to chronic stress (studies II and III)

To establish the effect of genetic background on the behavioral response to chronic psychosocial stress, we subjected mice from four inbred strains (129, BALB, D2, and B6) to 10-day CSDS. Subsequently, to assess their SA phenotype, we performed the SA test 24 hours after the last CSDS session. As the studied strains differed in their baseline social behavior during the SA test, we evaluated the behavior of the defeated mice individually for each strain by comparing them to the same-strain controls. We then assigned the defeated mice with SI ratios within and above one standard deviation from the same-strain control mean as stress-resilient (i.e., behaviorally resembling controls). The remaining defeated mice, or those with SI ratios below one standard

deviation from the mean, were defined as stress-susceptible. In both studies, we observed a distinct response to chronic stress, detected as the differences in distribution of susceptible and resilient mice, between the compared strains (Fig. 12, Pearson's chi-square, $\chi 2$ = 60.38, P = 7.76E^{-14} and $\chi 2$ = 63.401, P = 1.10E^{-13}, respectively for studies II and III). The B6 and D2 strains, selected for all subsequent analyses, represented the phenotypic extremes for each study as only 30% to 31% of B6 defeated mice, but 89% to 95% of D2 mice, were susceptible to chronic psychosocial stress (Fig. 12 and Fig. 13). In both studies II and III, the susceptible mice from all four strains spent significantly less time in the IZ and significantly more time in the corners during the social target trial than in the no-target trial (Table 13).

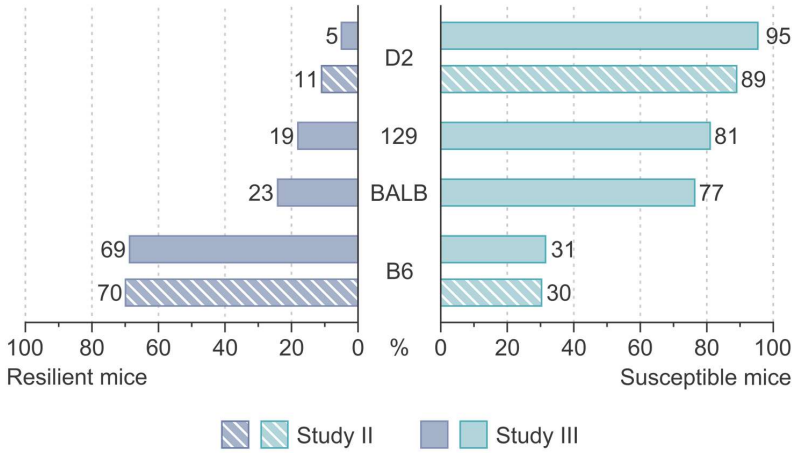

Figure 12. Percentage of mice resilient and susceptible to stress in the four mouse strains subjected to 10-day chronic social defeat stress (CSDS). The bars show the proportion of resilient (left) and susceptible (right) mice in each strain and study. *n* (study II) = D2: Susceptible = 62, Resilient = 8; B6: Susceptible = 34, Resilient = 78; *n* (study III) = D2: Susceptible = 40, Resilient = 2; 129: Susceptible = 13, Resilient = 3; BALB: Susceptible = 33, Resilient = 10; B6: Susceptible = 32, Resilient = 70; 129: 129S2/SvPasCrl; B6: C57BL/6NCrl; BALB: Balb/cAnNCrl; D2: DBA/2NCrl strain.

To further determine the influence of genetic background on response to chronic stress, we assessed the locomotor behavior of the control and defeated mice measured as distance moved during the SA test (Table 13) and OF test (Table 14). While we did not observe differences in distance travelled between the defeated and control 129 and BALB mice in either of the tests, in both studies II and III the B6 and D2 susceptible mice moved significantly less than the same strain-controls during the no-target trial of the SA test. Additionally, in study III, B6 susceptible and D2 resilient mice moved less than the same-strain controls in the OF test. In study II, D2

resilient mice moved significantly more than D2 susceptible mice, however, we did not observe a similar difference in the B6 strain. This result was not validated in study III, most likely due to the small number of animals per group.

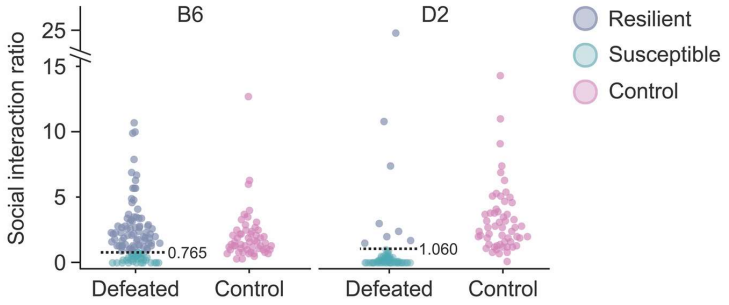

Figure 13. Social interaction (SI) ratios in the social avoidance (SA) test of the B6 and D2 strains subjected to 10-day CSDS in study II. SI ratio border values for the B6 and D2 strains are marked with dotted lines. *n* = B6: Susceptible = 34, Resilient = 78, Control = 56; D2: Susceptible = 62, Resilient = 8, Control = 56. Outliers criterion: IQR > 3. B6: C57BL/6NCrl; CSDS: Chronic social defeat stress; D2: DBA/2NCrl strain; IQR: interquartile range; SA: Social avoidance.

To assess if chronic psychosocial stress affects despair behavior and anxiety-like behavior, we performed the forced swim test (FST) and elevated zero maze (EZM), respectively. Susceptible mice showed increased anxiety-like, but not despair, behavior compared to the controls (Table 14). Furthermore, the latency to immobility during the FST, used as a measure of active stress coping (Commons et al., 2017; Anyan and Amir, 2018), was highly correlated with the SI ratio in the D2 defeated mice but not in the same-strain control group or the B6 control or defeated mice (Table 14). This suggests that defeated D2 mice with higher resilience to CSDS also showed a more active coping strategy than mice with higher SA.

Table 13. Summary of main behavioral results obtained during social avoidance (SA) test performed after 10 days of chronic social defeat stress (CSDS).

Study	Analysis	Description of the statistical test	Value	Mouse strain: B6			D2			129			BALB		
				Con	Res	Sus	Con	Res	Sus						
II	Time in IZ (s)	Mixed ANOVA (phenotype*trial), *post hoc* comparison of no-target and target trials	*n*	34[a]	78[a]	56[a]	56	8	62	N/A					
			P	**8.98E-08**	**2.03E-17**	**2.50E-04**	**2.33E-11**	**0.003**	**1.26E-11**						
			t	-24.1	-33.2	13.4	-36.6	-17.6	25.3						
	Time in corners (s)		*P*	0.332	0.210	**0.001**	**5.37E-08**	0.626	**2.20E-05**						
			t	3.8	5.0	-23.8	20.8	5.9	-21.6						
				Sus vs Con	**Res vs Con**	**Sus vs Res**	**Sus vs Con**	**Res vs Con**	**Sus vs Res**						
	Distance travelled (cm) (no-target trial)	One-way ANOVA (phenotype*trial), post hoc comparison of phenotypes	*P*	**3.00E-03**	**1.80E-05**	0.443	**0.002**	0.178	**0.003**						
			t	157.0	193.1	36.1	207.5	-167.7	-375.2						
				Con	**Res**	**Sus**	**Con**	**Res**	**Sus**	**Con**	**Res**	**Sus**	**Con**	**Res**	**Sus**
III	Time in IZ (s)	Mixed ANOVA (phenotype*trial), *post hoc* comparison of no-target and target trials	*n*	72[a]	70[a]	32[a]	39	2	40	7	3	3	34	10	33
			P	**1.87E-12**	**3.90E-21**	**2.95E-08**	**1.39E-12**	0.128	**3.02E-14**	0.024	0.084	**9.82E-08**	**5.35E-11**	0.018	**4.80E-09**
			t	-21.6	-31.6	24.5	-29.1	-13.8	31.8	-26.7	-25.3	77.9	-37.6	-18.4	32.8
	Time in corners (s)		*P*	0.135	0.017	**2.99E-09**	0.065	0.115	**2.43E-06**	0.147	0.224	**0.003**	0.232	0.269	**1.55E-08**
			t	2.6	6.2	-28.4	7.2	-23.1	-26.2	12.3	10.2	-33.7	-2.5	-2.9	-38.9
				Sus vs Con	**Res vs Con**	**Sus vs Res**	**Sus vs Con**	**Res vs Con**	**Sus vs Res**	**Sus vs Con**	**Res vs Con**	**Sus vs Res**	**Sus vs Con**	**Res vs Con**	**Sus vs Res**
	Distance travelled (cm) (no-target trial)	One-way ANOVA (phenotype*trial), post hoc comparison of phenotypes	*P*	**7.23E-05**	**1.11E-08**	**0.006**	**0.031**	**1.80E-06**	0.552	0.901	0.224	0.444	0.628	0.804	0.516
			t	179.5	335.5	156.0	384.8	280.4	-104.5	19.8	133.4	113.6	59.3	-20.7	-80.0

[a] Control, resilient, and susceptible B6 mice included in the SA test of studies II and III are partially overlapping as 12 controls, 16 resilient, and 5 susceptible mice are identical between the groups.

All P-values (*P*) exceeding the statistical threshold for significance after adjustment for multiple testing ($P < 0.0167$) are written in bold. 129: 129S2/SvPasCrl; B6: C57BL/6NCrl; BALB: Balb/cAnNCrl; Con: Control; CSDS: Chronic social defeat stress; D2: DBA/2NCrl; IZ: Interaction zone; *n*: Number of animals in each group; Res: Resilient; SA: Social avoidance; Sus: Susceptible; *t*: Mean difference.

Table 14. Summary of main behavioral results obtained during forced swim test (FST), elevated zero maze (EZM), and open field test performed after 10 days of chronic social defeat stress (CSDS).

Test	Study	Analysis	Description of statistical test	Value	Mouse strain: B6			D2		129			BALB		
					Control	Defeated		Control	Defeated						
FST[a]	II	Immobility time during min 2-6	One-way ANOVA (phenotype*trial), post hoc comparison of phenotypes	*n*	28	53		8	6						
				P	0.691	0.852		0.759	**0.009**						
				t	-0.1	0.0		-0.130	0.920						
					Sus vs Con	**Res vs Con**	**Sus vs Res**								
	III	Immobility time during min 2-6	One-way ANOVA (phenotype*trial), post hoc comparison of phenotypes	*n*	Con = 28, Res =32, Sus = 21										
				P	0.265	0.278	0.882								
				t	15.74	13.71	2.031								
					Sus vs Con	**Res vs Con**	**Sus vs Res**								
EZM	III	Time in open zones (s)	One-way ANOVA (phenotype*trial), post hoc comparison of phenotypes	*n*	Con = 20, Res =29, Sus = 11										
				P	**0.004**	0.088	0.077								
				t	-19.0	-8.4	-10.6								
					Sus vs Con	**Res vs Con**	**Sus vs Res**	**Sus vs Con**		**Sus vs Con**	**Res vs Con**	**Sus vs Res**	**Sus vs Con**	**Res vs Con**	**Sus vs Res**
OF	III	Distance tranvelled (cm) during OF test	One-way ANOVA (phenotype*trial), post hoc comparison of phenotypes or Independent t-test	*n*	Con = 20, Res =19, Sus = 4			Con = 19, Sus = 22		Con = 7, Res =3, Sus = 13			Con = 18, Res =6, Sus = 19		
				P	0.328	**0.007**	0.511	**8.0E-04**		0.057	0.404	0.582	0.348	0.739	0.743
				t	-175.4	-293.5	118.1	-209.6		-232.9	-144.8	-88.1	-82.4	-41.7	-40.7

[a] Results included in the studies II and III contain information from the same forced swim test (FST).

All *P*-values (*P*) exceeding the statistical threshold for significance after adjustment for multiple testing ($P < 0.0167$) are written in bold. 129: 129S2/SvPasCrl; B6: C57BL/6NCrl; BALB: Balb/cAnNCrl; Con: Control; D2: DBA/2NCrl; EZM: Elevated zero maze; FST: Forced swim test; IZ: Interaction zone; *n*: Number of animals in each group; OF: Open field; Res: Resilient; Sus: Susceptible; *t*: Mean difference.

To investigate the metabolic effect of chronic psychosocial stress, we weighed all defeated and control mice before and after CSDS. In the B6 strain, chronic stress did not have a significant effect on body weight as both control and defeated mice gained weight throughout the duration of the experiment (mixed-design repeated measures ANOVA, $P = 9.45E^{-46}$ and $P = 2.05E^{-44}$, in studies II and III, respectively). 129 and BALB controls gained weight during CSDS ($P = 0.012$ and $P = 4.90E^{-5}$, respectively), while the weight of the defeated mice in both of these strains did not change. Furthermore, BALB susceptible mice gained significantly less weight than the same-strain controls ($P = 0.006$). Conversely, in the D2 strain, the body weight of all defeated animals decreased during the chronic psychosocial stress (mixed-design repeated measures $P < 0.001$ and $P < 0.004$, in studies II and III, respectively) (Fig. 14).

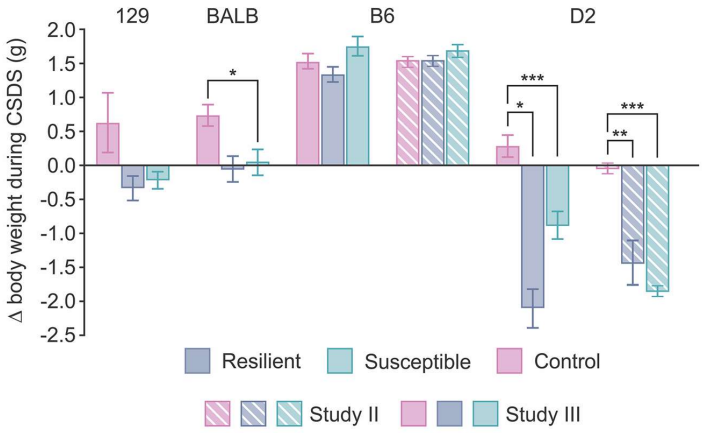

Figure 14. Difference in body weight before and after chronic social defeat stress. The figure shows mean ±1 SEM. * = $P < 0.05$, ** = $P < 0.01$, *** = $P < 0.001$, see text for exact *P*-values. *n* (study II) = B6: Susceptible = 34, Resilient = 77, Control = 55; D2: Susceptible = 55, Resilient = 6, Control = 59; *n* (study III), see Figure 2. Outlier criterion: modified Z-score > 3.5. Outliers (study II): *n* = B6: Resilient = 1, Control = 4; D2: Susceptible = 7, Resilient = 2, Control = 3. Inferential statistical testing by one-way ANOVA with Bonferroni correction. B6: C57BL/6NCrl; CSDS: Chronic social defeat stress; D2: DBA/2NCrl strain.

5.2.2 Differential gene expression in B6 and D2 strains following CSDS (study III)

To detect DE mRNAs (data sets A-C) and to establish which biological pathways are dysregulated following CSDS, we performed gene expression (RNA-seq) profiling in the PFC_M, HIP_V, and BNST. We chose the B6 and D2 strains for these analyses as they represented the phenotypic extremes in their distribution of susceptible and resilient mice following CSDS (Fig. 12 and Fig. 13). In all data sets, we compared the stress-resilient, stress-susceptible, and same-strain control mice. However, we were not able to examine gene expression levels of resilient D2 mice for the PFC_M and HIP_V due to low numbers of resilient animals in those groups. Furthermore, it is important to note that data sets A and B contained seven of the same mice (n = B6: Resilient = 2, Control = 2; D2: Susceptible = 2, Control = 1). Unless specified otherwise, DE thereafter refers to $P < 0.05$ and $|FC| \geq 1.2$.

Genetic background affects differential gene expression in the PFC_M *and* HIP_V *(study III)*

We first examined the transcriptional response in the PFC_M and HIP_V of stress-susceptible B6 and D2 mice and stress-resilient B6 mice. We observed differences in the number of DE genes between the strains in both brain regions (PFC_M, *n* = 1146, B6; *n* = 261, D2; HIP_V, *n* = 6633, B6; *n* = 1474, D2; Fig. 15; see also Fig. 10 for further explanation on how to read Fig. 15-16). In the PFC_M, only 32 (2.3%) of the DE genes were common to the susceptible vs control comparisons in the B6 and D2 strains, with most of them (*n* = 25; 78%) DE in the same direction between the strains. We observed a much larger number of DE genes shared between the strains (*n* = 1376; 20.4%) in the same comparison in the HIP_V. Most of them were common to the B6 resilient vs control (*n* = 1074, 78.0%) and B6 susceptible vs control (*n* = 807; 58.7%) or both (*n* = 588; 42.7%) comparisons. Notably, all of them were DE in the same direction. Taken together, our results suggest that while in the HIP_V the transcriptional profiles are more similarly affected by the chronic psychosocial stress, regardless of the mouse genetic background the strain effect is more prominent in the PFC_M.

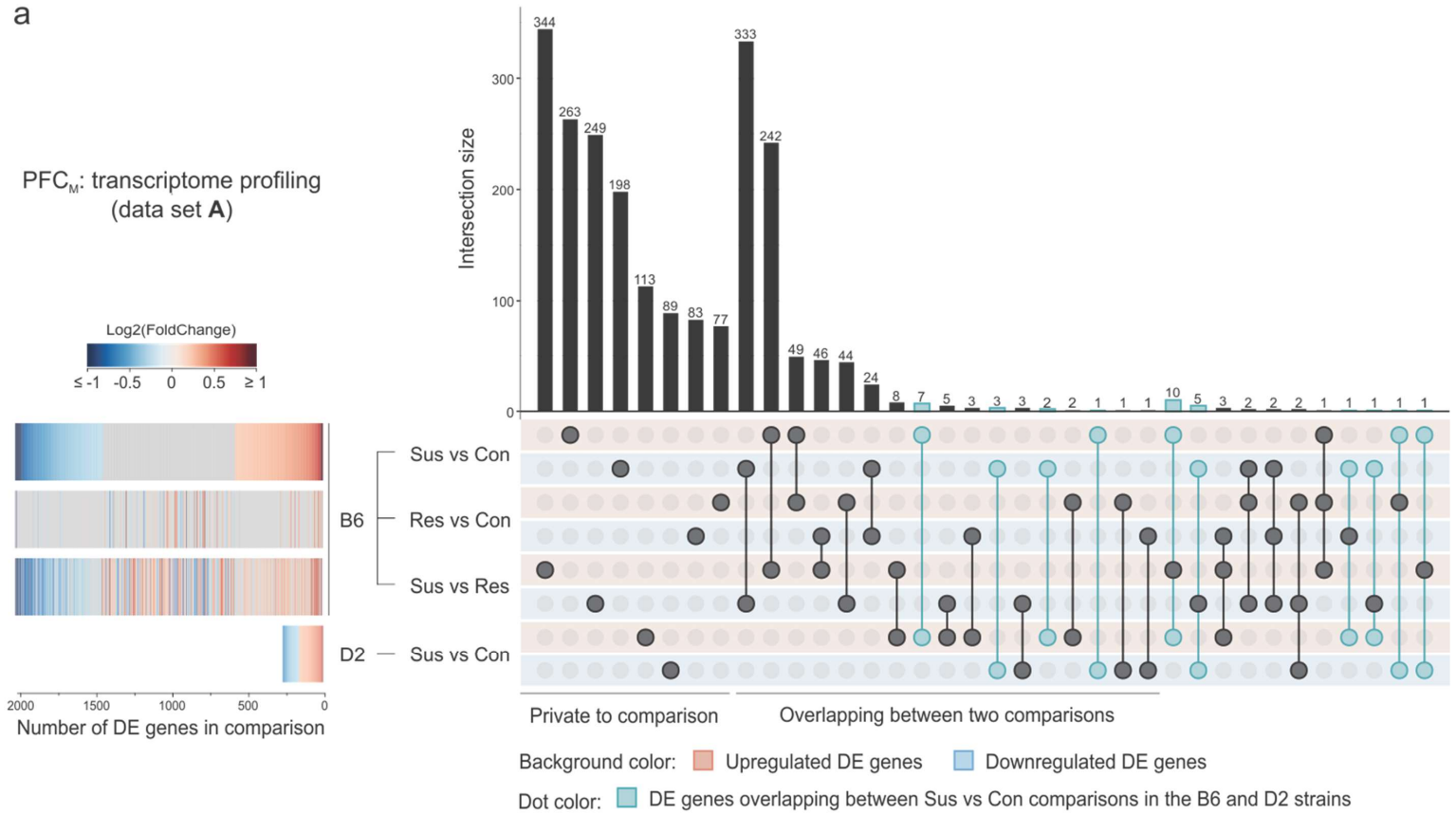

Figure 15. Distinct transcriptional stress response in PFC$_M$ and HIP$_V$ of the D2 and B6 strains subjected to CSDS. Overlap of the DE genes between stress-susceptible, stress-resilient, and control mice in the **(a)** medial prefrontal cortex (PFC$_M$) and **(b)** ventral hippocampus (HIP$_V$). Within the union heatmaps (left), the DE genes are rank-ordered by FC in the susceptible vs control comparison, separately for each strain and –omics data set. B6: C57BL/6NCrl; Con: Control; CSDS: Chronic social defeat stress; D2: DBA/2NCrl; DE: Differentially expressed; PFC$_M$: medial prefrontal cortex; Res: Resilient; Sus: Susceptible; HIP$_V$: ventral hippocampus. See also Fig. 10.

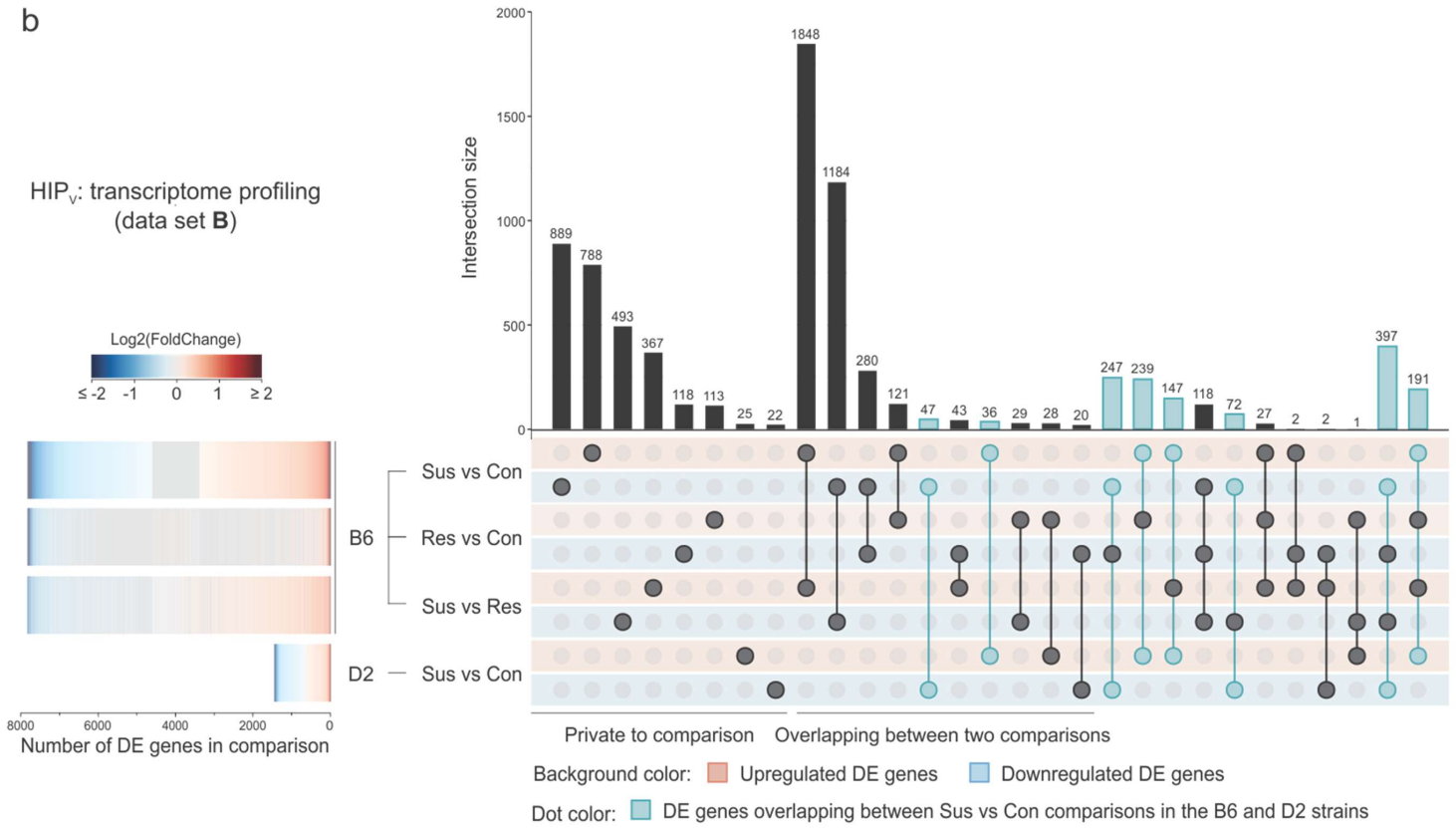

Figure 15. Distinct transcriptional stress response in PFC_M and HIP_V of the D2 and B6 strains subjected to CSDS. Overlap of the DE genes between stress-susceptible, stress-resilient and control mice in the **(a)** medial prefrontal cortex (PFC_M) and **(b)** ventral hippocampus (HIP_V). Within the union heatmaps (left), the DE genes are rank-ordered by FC in the susceptible vs control comparison, separately for each strain and –omics data set. B6: C57BL/6NCrl; Con: Control; CSDS: Chronic social defeat stress; D2: DBA/2NCrl; DE: Differentially expressed; PFC_M: medial prefrontal cortex; Res: Resilient; Sus: Susceptible; HIP_V: ventral hippocampus. See also Fig. 10.

Overlapping DE genes in the BNST show divergent expression profiles in stress-susceptible B6 and D2 mice (studies II and III)

While we detected a similar number of uniquely DE genes (data set C) in the BNST of both B6 and D2 strains (*n* = 1638, B6; *n* = 1441, D2), their overall distribution across the comparisons and the directionality of the expression of the genes common to both strains differed (Fig. 16). In the B6 strain we identified the smallest number of DE genes when comparing the resilient and control groups (*n* = 91, 5.6% of all DE genes). In contrast, in the D2 strain this comparison had the largest number of DE genes (*n* = 483; 35.5% of all DE genes). Within this comparison, only a few DE genes (*n* = 13) were common to both strains. Furthermore, we detected similar numbers of DE genes between the strains in the susceptible vs control comparison (*n* = 884, B6; *n* = 811, D2) with a larger overlap (*n* = 194) between the strains. Importantly, all genes common to both strains were DE in opposite directions and significantly enriched (P_{FDR} < 0.05) for oligodendrocyte, translation, and mitochondria-related gene sets (Table 15) and GO terms (Table 16) in the gene set enrichment and Gene Ontology term enrichment analyses. Overall, our findings show a vastly divergent transcriptional CSDS-induced response in the B6 and D2 strains.

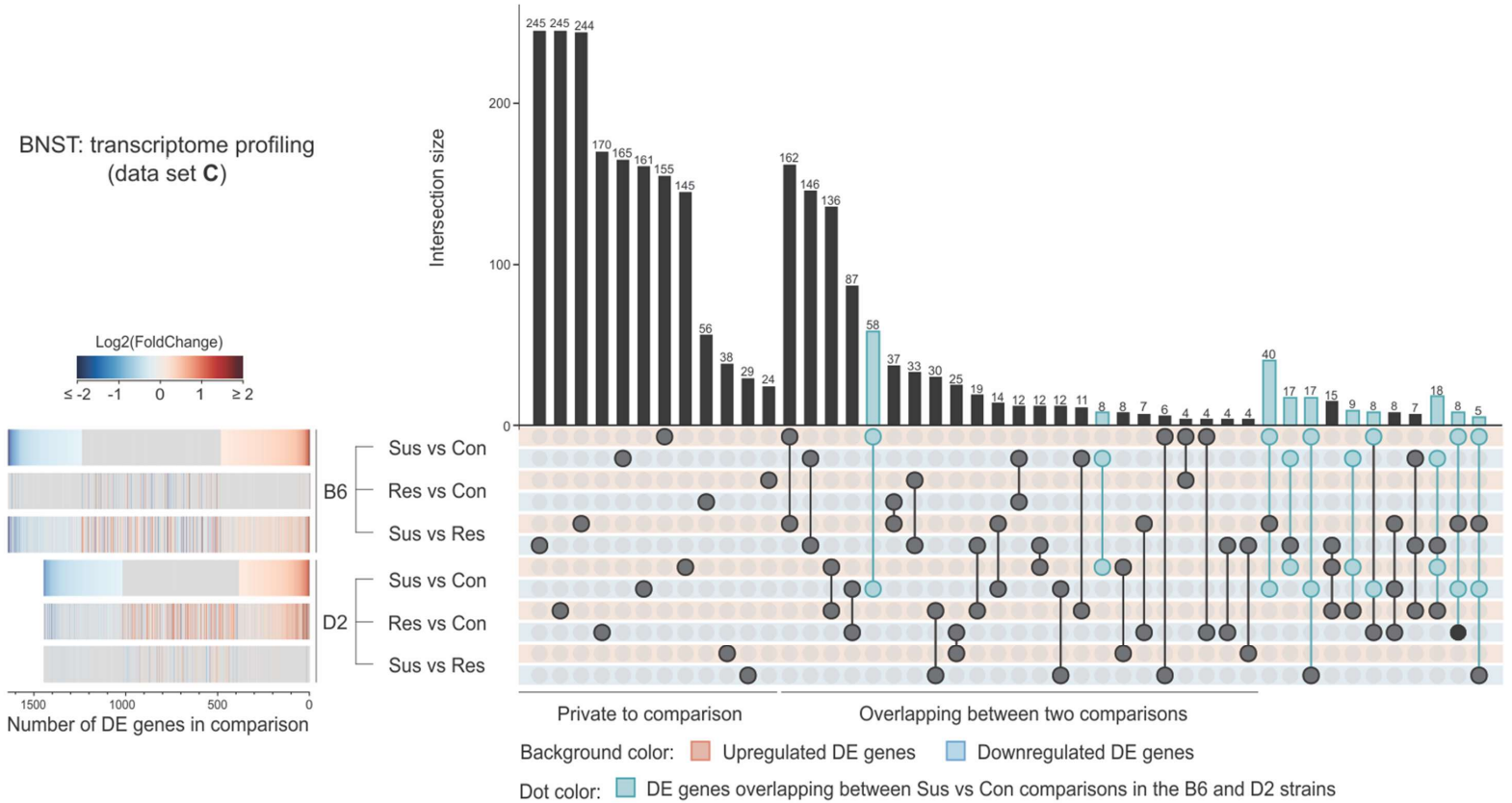

Figure 16. Distinct transcriptional stress response in the BNST of the D2 and B6 strains subjected to CSDS. Overlap of the DE genes between stress-susceptible, stress-resilient, and control mice. Within the union heatmaps (left), the DE genes are rank-ordered by FC in the susceptible vs control comparison, separately for each strain and –omics data set. Intersections including less than four genes are not shown due to space limits. B6: C57BL/6NCrl; BNST: Bed nucleus of the stria terminalis; Con: Control; CSDS: Chronic social defeat stress; D2: DBA/2NCrl; DE: Differentially expressed; Res: Resilient; Sus: Susceptible. See also Fig. 10.

Table 15. Top 30 significantly enriched gene sets (P_{FDR} < 0.05) for the DE genes overlapping between the BNST B6 and D2 susceptible vs control comparisons (data set C).

Source	Gene set name	Number of genes in gene set (K)	Number of DE genes in gene set (k)	k/K	*P*	P_{FDR}
Hsiao	Housekeeping genes	389	37	0.095	2.31E-41	1.10E-37
Blalock	Alzheimer's disease (down)	1237	42	0.034	1.32E-28	3.14E-25
KEGG	Ribosome	88	14	0.159	2.05E-19	3.25E-16
Kim	Bipolar disorder oligodendrocyte density correlation (up)	682	26	0.038	4.97E-19	5.91E-16
Martens	Tretinoin response (down)	841	28	0.033	6.67E-19	6.36E-16
KEGG	Parkinson's disease	133	15	0.113	2.25E-18	1.78E-15
Mootha	VOXPHOS	87	13	0.149	9.71E-18	6.61E-15
Pujana	*BRCA1* -PCC network	1652	35	0.021	2.60E-17	1.55E-14
Reactome	Influenza life cycle	203	16	0.079	5.36E-17	2.83E-14
KEGG	Alzheimer's disease	169	15	0.089	8.74E-17	3.78E-14
Reactome	Influenza viral RNA transcription and replication	169	15	0.089	8.74E-17	3.78E-14
Spielman	Lymphoblast European vs Asian (up)	479	21	0.044	9.53E-17	3.78E-14
Tien	Intestine probiotics 6 hr (up)	55	11	0.200	1.09E-16	3.99E-14
Reactome	Nonsense mediated decay enhanced by the exon junction complex	176	15	0.085	1.61E-16	5.49E-14
Reactome	SRP-dependent cotranslational protein targeting to membrane	179	15	0.084	2.08E-16	6.61E-14
KEGG	Huntington's disease	185	15	0.081	3.42E-16	1.01E-13
Mootha	Mitochondria	447	20	0.045	3.63E-16	1.01E-13
Reactome	Metabolism of RNA	330	18	0.055	3.80E-16	1.01E-13
Reactome	Metabolism of mRNA	284	17	0.060	5.58E-16	1.40E-13
Reactome	Peptide chain elongation	153	14	0.092	6.22E-16	1.48E-13
Kim	All disorders oligodendrocyte number correlation (up)	756	24	0.032	7.45E-16	1.69E-13
Pujana	*CHECK2* -PCC network	779	24	0.031	1.44E-15	3.12E-13
Mootha	*PGC*	420	19	0.045	1.69E-15	3.50E-13
Reactome	Respiratory electron transport ATP synthesis by chemiosmotic coupling and heat production by uncoupling proteins	98	12	0.122	2.20E-15	4.37E-13
KEGG	Oxidative phosphorylation	135	13	0.096	3.58E-15	6.81E-13
Reactome	3'-UTR mediated translational regulation	176	14	0.080	4.47E-15	8.18E-13
Reactome	Translation	222	15	0.068	5.18E-15	9.14E-13
Reactome	TCA cycle and respiratory electron transport	141	13	0.092	6.34E-15	1.08E-12
Pujana	*ATM* -PCC network	1442	30	0.021	1.07E-14	1.75E-12
Dazard	UV response cluster G1	67	10	0.149	6.34E-14	1.01E-11

Analysis performed with MSigDB v6.0 C2 curated gene sets (Mootha et al., 2003; Subramanian et al., 2005). *ATM*: Ataxia-telangiectasia mutated serine/threonine kinase; B6: C57BL/6NCrl; BNST: bed nucleus of the stria terminalis; *BRCA1*: Breast cancer, DNA repair associated; *CHECK2*: Checkpoint kinase 2; D2: DBA/2NCrl; DE: differentially expressed; PCC: Pearson correlation coefficient; *PGC:* Peroxisome proliferator-activated receptor gamma coactivator 1-alpha (*PPARGC1A*); TCA: Tricarboxylic acid; VOXPHOS: oxidative phosphorylation genes.

Table 16. Top 10 significantly enriched Gene Ontology (GO) terms (P_{FDR} < 0.05) for each GO category within the DE genes overlapping between the BNST B6 and D2 susceptible vs control comparisons (data set C).

GO ID	GO term	GO category	Number of all genes in GO term	Number of DE genes in GO term	*P*	P_{FDR}
GO:0045333	Cellular respiration	Biological processes	134	12	2.37E-09	1.23E-05
GO:0046034	ATP metabolic process	Biological processes	163	13	1.87E-09	1.46E-05
GO:0009141	Nucleoside triphosphate metabolic process	Biological processes	214	14	4.84E-09	1.88E-05
GO:0009199	Ribonucleoside triphosphate metabolic process	Biological processes	193	13	1.26E-08	2.17E-05
GO:0009126	Purine nucleoside monophosphate metabolic process	Biological processes	189	13	9.95E-09	2.21E-05
GO:0015980	Energy derivation by oxidation of organic compounds	Biological processes	194	14	1.48E-09	2.29E-05
GO:0009161	Ribonucleoside monophosphate metabolic process	Biological processes	192	13	1.19E-08	2.31E-05
GO:0009205	Purine ribonucleoside triphosphate metabolic process	Biological processes	189	13	9.95E-09	2.58E-05
GO:0009144	Purine nucleoside triphosphate metabolic process	Biological processes	198	13	1.68E-08	2.61E-05
GO:0009167	Purine ribonucleoside monophosphate metabolic process	Biological processes	188	13	9.38E-09	2.91E-05
GO:0098800	Inner mitochondrial membrane protein complex	Cellular component	135	21	6.33E-20	1.24E-16
GO:0044455	Mitochondrial membrane part	Cellular component	216	23	2.22E-18	2.16E-15
GO:0005743	Mitochondrial inner membrane	Cellular component	398	27	8.76E-17	5.70E-14
GO:0043209	Myelin sheath	Cellular component	212	21	2.76E-16	1.35E-13
GO:0019866	Organelle inner membrane	Cellular component	440	27	9.10E-16	3.55E-13
GO:0098798	Mitochondrial protein complex	Cellular component	264	22	1.47E-15	4.78E-13
GO:0005740	Mitochondrial envelope	Cellular component	617	30	7.39E-15	2.06E-12
GO:0070469	Respiratory chain	Cellular component	89	14	1.01E-13	2.47E-11
GO:0031966	Mitochondrial membrane	Cellular component	575	27	4.15E-13	9.01E-11
GO:0044429	Mitochondrial part	Cellular component	799	31	8.00E-13	1.56E-10
GO:0003954	NADH dehydrogenase activity	Molecular function	29	7	1.30E-08	1.97E-05
GO:0050136	NADH dehydrogenase (quinone) activity	Molecular function	26	7	6.81E-09	3.09E-05
GO:0016655	Oxidoreductase activity, acting on NAD(P)H, quinone or similar compound as acceptor	Molecular function	37	7	5.67E-08	6.43E-05
GO:0009055	Electron transfer activity	Molecular function	68	8	1.74E-07	1.57E-04
GO:0015078	Proton transmembrane transporter activity	Molecular function	116	9	7.74E-07	5.85E-04
GO:0016676	Oxidoreductase activity, acting on a heme group of donors, oxygen as acceptor	Molecular function	21	5	1.80E-06	9.08E-04
GO:0016675	Oxidoreductase activity, acting on a heme group of donors	Molecular function	22	5	2.20E-06	9.96E-04
GO:0004129	Cytochrome-c oxidase activity	Molecular function	21	5	1.80E-06	1.02E-03
GO:0015002	Heme-copper terminal oxidase activity	Molecular function	21	5	1.80E-06	1.17E-03
GO:0016651	Oxidoreductase activity, acting on NAD(P)H	Molecular function	80	7	6.47E-06	2.67E-03

Analysis performed with topGO R package (Alexa et al., 2006). ATP: Adenosine triphosphate; B6: C57BL/6NCrl; BNST: bed nucleus of the stria terminalis; D2: DBA/2NCrl; DE: differentially expressed; GO: Gene ontology; NAD(P)H: Nicotinamide adenine dinucleotide.

5.2.3 Oligodendrocyte-related genes are differentially expressed after CSDS (study III)

We performed GSEA to identify biological pathways and gene sets affected by chronic psychosocial stress in the PFC_M, HIP_V, and BNST. We identified five gene sets significantly enriched ($P_{FRD} < 0.05$) in at least two comparisons and all analyzed brain structures (Fig. 17), of which ageing and oligodendrocyte (OLG)-related were the most prominent. Notably, both of the aging-related gene sets consisted of a functionally diverse group of genes ($n = 301$), which were also significantly overrepresented in the "Lein: Oligodendrocyte markers" gene set ($P_{FDR} = 1.2E^{-16}$). We further investigated the oligodendrocyte-related genes to determine if OLG progenitor cells (OPCs) or mature OLGs cell populations predominantly contributed to the observed dysregulation of the gene sets of interest. The transcriptomic profiles associated with chronic psychosocial stress were stronger in mature OLG markers (Fig. 18), a finding which was further validated with q-RT-PCR by investigating the expression of five markers of mature OLG (*Opalin*, *Ermn*, *Mbp*, *Mobp*, and *Plp1*).

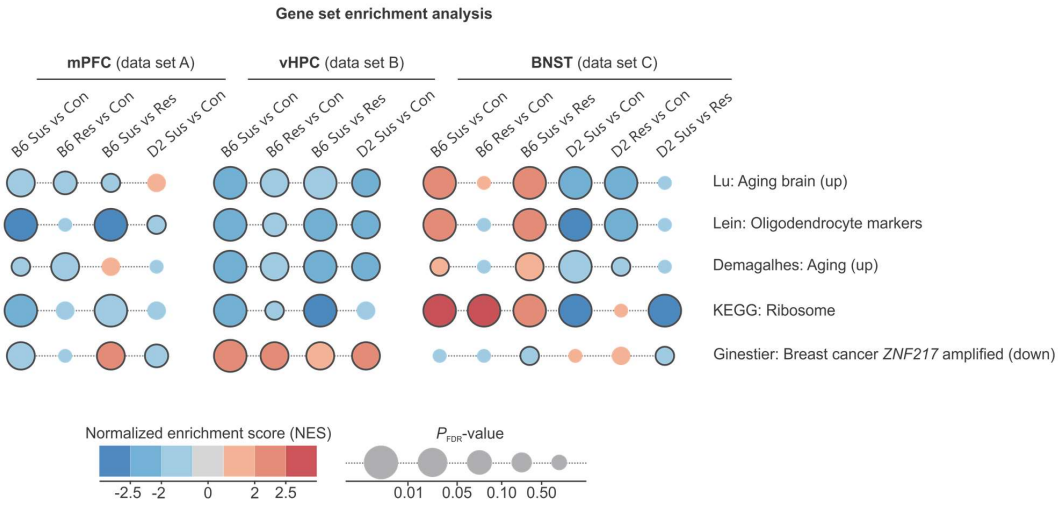

Figure 17. Converging gene set enrichment analysis (GSEA) shows dysregulation of aging and oligodendrocyte-related gene set. Heatmap showing the top five enriched gene sets overlapping between PFC_M, HIP_V, and BNST in the stress-susceptible and resilient mice in comparison to same-strain controls. A positive (or negative) NES indicates overrepresentation at the top (or bottom, respectively) of the ranked list of upregulated (or downregulated, respectively) genes. Gene sets are ordered by P_{FDR}-value and frequency. P_{FDR}-values < 0.25 are marked with black outlines around the circles. B6: C57BL/6NCrl; BNST: bed nucleus of the stria terminalis; Con: control; D2: DBA/2NCrl; HIP_V: ventral hippocampus; PFC_M: medial prefrontal cortex; NES: normalized enrichment score; Res: resilient; Sus: susceptible.

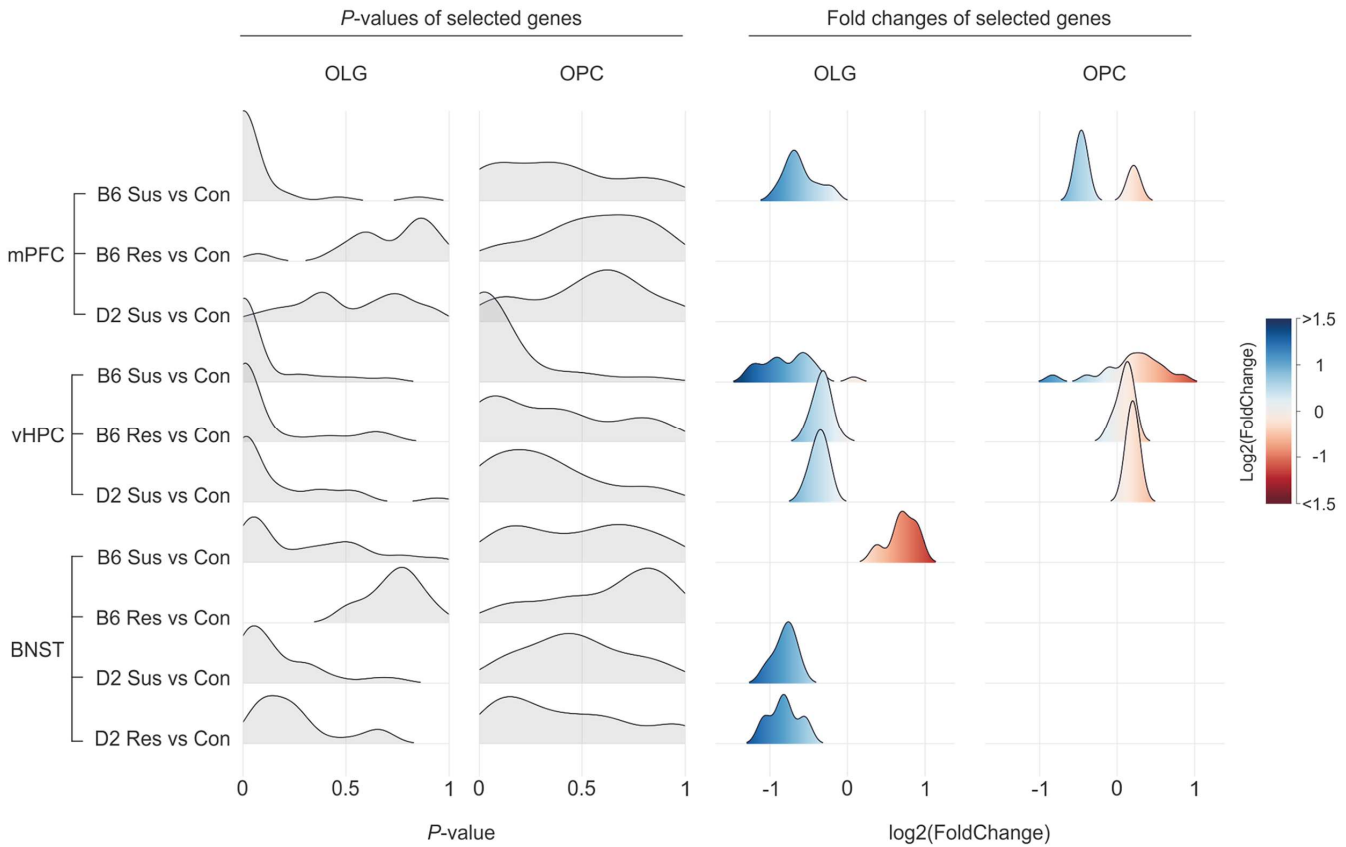

Figure 18. Mature oligodendrocytes (OLGs), rather than oligodendrocyte progenitor cells (OPCs), predominantly contribute to the observed differentially expressed pathways following chronic psychosocial stress. Combined density plots showing the significance (*P*-values) and expression FC (log2FoldChange; for $P < 0.05$) of OLG-specific and OPC-specific genes in the PFC_M, HIP_V, and BNST susceptible vs control and resilient vs control comparisons. B6: C57BL/6NCrl; BNST: bed nucleus of the stria terminalis; Con: control; D2: DBA/2NCrl; HIP_V: ventral hippocampus; PFC_M: medial prefrontal cortex; OPC: oligodendrocyte progenitor cells; OLG: (mature) oligodendrocytes; Res: resilient; Sus: susceptible.

Our analyses showed a high correlation between the RNA-seq and q-RT-PCR results in all three brain structures and comparisons (mean r = 0.82). Furthermore, we did not observe any significant main effect of the group (susceptible, resilient, or control mice) on expression levels of any of the five genes in the whole cortex (without PFC_M) or dorsal hippocampus as measured by q-RT-PCR (mixed ANOVA, B6, $P \geq 0.423$; D2, $P \geq 0.060$). While in the hypothalamus we observed lower expression of *Opalin* in the D2 susceptible mice in comparison to the same-strain controls (Student's t-test, $P = 0.006$), the expression levels of all other investigated genes did not differ within any of the other regions. Lastly, we detected no differences in the thickness of the corpus callosum between any of the groups in either strain after CSDS (*post hoc* by Fisher's LSD, $P = 1.000$), as measured in brain sections stained with an anti-CNPase myelin-binding antibody.

5.2.4 Susceptibility to chronic psychosocial stress in the BNST is associated with myelin thickness in the B6 strain (study III)

We next aimed to establish if the observed OLG-related differences in gene expression after CSDS (see Fig. 17 and 18) could be associated with alterations in axon myelination. To do so, we performed TEM of myelinated axons (Fig. 18a) in the PFC_M, HIP_V, and BNST of B6 and D2 mice (data set F). We analyzed stress-susceptible, stress-resilient, and same-strain control mice. The information below includes only a summary of the author's own BNST results.

We observed strain-specific differences between the groups in myelin thickness and g ratio (i.e., the ratio of the inner axonal diameter to the outer axonal diameter). Specifically, the B6 susceptible mice had thicker myelin in the BNST compared to resilient mice ($P = 2.67E^{-7}$). As different types of axonal projections are known to differ in axon diameter (Innocenti and Caminiti, 2017), we subsequently subdivided the axons into three size groups, specifically small, medium, and large axons (diameter: small < 0.52 µm, medium = 0.52-0.81 µm, and large > 0.81 µm; see also section 4.5). We found thicker myelin in the axons of medium size in the B6 susceptible group in comparison to the controls and resilient mice ($P = 0.002$ and $P = 0.001$, respectively). Concurrent to myelin thickness, we observed a smaller g ratio (see section 4.5) in the susceptible mice than those of the controls and the resilient mice ($P = 3.33E^{-4}$ and $P = 3.11E^{-11}$, respectively).

5.2.5 Differential protein and miRNA expression in the BNST following CSDS (study II)

To establish which biological pathways are dysregulated in the BNST following CSDS on both transcriptome and proteome levels, we further performed proteomic profiling via liquid chromatography-tandem mass spectrometry (data set D) in study II. As in the BNST gene expression experiment (data set C), we chose the B6 and D2 strains for these analyses as they represented the phenotypic extremes in their distribution of susceptible and resilient mice following CSDS (Fig. 12 and Fig. 13). Moreover, in the BNST of the B6 strain, we performed AGO2 RNA immunoprecipitation-sequencing (AGO2 RIP-seq) of active microRNAs (miRNAs) and their mRNA targets (data sets G and H, respectively). In all data sets, we compared the stress-resilient, stress-susceptible, and same-strain control mice. Data sets C and D were collected from the same cohorts of animals, with each cohort being equally divided by the SI ratios between both transcriptomic and proteomic experiments. Data sets G and H (AGO2 RIP-seq) were prepared from much larger amounts of starting material and therefore required an additional cohort of animals.

Distinct differences in protein abundance after CSDS in the B6 and D2 strains

To test whether the differences in mRNA expression were also present at the protein level, we examined protein abundance in stress-susceptible, stress-resilient, and control B6 and D2 mice. We identified 1191 distinct labeled proteins, of which 9.8% (*n* = 117) showed differences in abundance in at least one of the comparisons in the B6, D2, or both strains (Fig. 19). Furthermore, similarly to the DE genes, only a small number of DE proteins (*n* = 27, 23%) were shared between at least two comparisons within or between the B6 and D2 strains. We found only one protein to be DE between the same comparison (i.e., susceptible vs resilient) in both strains (see Fig. 19; circles marked in purple), namely protein phosphatase 1 regulatory subunit 1B (PPP1R1B), also known as dopamine- and cAMP-regulated neuronal phosphoprotein (DARPP-32). PPP1R1B was expressed at a lower level in the B6 susceptible mice and at a higher level in the D2 mice in comparison to their respective same-strain resilient groups. Taken together, we identified discrete changes in protein abundance after CSDS in the B6 and D2 strains.

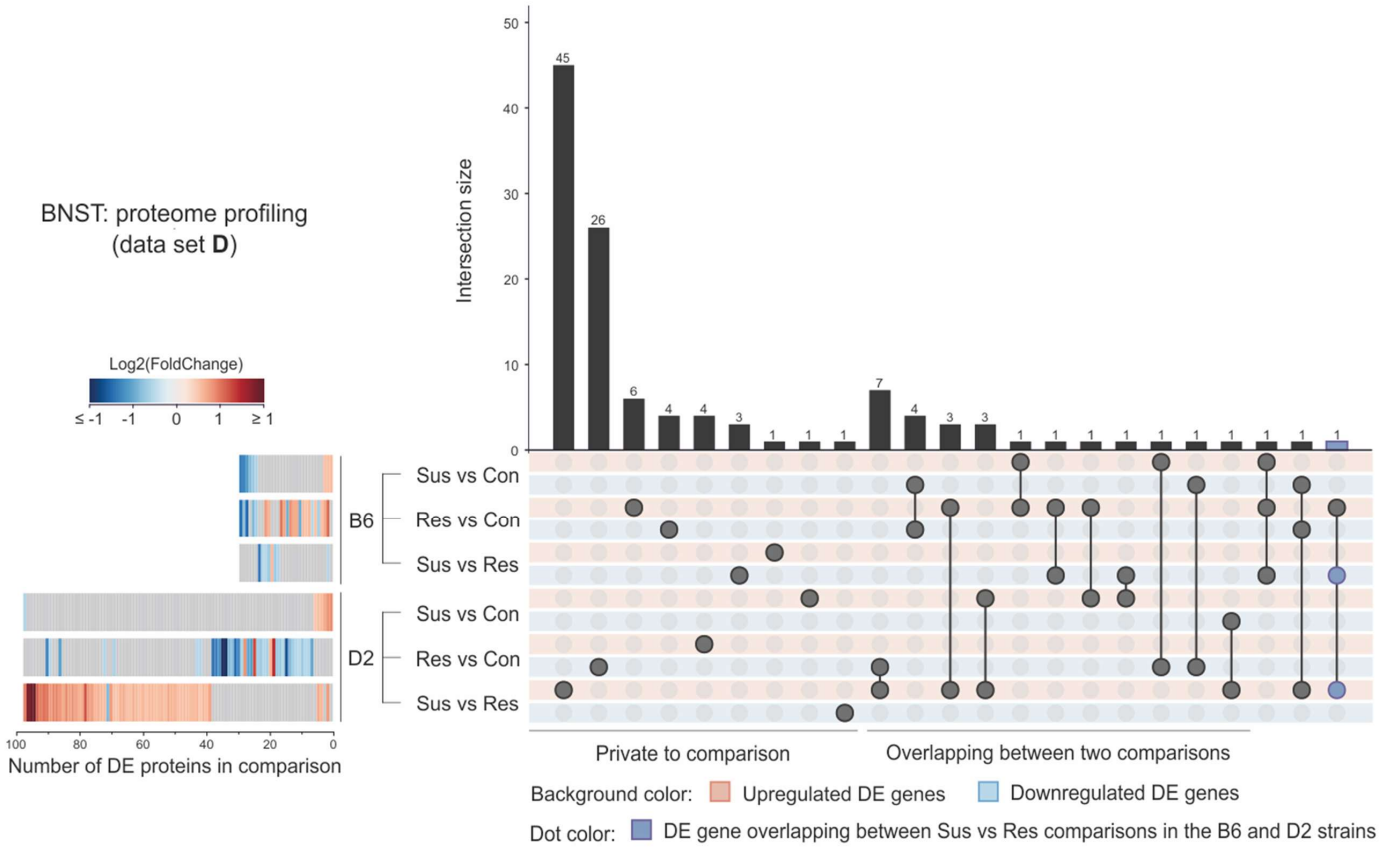

Figure 19. Discrete proteome profiles in the BNST of the D2 and B6 mice subjected to CSDS. Overlap of the DE proteins between stress-susceptible, stress-resilient, and control mice. Within the union heatmaps (left), the DE genes are rank-ordered by FC in the susceptible vs control comparison, separately for each strain and –omics data set. B6: C57BL/6NCrl; BNST: Bed nucleus of the stria terminalis; Con: Control; CSDS: Chronic social defeat stress; D2: DBA/2NCrl; DE: Differentially expressed; Res: Resilient; Sus: Susceptible. See also Fig. 10.

Isolation of active miRNAs and their mRNA targets in the BNST

Comprehensive tissue and gene-specific analyses have previously shown that, in general, only 30% to 40% of variance in protein abundance can be accounted for by mRNA expression due to translational, protein-degradation, and post-transcriptional processes (e.g., regulation by non-coding RNAs such as miRNAs) (Vogel and Marcotte, 2012; Bauernfeind and Babbitt, 2017). To isolate and study stress-responsive miRNAs and their bound mRNA targets, we performed AGO2 RNA immunoprecipitation-sequencing (AGO2 RIP-seq) in the B6 strain. Although the numbers of identified DE miRNAs were similar between all analyzed comparisons (*n* = 142, B6 susceptible vs control; *n* = 150, B6 resilient vs control; *n* = 112, B6 susceptible vs resilient; Fig. 20a), the numbers of their DE mRNA targets were not (*n* = 2994, B6 susceptible vs control; *n* = 2075, B6 resilient vs control; *n* = 487, B6 susceptible vs resilient; Fig. 20b). Notably, almost all detected DE miRNAs and mRNAs shared between the susceptible vs control and resilient vs control comparisons were expressed in the same direction (95.1% and 100%, respectively, for common DE miRNAs and mRNAs). Overall, although the DE miRNA profiles were largely private to the comparisons, the profiles common to both were expressed in the same direction, thus indicating a shared stress-related response in both the resilient and the susceptible mice.

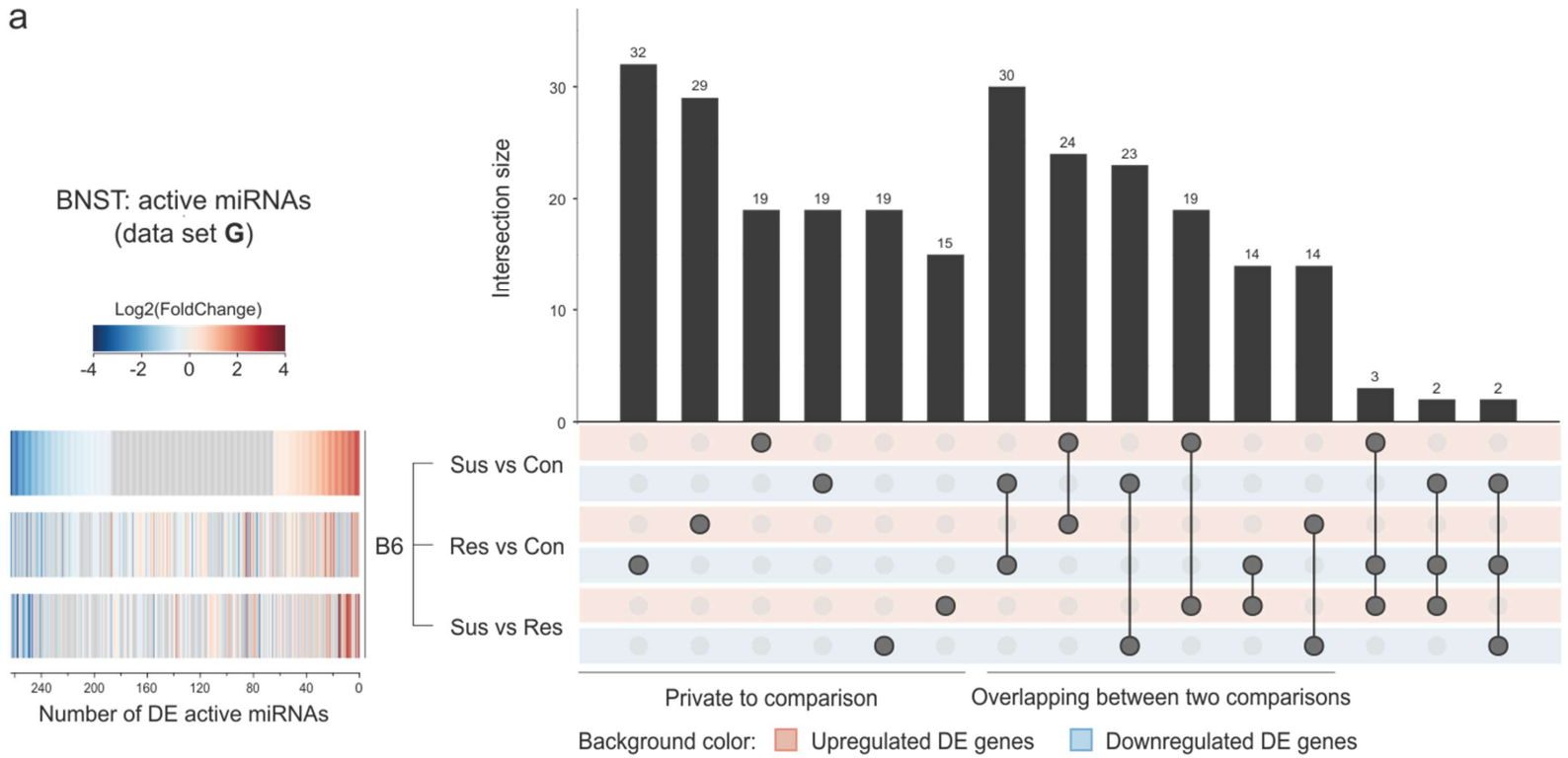

Figure 20. Stress-responsive miRNAs and their mRNA targets in the BNST of the B6 mice after CSDS. Overlap of the active AGO2-associated DE **(a)** miRNAs and their **(b)** bound mRNA targets between stress-susceptible, stress-resilient, and control B6 mice. Within the union heatmaps (left), the DE miRNAs and mRNAs are rank-ordered by FC in the susceptible vs control comparison, separately for each strain and –omics data set. B6: C57BL/6NCrl; BNST: Bed nucleus of the stria terminalis; Con: Control; CSDS: Chronic social defeat stress; D2: DBA/2NCrl; DE: Differentially expressed; Res: Resilient; Sus: Susceptible. See also Fig. 10.

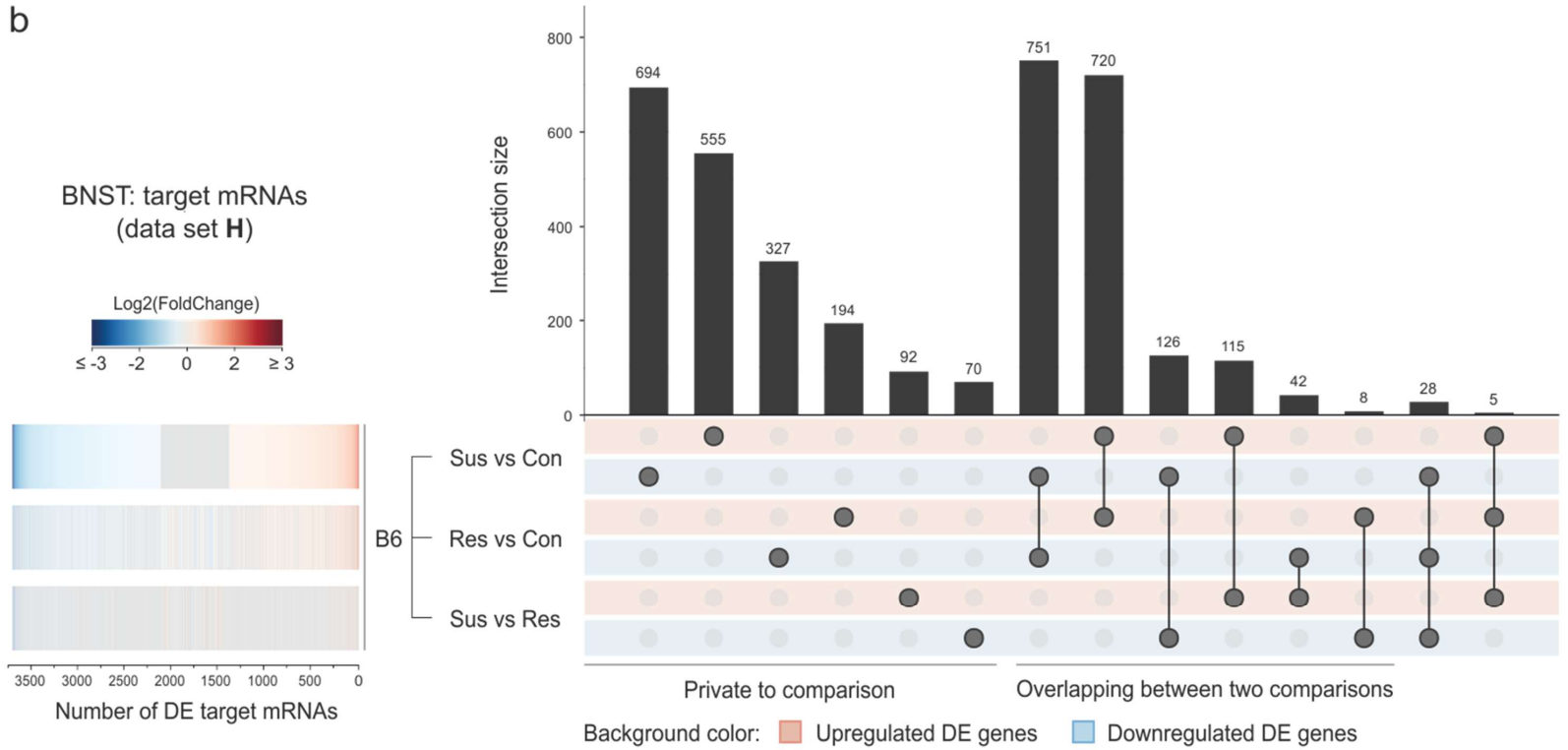

Figure 20. Stress-responsive miRNAs and their mRNA targets in the BNST of the B6 mice after CSDS. Overlap of the active AGO2-associated DE **(a)** miRNAs and their **(b)** bound mRNA targets between stress-susceptible, stress-resilient, and control B6 mice. Within the union heatmaps (left), the DE miRNAs and mRNAs are rank-ordered by FC in the susceptible vs control comparison, separately for each strain and –omics data set. B6: C57BL/6NCrl; BNST: Bed nucleus of the stria terminalis; Con: Control; CSDS: Chronic social defeat stress; D2: DBA/2NCrl; DE: Differentially expressed; Res: Resilient; Sus: Susceptible. See also Fig. 10.

5.2.6 DE genes and proteins in the BNST are enriched for gene sets and biological pathways engaged in translational control and mitochondrial function (study II)

To establish which biological pathways were dysregulated by CSDS, we performed GSEA and Ingenuity Pathway Analysis (IPA) of transcriptomic and proteomic data sets (C and D, respectively). We observed 16 top significantly dysregulated ($P < 0.05$) canonical pathways common to at least one-third of the comparisons in both data sets combined (Fig. 21a) and four top significantly enriched gene sets (Fig 21b; $P_{FDR} < 0.25$, in accordance with recommended stringency threshold by Subramanian et al. 2005) common to at least half of the comparisons. We found several significantly dysregulated mitochondria-related and Ca^{2+} and cAMP-mediated signaling canonical pathways, genes, or both. Interestingly, at the transcriptome level, the oxidative phosphorylation pathway was expressed at a higher level in the B6 (Z-score = 4.90, $P = 1.55E^{-11}$) but on a lower level in the D2 (Z-score = -5.57, $P = 1.59E^{-9}$) susceptible mice in comparison to the same-strain controls. An analogous pattern of expression was observed in the same comparison for the eIF2 signaling pathway (B6, Z-score = 4.36, $P = 5.46E^{-11}$; D2, Z-score = -3.46, $P = 8.40E^{-5}$). Furthermore, the Protein Kinase A and the dopamine-DARPP32 feedback in cAMP signaling pathways were upregulated at the protein level in the B6 resilient vs control mice ($P = 2.21E^{-6}$ and $P = 2.14E^{-5}$, respectively) and the D2 susceptible group in comparison to the D2 resilient one ($P = 1.42E^{-4}$ and $P = 1.10E^{-4}$, respectively). Overall, our findings show significant genetic background-specific dysregulation of pathways related to mitochondrial function and transcriptional control after CSDS.

Beta-estradiol, testosterone, and RICTOR predicted as shared upstream regulators of DE genes

To determine the transcriptional regulators behind the detected differences in gene and protein expression in the BNST, we conducted IPA Upstream Regulator Analysis (QIAGEN Inc., 2018). The purpose of the analysis is to examine the data sets for known targets of transcription regulators and compare the directionality of the gene expression to the information included in the Ingenuity Knowledge Base. Within the beta-estradiol cluster, the target genes were predicted to be significantly downregulated at both the transcriptome and proteome level in the B6 and D2 resilient mice in comparison to the controls (B6, $P = 0.002$ and $P = 0.010$; D2, $P = 1.08E^{-5}$, $P = 0.015$).

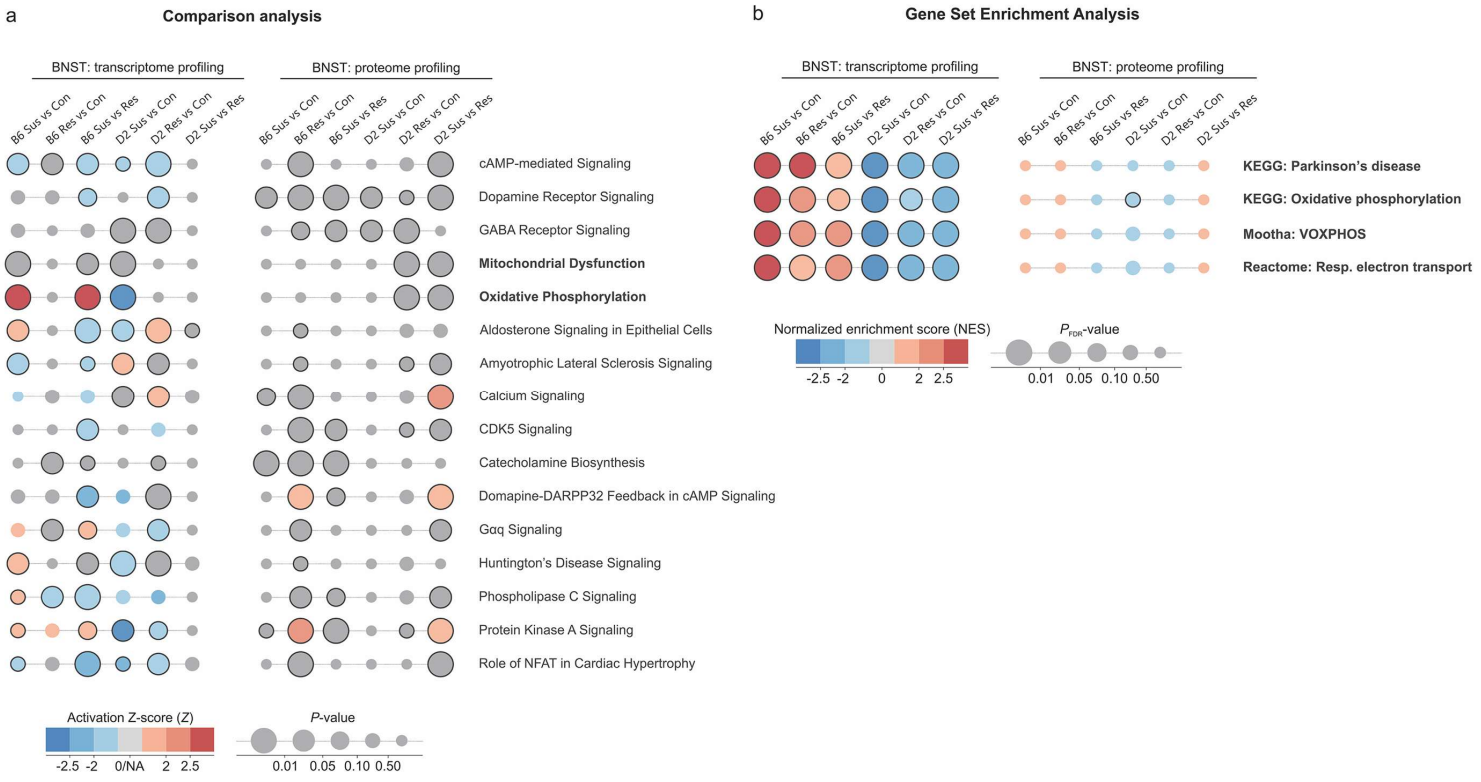

Figure 21. BNST transcriptomic and proteomic analyses implicate dysregulation of mitochondria-related and Ca^{2+} and cAMP-mediated gene sets and canonical pathways in the following CSDS. (a) Merged heatmap showing the top 16 overlapping canonical pathways ($P < 0.25$ indicated by a black outline) and **(b)** top four gene sets (P_{FDR}-values < 0.25 indicated by a black outline). Mitochondria-related pathways and gene sets are written in bold. The IPA Z-score, predicting the activation (red) or inhibition (blue) of the respective signaling pathway, is marked in color. See also Figure 17 for additional description of normalized enrichment score (NES) in panel **(b)**. cAMP: Cyclic adenosine monophosphate; CDK5: Cell division protein kinase 5; Con: Control; D2: DBA/2NCrl; DARPP-32: Dopamine- and cAMP-regulated phosphoprotein; Gαq: Guanine nucleotide-binding protein G(q) subunit alpha; GABA: Gamma-aminobutyric acid; IPA: Ingenuity Pathway Analysis; KEGG: Kyoto Encyclopedia of Genes and Genomes; NAFT: Nuclear factor of activated T-cells; Res: Resilient; Sus: Susceptible; VOXPHOS: Genes involved in oxidative phosphorylation.

Furthermore, at the transcriptome level, the genes within the testosterone cluster were predicted to be significantly upregulated in the B6 and downregulated in the D2 susceptible groups in comparison to both the control and resilient groups (B6, $P = 0.033$ and $P = 0.018$; D2, $P = 0.004$ and $P = 0.012$). Notably, five of the genes predicted to be regulated by both hormones were highly DE (|FC| ≥ 1.8) between susceptible and control mice in either (B6, *Top2a*; D2*, Crhr2, Esr1, Igf1*) or both (*Sstr2*) strains (Table 17). Moreover, rapamycin-insensitive companion of mTOR (RICTOR) was detected as the most significant potential upstream regulator in the B6 and D2 strains. Specifically, the RICTOR cluster was downregulated in the B6 susceptible mice in comparison to the control and resilient groups (Z-score = -4.94, $P = 3.43E^{-16}$ and Z-score =-3.03, $P = 4.88E^{-4}$, respectively) and upregulated in the same comparisons in the D2 mice (Z-score = 6.63, $P = 1.86E^{-17}$ and Z-score = 3.74, $P = 9.13E^{-8}$, respectively). In summary, although the main three predicted upstream regulators were identical in both strains, their predicted activation pattern was opposite in the B6 and D2 strains.

Table 17. Top differentially expressed ($P < 0.05$ and |FC| ≥ 1.8) genes (data set A) included in the predicted beta-estradiol and testosterone IPA upstream regulator clusters.

Upstream regulator cluster	Gene symbol	DE genes in the B6 strain (data set A)						DE genes in the D2 strain (data set A)					
		Sus vs Con		Res vs Con		Sus vs Res		Sus vs Con		Res vs Con		Sus vs Res	
		FC	*P*	FC	*P*	FC	*P*	FC	*P*	FC	*P*	FC	*P*
Beta-estradiol, Testosterone	*Top2a*	2.5777	0.0112	-	-	2.29	0.0233	-	-	2.18	0.0226	-2.14	0.0207
	Crhr2	-	-	-	-	-	-	2.23	0.0147	3.83	<0.001	-1.72	0.0498
	Esr1	-	-	-	-	-	-	2.32	0.0286	2.33	0.0488	-	-
	Igf1	-	-	-	-	-	-	-1.80	0.0142	-2.29	0.0074	-	-
	Sstr2	-1.822	0.0441	-	-	-2.79	0.0008	2.87	0.0011	-	-	-	-

Data generated from mouse BNST after exposure to CSDS. All non-significant results ($P > 0.05$) are indicated by a hyphen ("-"). B6: C57BL/6NCrl; Con: Control; *Crhr2:* Corticotropin releasing hormone receptor 2; D2: DBA/2NCrl; DE: Differentially expressed*; Esr1:* Estrogen receptor 1 alpha; FC: Fold change; *Igf1:* Insulin-like growth factor 1; IPA: Ingenuity Pathway Analysis, Res: Resilient*; Sstr2*: Somatostatin receptor 2; Sus: Susceptible; *Top2a*: Topoisomerase II alpha.

Analysis of active miRNAs and their mRNA targets in the BNST of CSDS-subjected B6 mice reveals lower levels of miR-34c and miR-99b and higher levels of miR-15b after stress

To detect active DE miRNAs (data set G) and their bound mRNA targets (data set H), we performed AGO-RIP-seq followed by analysis with microRNA Target Filter tool implemented in Ingenuity Pathway Analysis (IPA) software (QIAGEN Inc., 2018). The aim of the analysis was to provide insight into the biological role of the identified DE miRNAs by using TargetScan-predicted

miRNA-mRNA interactions (Agarwal et al. 2015) and experimentally validated interactions from miRecords (Xiao et al., 2009), TarBase (Karagkouni et al., 2018), and miRNA-associated findings from published literature (QIAGEN Inc., 2018). We identified several dozen (*n* = 59, susceptible vs control; *n* = 72, resilient vs control; *n* = 36, susceptible vs resilient) DE miRNAs that repressed from one to many (maximum *n* = 60) co-immunoprecipitated DE experimentally validated or computationally predicted (high confidence) mRNA targets. Table 18 shows miRNA-mRNA interactions selected with the highest confidence (i.e., based on at least three miRNA IPA Target Filter sources). Collectively, and consistent with the literature (Leung and Sharp, 2010), our results suggest that miRNA regulation of gene expression is not only influenced by the specificity of the interaction but also by the relative cellular concentrations of miRNAs and their mRNA targets.

Table 18. Detected DE miRNAs with their predicted DE target genes in the B6 BNST after CSDS.

	DE miRNA in the B6 strain (data set G)							DE mRNA in the B6 strain (data set H)					
miRNA	**Sus vs Con**		**Res vs Con**		**Sus vs Res**		**Target gene**[a]	**Sus vs Con**		**Res vs Con**		**Sus vs Res**	
	FC	***P***	**FC**	***P***	**FC**	***P***		**FC**	***P***	**FC**	***P***	**FC**	***P***
miR-34c	-2.84	0.004	-1.77	0.041	-	-	*Jag1*	-1.41	0.020	-1.32	0.045	-	-
miR-126a	-	-	1.21	0.011	-	-	*Irs1*	-	-	1.21	0.023	-	-
miR-15b	1.35	0.003	1.33	0.002	-	-	*Dmtf1*	1.20	0.006	1.23	0.002	-	-
miR-33	1.25	0.047	-	-	-	-	*Abca1*	1.21	0.002	-	-	-	-
miR-18a	3.22	0.026	2.59	0.034	-	-	*Esr1*	1.75	0.006	-	-	-	-
miR-99b	-1.50	<0.001	-1.22	0.005	-1.22	0.011	*Igf1r*	-	-	-	-	-1.21	0.039

All presented miRNA-mRNA interactions were predicted by Ingenuity Expert Findings, TargetScan, and miRecords, with the exception of miR-15b and *Dmtf1* interaction, which was predicted by TarBase, TargetScan, and miRecords. All non-significant results (*P* > 0.05) are indicated by a hyphen ("-"). Abca1: ATP-binding cassette transporter; B6: C57BL/6NCrl; Con: Control; Dmtf1: Cyclin D binding Myb-like transcription factor 1; Esr1: Estrogen receptor 1; Igf1r: Insulin-like growth factor 1 receptor; Jag1: Jagged1; Irs1: Insulin receptor substrate 1; Res: Resilient; Sus: Susceptible.

Converging multi-omics analysis implies dysregulation of CYCS and PPP1R1B following CSDS

We then investigated the shared DE genes and proteins with the implicated dysregulated canonical pathways (Fig. 21a) and enriched gene sets (Fig. 21b) identified in the BNST of both B6 and D2 mice. To determine the influence of genetic background on divergent regulation of mitochondria-related pathways, we included the comparison of B6 and D2 controls in the analysis (see S6 Table in Manuscript II). We examined similarities in expression patterns within at least one comparison (susceptible vs control, resilient vs control, susceptible vs resilient) between at least two BNST data sets (C, D, G and H; see Fig. 9). We identified three DE molecules

(*Cycs*, *Pcsk1n*, and *Atp6v1e1*) within the mitochondria-related canonical pathways (see Fig. 21a-b pathways and gene sets written in bold) and four molecules (*Adcy5*, *Ppp1r1b*, *Pcp4l1*, and *Ppp3ca*) in all other top IPA canonical pathways dysregulated after CSDS (Fig. 21a). An overview of the converging analysis is shown in Figure 22 (see pages 82-83). Two of the selected molecules, CYCS (Cytochrome c somatic) and PPP1R1B, previously associated with psychiatric diseases and disorders, including anxiety disorders (Hroudova and Fisar, 2011; Davis et al., 2012; Jin et al., 2015; Kovalenko et al., 2016; Scaini et al., 2017), were further successfully validated by Western blot analysis (see Fig. 23 for observed differences between the groups).

Figure 22. Circos heatmap showing overlap of DE genes and proteins included in the canonical pathways and gene sets dysregulated after chronic psychosocial stress. *See pages 82 and 83*. Merged heatmap showing the *P*-values and expression fold changes (log2FoldChange) of susceptible vs control, resilient vs control, and susceptible vs resilient groups in the BNST of B6 and D2 strains after CSDS. Only the molecules that are DE in at least one of the comparisons are included. DE genes and proteins common to both –omics data sets (C and D) were preselected based on Table S3. Significantly DE molecules ($P < 0.05$) are shown in solid colors, while those that did not exceed the cut-off ($P \geq 0.05$) are shown in diagonal stripe pattern. B6: C57BL/6NCrl; C: Control; D2: DBA/2NCrl; R: Resilient; S: Susceptible. Figure adapted from Article II.

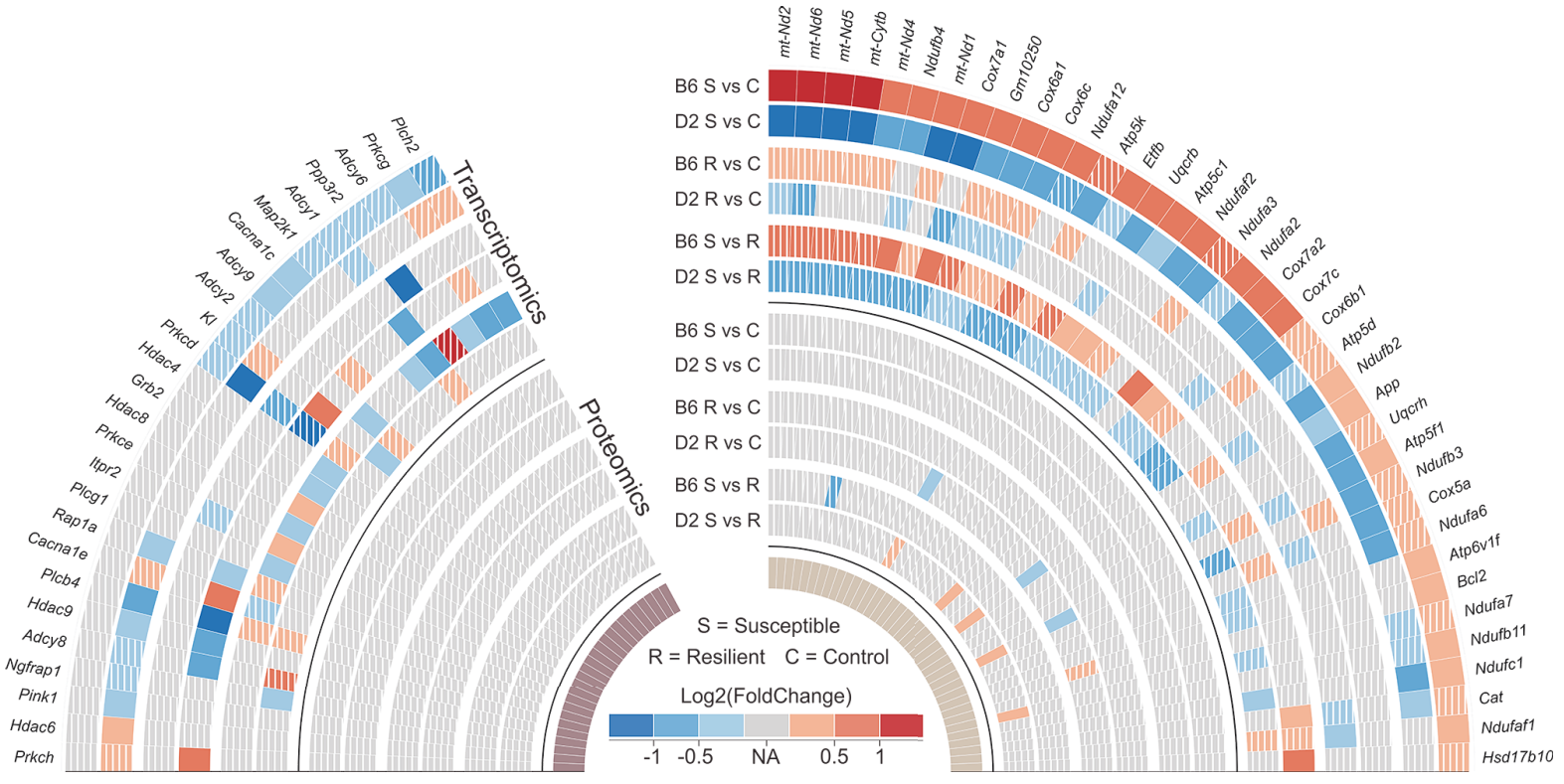

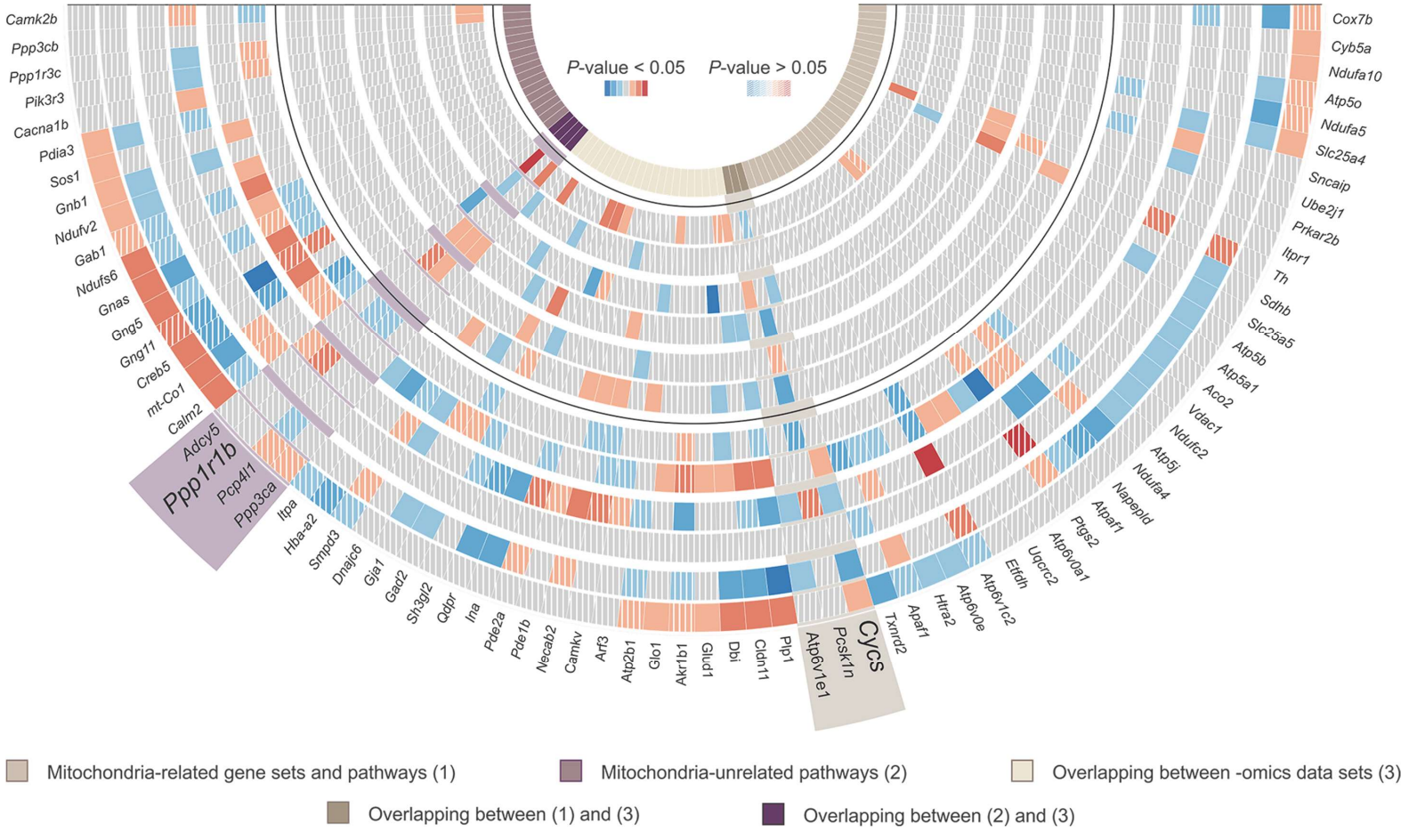
P-value < 0.05
P-value > 0.05
Camk2b
Ppp3cb
Ppp1r3c
Pik3r3
Cacna1b
Pdia3
Sos1
Gnb1
Ndufv2
Gab1
Ndufs6
Gnas
Gng5
Gng11
Creb5
mt-Co1
Calm2
Adcy5
Ppp1r1b
Pcp4l1
Ppp3ca
Itpa
Hba-a2
Smpd3
Dnajc6
Gja1
Gad2
Sh3gl2
Qdpr
Ina
Pde2a
Pde1b
Necab2
Camkv
Arf3
Atp2b1
Glo1
Akr1b1
Gld1
Dbi
Cldn11
Plp1
Atp6v1e1
Pcsk1n
Cycs
Txnrd2
Apaf1
Htra2
Atp6v0e
Atp6v1c2
Etfdh
Uqcrc2
Atp6v0a1
Pgs2
Alpaf1
Napepld
Ndufa4
Atp5j
Ndufc2
Vdac1
Aco2
Atp5a1
Atp5b
Slc25a5
Sdhb
Th
Itpr1
Prkar2b
Ube2j1
Sncaip
Slc25a4
Ndufa5
Atp5o
Ndufa10
Cyb5a
Cox7b
Mitochondria-related gene sets and pathways (1)
Mitochondria-unrelated pathways (2)
Overlapping between -omics data sets (3)
Overlapping between (1) and (3)
Overlapping between (2) and (3)

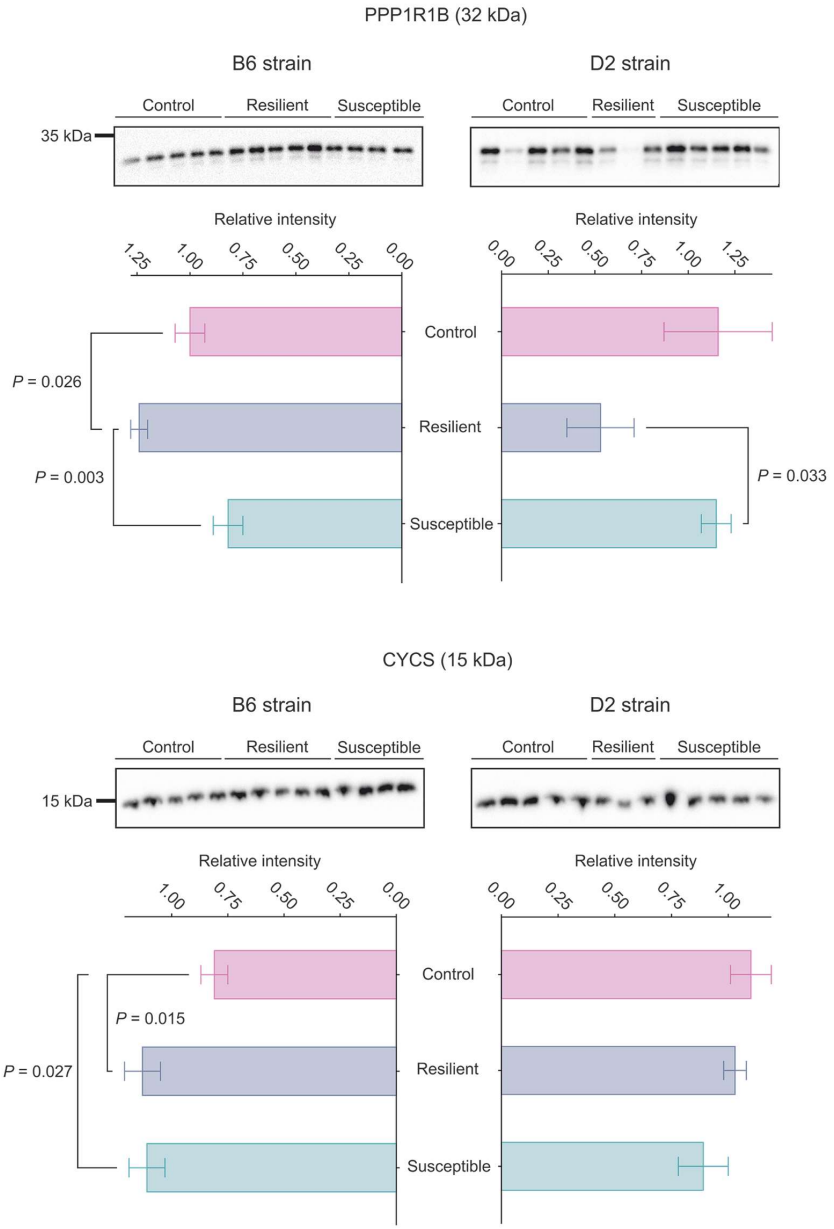

Figure 23. Western blot analysis confirms significant differences in PPP1R1B and CYCS proteins in the BNST between the stress-susceptible and stress-resilient mice. B6: C57BL/6NCrl; CYCS: Cytochrome c, somatic; D2: DBA/2NCrl; PPP1R1B: Protein phosphatase 1 regulatory subunit 1B.

5.2.7 Gene expression profiling of blood cells from stressed mice and panic disorder patients after exposure-induced panic attack reveals dysregulation of mitochondria-related pathways

We then aimed to determine which canonical pathways and gene sets could be identified as stress-responsive from easily accessible tissue (i.e., blood cells) collected from both mice and humans and if any of them were shared with the findings obtained from BNST gene expression (data set C). We performed RNA-seq and miRNA-seq (data sets I and J, respectively) and subsequently compared B6 and D2 stress-susceptible mice to the same-strain controls, and B6 susceptible mice to the B6 resilient group. D2 resilient mice were not included in the analysis as we were not able to obtain a sufficient amount of blood. Importantly, all blood cell samples were collected from the same animals as those used for BNST transcriptome profiling (data set C). The human sample (data set K) consisted of individuals diagnosed with PD who underwent exposure-induced panic attack as a part of exposure therapy. We compared blood cell gene expression profiles from samples collected at 1-hour and 24-hour post-exposure to a baseline measurement.

We detected similar numbers of DE genes in the B6 and D2 susceptible mice in comparison to the same-strain controls (B6, n = 568 and D2, n = 771), of which 112 were shared between the strains. Notably, similarly to the BNST, the majority (n = 102, 91.1%) differed in their directionality of expression (Fig. 24a). To identify dysregulated canonical pathways and gene sets, we performed hypergeometric statistic using the MSigDB C2 collection (Mootha et al., 2003; Subramanian et al., 2005). We observed significant enrichment ($P_{FDR} < 0.05$) of over 100 gene sets, including the Alzheimer's disease gene set containing the largest number of shared DE genes (Table 19). Furthermore, we examined the expression patterns of all DE genes common to the BNST and blood cells data sets (C and I, respectively) and observed a moderate positive correlation between them (Pearson's correlation, r = 0.410, $P = 2.93E^{-33}$). Taken together, our results show similar patterns of the expression profiles in the BNST (data set C) and blood cells (data set I) after CSDS.

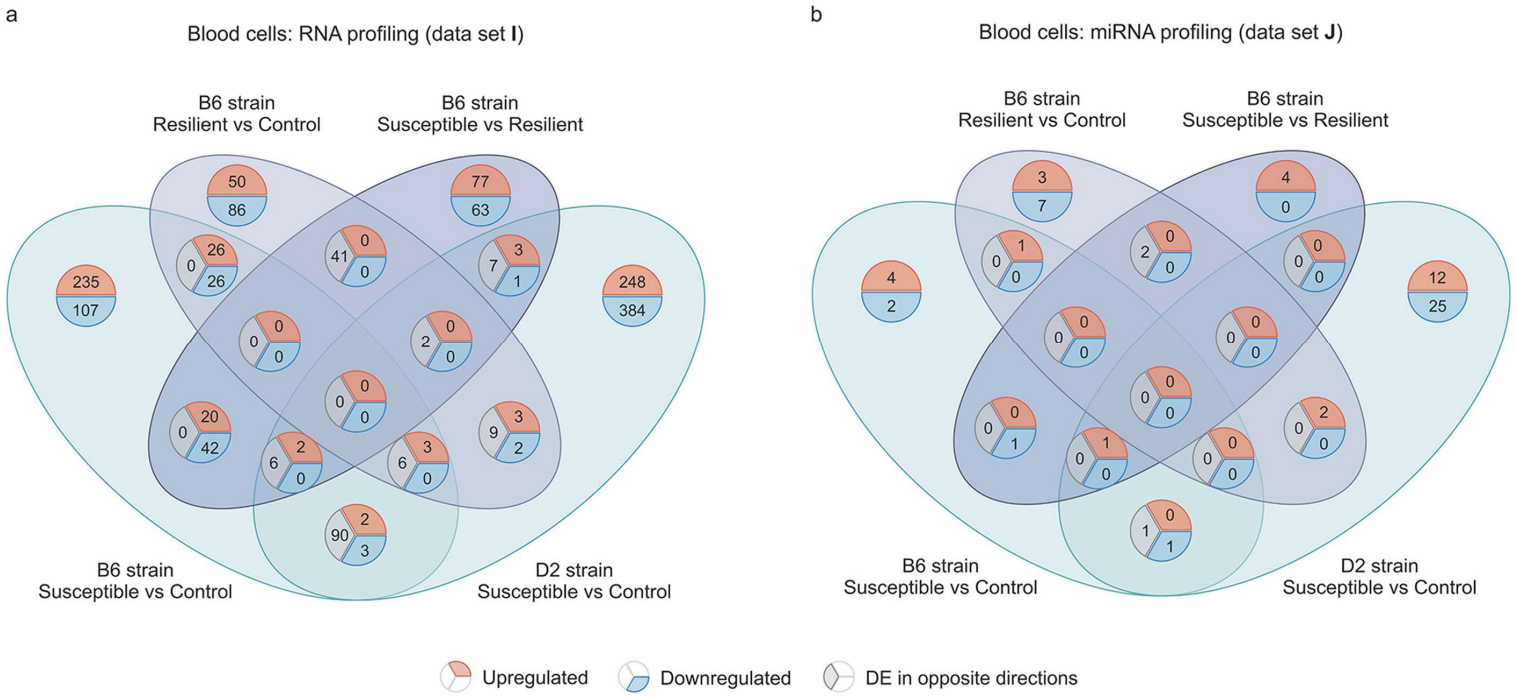

Figure 24. Venn diagrams showing the overlap between the top significantly differentially expressed (a) genes (data set I), (b) miRNAs (data set J) in the B6 and D2 mice subjected to CSDS. Transcriptome profiling from the BNST (data set C) and blood cells (data sets I and J) were performed from the same mice, with the exception of D2 resilient mice, as we were not able to obtain sufficient amount of blood from that group. B6: C57BL/6NCrl; D2: DBA/2NCrl; DE: Differentially expressed.

Table 19. Top significantly enriched gene sets (P_{FDR} < 0.05) for the DE genes overlapping between the blood cells of B6 and D2 susceptible vs control comparisons (data set G).

Source	Gene set name	Number of genes in gene set (K)	Number of DE genes in gene set (k)	k/K	*P*	P_{FDR}
Blalock	Alzheimer's disease (down)	1237	17	0.014	1.75E-09	1.55E-06
Diaz	Chronic myelogenous leukemia (up)	1382	16	0.012	5.94E-08	2.83E-05
Pilon	*KLF1* targets (down)	1972	16	0.008	6.30E-06	1.15E-03
Graessmann	Apoptosis by doxorubicin (up)	1142	15	0.013	3.15E-08	1.67E-05
Yoshimura	*MAPK8* targets (up)	1305	15	0.012	1.76E-07	6.99E-05
Pujana	*BRCA1* -PCC network	1652	14	0.009	1.57E-05	2.34E-03
Chen	Metabolic syndrome network	1210	13	0.011	2.62E-06	5.87E-04
Reactome	Hemostasis	466	12	0.026	5.42E-10	1.29E-06
Graessmann	Response to MC and doxorubicin (up)	612	12	0.020	1.14E-08	7.72E-06
Kim	All disorders oligodendrocyte number correlation (up)	756	12	0.016	1.13E-07	4.89E-05
Krige	Response to tosedostat 6 hr (down)	911	12	0.013	8.13E-07	2.28E-04
Gobert	Oligodendrocyte differentiation (down)	1080	12	0.011	4.67E-06	9.42E-04
Marson	Bound by *FOXP3* unstimulated	1229	12	0.010	1.70E-05	2.36E-03
Pujana	*ATM* -PCC network	1442	12	0.008	7.92E-05	6.28E-03
Acevedo	Liver cancer (up)	973	11	0.011	1.02E-05	1.69E-03
Dodd	Nasopharyngeal carcinoma (down)	1375	11	0.008	2.24E-04	1.39E-02
Reactome	Platelet activation signaling and aggregation	208	10	0.048	3.90E-11	1.86E-07
Lindgren	Bladder cancer cluster 2B	392	10	0.026	1.75E-08	1.04E-05
Nuytten	*NIPP1* targets (down)	848	10	0.012	1.84E-05	2.43E-03
Bystrykh	Hematopoiesis stem cell QTL transcripts	882	10	0.011	2.57E-05	3.06E-03
Krige	Response to tosedostat 24 hr (down)	1011	10	0.010	8.02E-05	6.28E-03
Marson	Bound by *FOXP3* stimulated	1022	10	0.010	8.76E-05	6.62E-03
Bruins	UVC response late	1137	10	0.009	2.08E-04	1.32E-02

Analysis performed with MSigDB v6.0 C2 curated gene sets (Mootha et al., 2003; Subramanian et al., 2005). *ATM*: Ataxia-telangiectasia mutated serine/threonine kinase; B6: C57BL/6NCrl; *BRCA1*: Breast cancer, DNA repair associated; D2: DBA/2NCrl; DE: Differentially expressed; *FOXP3:* Forkhead box P3; *KLF1:* Krueppel-like factor 1; *MAPK8*: Mitogen-activated protein kinase *8;* MC: Medium concentrate; NIPP1: Nuclear inhibitor of protein phosphatase-1; PCC: Pearson correlation coefficient; QTL: Quantitative trait locus; UVC: Ultraviolet C.

To examine the DE miRNAs in blood cells after chronic stress, we performed miRNA-seq followed by DE analysis (data set J). B6 susceptible and resilient groups had similar numbers of DE miRNAs (n = 11 and n = 15, respectively, Fig. 24b), which was consistent with our findings of active AGO2-associated miRNAs in the BNST (data set G). Furthermore, we detected three DE miRNAs shared between the B6 and D2 susceptible vs control comparisons (miR-181b, miR-148a, and miR-592), two of which had opposite expression patterns (miR-148a and miR-181b, Table 20). Additionally, we identified two DE miRNAs (miR-3076 and miR-34c) as common to both blood cell and BNST data sets (J and G, respectively), with miR-34c being expressed at a lower level in B6 resilient mice in comparison to the same-strain controls in both. Taken together, our results show two interesting candidate miRNAs that have been previously implicated in psychiatric diseases and disorders. Notably, miR-148a has been previously associated with PD (Muinos-Gimeno et al., 2011) and miR-181b has been proposed as a marker for Alzheimer's disease (Femminella et al., 2015). Furthermore, high levels of miR-181b have been correlated with increase in mitochondrial oxidative stress and DNA damage, an early systematic process in the pathophysiology of Alzheimer's disease (Schipper et al., 2007).

Table 20. DE miRNA in blood cells of B6 and D2 mice after CSDS (data set J).

miRNA	B6 strain						D2 strain	
	Sus vs Con		Res vs Con		Sus vs Res		Sus vs Con	
	FC	*P*	FC	*P*	FC	*P*	FC	*P*
mmu-miR-296-5p	-	-	-2.50	0.005	2.06	0.021	-	-
mmu-miR-6516-5p	-	-	-2.44	0.010	2.34	0.013	-	-
mmu-miR-503-5p	-	-	1.31	0.044	-	-	1.54	0.003
mmu-miR-6546-5p	-	-	1.46	0.020	-	-	1.40	0.035
mmu-miR-7a-5p	1.65	0.007	1.61	0.010	-	-	-	-
mmu-miR-5620-5p	-2.52	0.008	-	-	-2.50	0.008	-	-
mmu-miR-592-5p	-1.71	0.021	-	-	-	-	-1.71	0.021
mmu-miR-148a-5p	1.34	0.012	-	-	-	-	-1.26	0.042
mmu-miR-181b-5p	1.66	0.004	-	-	1.57	0.008	-1.41	0.038

Only miRNAs DE in at least two comparisons are shown. All non-significant results (P > 0.05 and |FC| < 1.2) are indicated by a hyphen ("-"). B6: C57BL/6NCrl; Con: Control; D2: DBA/2NCrl; DE: Differentially expressed; Res: Resilient; Sus: Susceptible.

Simultaneously, we performed DE analysis of microarray-based gene expression data from PD (PD) patient blood cells (see section 4.2 and Fig. 9; data set K), collected immediately and 24 hours after exposure-induced panic attack in comparison to baseline measurement. We detected 4185 significantly DE genes (P < 0.05) in either one or both time points. We detected a

larger number of DE genes directly after the exposure-induced panic attack (n = 2099) rather than 24 hours after (n = 1424), although a significant number of DE genes was shared between both (n = 692). We further analyzed the DE genes for overrepresentation of GO terms and reported higher than expected number of GO terms ($P_{FDR} < 0.05$) associated with mitochondria and translational control (Table 21). Taken together, while we identified higher expression levels of a number of genes at the time of the panic attack, which continued one day after the attack, a significant number of genes exhibit a postponed response to the stressful event, being DE only at the second timepoint.

Table 21. Top 30 significantly enriched gene sets (P_{FDR} < 0.05) for the DE genes overlapping between the panic disorder (PD) patients' blood cells (data set H) collected directly and 24h after exposure-induced panic attack in comparison to baseline measurement (0H and 24H, respectively).

GO ID	GO term	GO category	Number of all genes in GO term		Number of DE genes in GO term		*P*		P_{FDR}	
			0H	24H	0H	24H	0H	24H	0H	24H
GO:0006412	Translation	Biological processes	367	367	107	72	1.10E-11	2.52E-07	1.72E-07	1.97E-03
GO:0043043	Peptide biosynthetic process	Biological processes	392	392	110	76	2.92E-11	2.25E-07	2.29E-07	3.52E-03
GO:0006518	Peptide metabolic process	Biological processes	504	504	125	86	1.32E-09	4.19E-06	6.89E-06	1.64E-02
GO:0043604	Amide biosynthetic process	Biological processes	499	499	119	83	2.23E-08	1.49E-05	6.99E-05	2.12E-02
GO:0006119	Oxidative phosphorylation	Biological processes	83	83	36	28	3.68E-08	2.65E-07	8.24E-05	1.39E-03
GO:0002181	Cytoplasmic translation	Biological processes	62	62	28	21	6.21E-07	7.64E-06	7.48E-04	1.50E-02
GO:0042773	ATP synthesis coupled electron transport	Biological processes	65	65	26	22	8.89E-06	4.72E-06	5.80E-03	1.06E-02
GO:0042775	Mitochondrial ATP synthesis coupled electron transport	Biological processes	64	64	25	21	1.81E-05	1.14E-05	9.47E-03	1.98E-02
GO:0009144	Purine nucleoside triphosphate metabolic process	Biological processes	203	203	53	42	2.95E-05	3.33E-05	1.28E-02	3.73E-02
GO:0009205	Purine ribonucleoside triphosphate metabolic process	Biological processes	196	196	51	41	3.60E-05	2.71E-05	1.48E-02	3.54E-02
GO:0022904	Respiratory electron transport chain	Biological processes	83	83	29	23	3.75E-05	4.26E-05	1.51E-02	4.45E-02
GO:0009199	Ribonucleoside triphosphate metabolic process	Biological processes	200	200	51	41	6.15E-05	4.82E-05	2.24E-02	4.72E-02
GO:0046034	ATP metabolic process	Biological processes	166	166	44	37	8.44E-05	2.72E-05	2.87E-02	3.28E-02
GO:0009167	Purine ribonucleoside monophosphate metabolic process	Biological processes	203	203	51	45	1.01E-04	4.21E-06	3.10E-02	1.32E-02
GO:0009126	Purine nucleoside monophosphate metabolic process	Biological processes	204	204	51	45	1.05E-04	4.40E-06	3.16E-02	1.15E-02
GO:0044391	Ribosomal subunit	Cellular component	186	186	70	35	4.16E-12	7.26E-04	8.39E-09	3.76E-02
GO:0019866	Organelle inner membrane	Cellular component	470	470	122	81	1.74E-10	5.93E-06	1.17E-07	1.71E-03
GO:0005743	Mitochondrial inner membrane	Cellular component	410	410	111	70	1.66E-10	2.91E-05	1.67E-07	6.54E-03
GO:0005740	Mitochondrial envelope	Cellular component	661	664	152	102	1.79E-09	2.99E-05	7.22E-07	6.04E-03
GO:0098798	Mitochondrial protein complex	Cellular component	249	249	76	56	2.38E-09	1.27E-07	8.01E-07	2.56E-04
GO:0031966	Mitochondrial membrane	Cellular component	623	626	144	95	3.68E-09	7.59E-05	1.06E-06	9.02E-03
GO:0031967	Organelle envelope	Cellular component	1090	1093	221	152	6.19E-09	3.58E-05	1.39E-06	5.56E-03
GO:0031975	Envelope	Cellular component	1090	1093	221	152	6.19E-09	3.58E-05	1.56E-06	6.03E-03
GO:0015934	Large ribosomal subunit	Cellular component	115	115	45	28	1.21E-08	7.41E-05	2.44E-06	9.35E-03
GO:0044455	Mitochondrial membrane part	Cellular component	204	204	63	48	3.72E-08	4.66E-07	6.25E-06	4.70E-04
GO:1990904	Ribonucleoprotein complex	Cellular component	828	828	174	120	4.13E-08	5.06E-05	6.40E-06	7.30E-03
GO:0044429	Mitochondrial part	Cellular component	944	947	189	130	1.84E-07	2.15E-04	2.47E-05	2.07E-02
GO:0098800	Inner mitochondrial membrane protein complex	Cellular component	121	121	43	33	2.18E-07	2.00E-06	2.74E-05	1.34E-03
GO:0044424	Intracellular part	Cellular component	13598	13623	1904	1396	3.87E-07	1.38E-04	4.59E-05	1.46E-02
GO:0005622	Intracellular	Cellular component	13850	13875	1934	1423	4.77E-07	5.92E-05	5.34E-05	7.97E-03

Analysis performed with MSigDB v6.0 C2 curated gene sets (Mootha et al., 2003; Subramanian et al., 2005). ATP: Adenosine triphosphate.

5.2.8 Integrated GSEA shows mitochondria-related dysregulation in mice subjected to chronic psychosocial stress and panic disorder patients after exposure-induced panic attack

We performed a converging GSEA of blood cell transcriptomic data obtained from B6 and D2 mice susceptible to CSDS in comparison to the same-strain controls (data set I) and data collected from PD patients after exposure-induced panic attacks (data set K). We detected an enrichment of several gene sets related to translational control and mitochondria (Fig. 25), a result which was in agreement with our findings in the BNST data (Fig. 21). Notably, these gene sets displayed a similar pattern in both the blood cells of defeated D2 mice and the PD patients. In summary, these results suggest a common evolutionarily conserved role of mitochondrial pathways in the regulation of anxiety-related behavior in mammals.

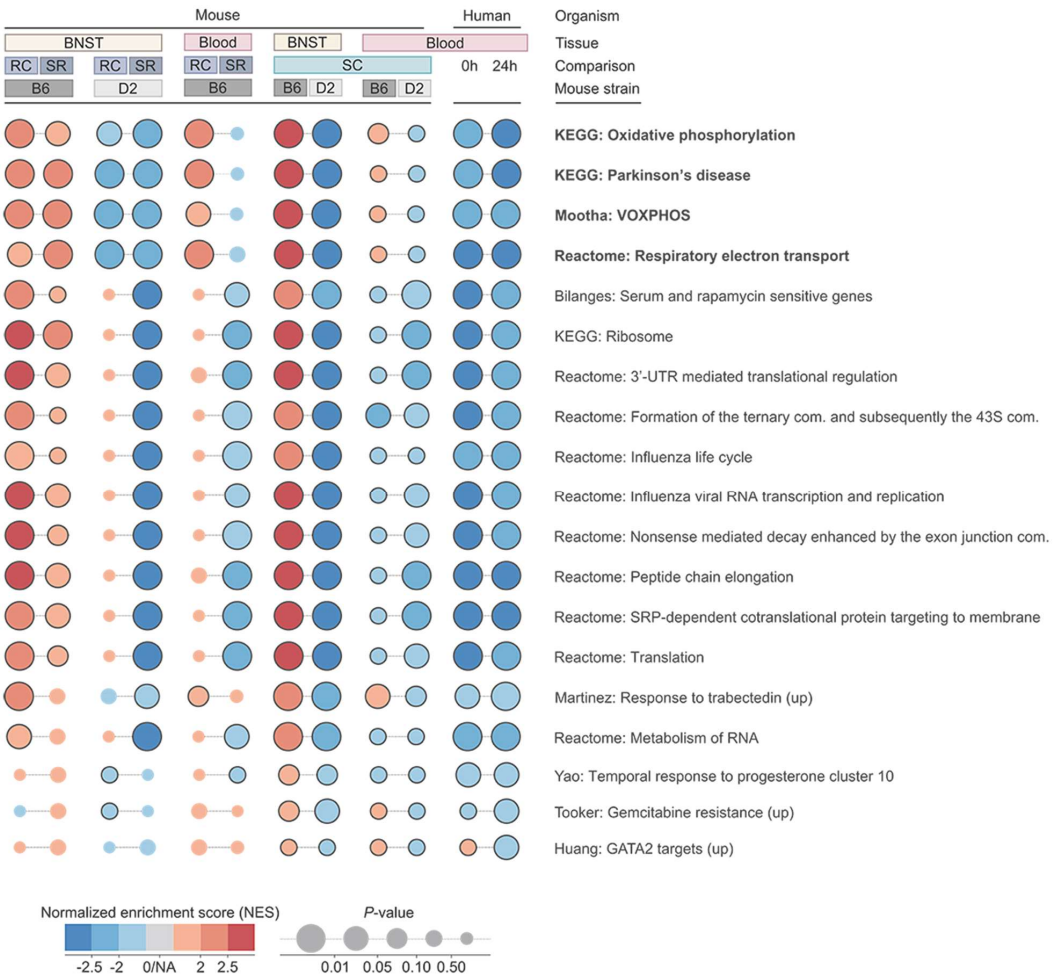

Figure 25. Merged heatmap showing the top overlapping gene sets between the gene expression data from CSDS-stressed mice (data sets C and I) and panic disorder (PD) patients' blood cells collected directly and 24 hours after exposure-induced panic attack (data set H). A positive (or negative) NES for a given gene set implicates overrepresentation at the top (or bottom, respectively) of the ranked list of upregulated (or downregulated, respectively) genes. Gene sets are ordered by frequency and then alphabetically. P_{FDR}-values < 0.25 are marked with black outlines around the circles. 3'-UTR: Three prime untranslated region; B6: C57BL/6NCrl; BNST: Bed nucleus of the stria terminalis; Com.: Complex; D2: DBA/2NCrl; GATA2: GATA-Binding Protein 2; KEGG: Kyoto Encyclopedia of Genes and Genomes; RC: Resilient vs control; SC: Susceptible vs control; SR: Susceptible vs resilient; SRP: signal recognition particle; VOXPHOS: genes involved in oxidative phosphorylation.

5.2.9 Susceptibility to chronic psychosocial stress in the BNST is associated with differences in mitochondria morphology in the B6 strain

We then aimed to determine if the observed mitochondria-related differences in gene and protein expression after CSDS (see Fig. 21) are associated with alterations in mitochondrial morphology. To test this, we performed TEM of mitochondria in the BNST of B6 and D2 mice (data set F). We compared stress-susceptible, stress-resilient, and same-strain control mice.

In TEM mitochondria analysis, we measured the number and size of mitochondrial cross-sections. Mitochondrial cross-sections were classified as *synaptic* provided that the synaptic density and vesicles were clearly identifiable. We observed that the mitochondrial cross-section diameter in the B6 susceptible mice was on average 8.4% shorter than in the B6 controls (Table 22). Furthermore, although the mean number of mitochondrial cross-sections was not affected by chronic stress, we observed a 39% higher number of pre-synaptic cross-sections in the B6 susceptible mice in comparison to the B6 control and a 46% smaller number of post-synaptic cross-sections in the resilient B6 mice than in the susceptible mice. Our findings were strain specific, which was further confirmed by the observed differences between the strains (Table 22). We therefore concluded that the changes in mitochondrial morphology in the BNST following CSDS are strain-dependent and consistent with our observed gene and protein differential expression.

Table 22. Differences in mitochondrial morphology after chronic social defeat stress.

Measurment			Differences within the B6 and D2 strains						Differences between the B6 and D2 strains		
			Sus vs Con		Res vs Con		Sus vs Res				
			B6	D2	B6	D2	B6	D2	Susceptible	Resilient	Control
Number of mitochondrial cross-sections	Total	*P*	-	-	-	-	-	-	0.013	-	0.054
		t	-	-	-	-	-	-	-2.150	-	-2.433
	Pre-synaptic comp.	*P*	0.015	-	-	-	-	-	-	0.012	-
		t	0.267	-	-	-	-	-	-	-0.167	-
	Post-synaptic comp.	*P*	-	-	-	-	0.038	-	-	-	0.014
		t	-	-	-	-	0.352	-	-	-	-0.097
Mitochondrial cross-section diameter (µm)	Maximal	*P*	0.003	-	-	-	-	-	0.041	-	-
		t	-0.035	-	-	-	-	-	-0.022	-	-
	Minimal	*P*	-	-	-	-	-	-	-	0.048	0.001
		t	-	-	-	-	-	-	-	0.020	0.021
	Maximal/minimal	*P*	-	-	-	-	-	0.003	<0.001	-	-
		t	-	-	-	-	-	0.080	-0.145	-	-

Con: Control; Comp.: Compartment; Res: Resilient; Sus: Susceptible; *t:* Mean difference.

6 Discussion

6.1 General implications

The studies presented in this work applied -omics and multi-omics approaches to establish the genetic architecture behind anxiety disorders and the molecular mechanisms that mediate susceptibility to psychosocial stress, a well-established factor for their onset and recurrence.

In study I, we performed a genome-wide linkage scan in an isolated homogenous population with a high reported incidence of acrophobia, a subtype of a specific phobia also known as fear of heights. Although we were not able to identify high-risk variants for the disorder, several of the variants were suggestive (LOD > 2.0). These were located on chromosomes 4q28, 8q24, and 13q21-q22. Our results imply that the genetic predisposition to acrophobia is likely to have a complex genetic architecture.

In the two remaining studies, we subjected two inbred mouse strains (B6 and D2) with different stress susceptibility to CSDS. CSDS is used as a model of psychosocial stress, a key feature of anxiety disorders (Gerra et al., 2000). To identify the core dysregulated molecules and pathways behind susceptibility to stress, we subsequently performed unbiased transcriptomic profiling followed by data integration of the analyzed data sets. We compared the stress-resilient, stress-susceptible, and same-strain control mice.

In study II, we investigated gene expression (including expression of active miRNAs and their mRNA targets) and protein abundance in the BNST. Furthermore, we performed transcriptome profiling in blood cells of CSDS-subjected mice and compared it to gene expression patterns from blood cells of PD patients who underwent exposure-induced panic attacks. We further followed with integrative GSEA of both mouse and human data, which showed global genetic background-specific significant enrichment of mitochondria-related gene sets. Interestingly, we observed lower expression of mitochondria-related genes in the D2 defeated mice and the PD patients. Additionally, we found differences in BNST mitochondrial morphology, as B6 susceptible mice had a significantly higher number of mitochondrial cross-sections in the pre-synaptic compartment than in B6 stress-resilient mice.

In study III, we analyzed gene expression data from three brain regions (the PFC_M, the HIP_V, and the BNST) followed by GSEA and data integration. The converging analyses showed genetic background-dependent over-representation of mature oligodendrocyte-related genes within

the DE genes. We followed this compelling finding with TEM measurements of myelinated axons in the BNST. Our results showed that B6 susceptible mice had thicker myelin in comparison to the B6 resilient group.

Overall, our results showed that anxiety disorders have a complex genetic architecture, most likely influenced by a spectrum of both common and rare variants (Bodmer and Bonilla, 2008; Smoller et al., 2009). Furthermore, they illustrated the large effect of genetic background on brain transcriptomic and proteomic response to chronic psychosocial stress, an important observation to improve the validity of translational studies. Finally, by identifying mitochondria-related pathways associated with anxiety-related behavior in both mice and human, our findings support the suitability of cross-species approaches in studying the biological mechanisms underlying anxiety disorders (Smoller et al., 2001; Ashbrook et al., 2015).

6.2 Genetic predisposition to acrophobia has a complex genetic architecture (study I)

6.2.1 Regions 4q28, 8q24, and 13q21-q22 show suggestive evidence for linkage to acrophobia

We detected three suggestive loci showing evidence of linkage to acrophobia on chromosomes 4q28, 8q24, and 13q21-q22 with the peaks on markers D4S2394 (LOD = 2.17), D8S373 (LOD = 2.09), and D13S162 (LOD = 2.22), respectively.

Markers D13S162 and D4S2394 showed the strongest and second strongest linkage to acrophobia in our study. To our knowledge, neither of the regions have been previously associated with anxiety disorders. Marker D4S2394 has previously provided evidence for linkage to schizophrenia in a study sample of Finnish schizophrenia families (Paunio et al., 2001). Interestingly, in our study this marker showed evidence of suggestive linkage to the pure acrophobia sample, but not to the acrophobia with comorbid schizophrenia (LOD = 0.52). Therefore, in our sample, the signal is mainly derived from the acrophobia and not the schizophrenia phenotype.

Marker D8S373 is located on the long arm of chromosome 8 (8q24.2-q24.3). Although in our study the marker did not provide evidence of linkage to schizophrenia (LOD = 0.51 and LOD = 0.00, in acrophobia with comorbid schizophrenia and pure schizophrenia subsets, respectively), it has been previously associated with this disease (Holmans et al., 2009) and with bipolar disorder (Avramopoulos et al., 2004; Gonzalez et al., 2014; Kaminsky et al., 2015). Region 8q24.2-q24.3 contains 49 genes, out of which *KCNQ3* (Wang et al., 1998; Avramopoulos et al., 2004), *ADCY8* (Avramopoulos et al., 2004; Wolf et al., 2014; Hu et al., 2015) have been previously implicated as a candidate genes for psychiatric diseases and disorders. Interestingly, *KCNQ3* has been identified as an active mediator of resiliency within the ventral tegmental area (VTA) dopaminergic (DA) neurons through studies conducted in mice subjected to CSDS (Friedman et al., 2016).

6.2.2 The genetic basis of fear of heights is highly complex

While the behavioral and physiological symptoms of acrophobia have been extensively studied (Coelho and Wallis, 2010; Steinman and Teachman, 2011; Brandt et al., 2015; Kapfhammer et al., 2016) and are shown to involve, among others, dizziness, sweating, and heart palpitation

(see also section 2.4.1), little is known about its genetic architecture. As in other complex anxiety disorders (see Introduction), research efforts are hindered by the heterogeneity of the human population and the ambiguity of the studied phenotypes (Peltonen et al., 2000).

Our study was conducted in an internal genetic isolate (Varilo et al., 1996; Hovatta et al., 1999; Wedenoja et al., 2008; Paunio et al., 2009), which offers several advantages in detecting both common (Stoll et al., 2013) and rare (Sullivan et al., 2012; Ott et al., 2015) variants associated with complex diseases as genetic, cultural, and environmental diversity are reduced. However, even in this genetic isolate and with sufficient statistical power, none of the loci reached the conventional genome-wide significance level (LOD = 3.3) (Lander and Kruglyak, 1995) and no locus was identified as a high-risk variant shared among the families. Together with our other results, this suggests that acrophobia has a complex genetic architecture. Our finding is consistent with a recent unpublished study conducted on a much larger heterogenous European population, where 392 genetic markers were shown to be associated with acrophobia (23andMe, 2018). However, it remains to be seen if the results from this study are reliable and reproducible.

6.2.3 How to define a true finding: the multiple testing problem

Due to the unknown inheritance pattern behind the fear of heights phenotype, our study consisted of a large number of genotyped markers (570) and six analyzed models. With each test, we increased the probability of observing type I error (false positive), which presents a difficulty when interpreting our findings without an adjustment of the significance threshold. However, as the performed analyses are not fully independent, the Bonferroni multiple testing correction (obtained by multiplication of the *P*-value by the number of independently performed tests) is not straightforward and might be considered overly conservative (Freimer and Sabatti, 2004). Consequently, avoidance of the type I error might inflate the type II error (false negative). Furthermore, such correction is not typically performed in linkage studies (Hiekkalinna and Terwilliger, personal communication). Therefore, we presented all results by the obtained LOD scores or corresponding uncorrected nominal *P*-values when applicable. We recognize that our study is of hypothesis-generating character and we rely on future research to replicate our findings.

6.3 Role of myelin and mitochondria in pathological anxiety (studies II and III)

6.3.1 Inbred mouse strains differ in their susceptibility to stress and coping strategies

We demonstrated that the more innately anxious strains (D2, 129, and BALB) have higher susceptibility to stress than the less anxious strain (B6). Only a few studies have investigated strain differences in response to repeated stress (Pothion et al., 2004; Mineur et al., 2006; Mozhui et al., 2010), including CSDS (Razzoli et al., 2011; Savignac et al., 2011). Similar to our results, the results from these studies showed that mice with higher basal anxiety levels have heightened anxiety-like behavior following stress exposure (Jacobson and Cryan, 2007; Millstein and Holmes, 2007) (see also section 6.3.4 for discussion on the significance of these findings to human anxiety).

We observed elevated latency to immobility in the FST in the D2 mice with higher levels of resilience to chronic stress. This observation was not true for the B6 strain. The behavior of the D2 mice can be interpreted as either an inability to maintain effort or adaptation aimed at energy conservation in the face of an inescapable situation (Arai et al., 2000; Petit-Demouliere et al., 2005) and has been previously shown to involve cognitive flexibility and executive dopaminergic functions (Tye et al., 2013; de Kloet and Molendijk, 2016). However, the construct validity of the FST is difficult to establish (Petit-Demouliere et al., 2005) and it is possible that the same passive behavior might involve different molecular mechanisms (David et al., 2003; Puglisi-Allegra and Ventura, 2012). Furthermore, consistent with other studies (Krishnan et al., 2007; Razzoli et al., 2011), we detected an increase in anxiety-like behavior in both B6 and D2 mice as measured by the OF test. Lastly, in both study II and III, we observed a decrease in body weight during CSDS in stress-susceptible and resilient D2 mice. In contrast, the same groups in the B6 strain gained weight, as did the B6 controls. Altogether, similar to earlier studies (Kulesskaya et al., 2014) our behavioral findings implicate an influence of genetic background on the adaptation of different stress-coping strategies (Wood and Bhatnagar, 2015).

6.3.2 Differential gene and protein expression is dependent on the genetic background

Consistent with our behavioral results, we observed strain- and brain region-specific divergent transcriptomic responses to chronic stress in the B6 and D2 mice. The specific findings within and between the studied brain structures are discussed below.

Differences and similarities between the PCF_M, HIP_V, and BNST

Although the HIP_V transcriptomic profiles in the B6 and D2 susceptible mice were highly similar to the same-strain controls (i.e., included a large number of shared genes DE in the same direction in both strains), the profiles of PFC_M and BNST were not. This finding may reflect the discrete role of these structures in processing anxiety-related behavior or the variation in their organization, or both (Chadick et al., 2014; Carlen, 2017). In healthy individuals, PFC_M and HIP_V are both part of a circuit involved in distinguishing danger from safety. This process might be impaired in people suffering from pathological anxiety due to abnormal activity in the PFC_M (Robinson et al., 2014). Furthermore, the BNST is involved in processing of information related to threat response through maintaining a vast connectivity network with other brain structures, including the PFC_M and HIP_V (Kim et al., 2013; Myers et al., 2014). As PFC_M, the BNST is implicated in increased responses to uncertainty in individuals with pathological anxiety (Somerville et al., 2010; Lebow and Chen, 2016). Interestingly, in all analyzed brain regions of the B6 mice subjected to CSDS, we identified the lowest number of DE genes in the resilient vs control comparisons. This result is consistent with the behavioral results, as resilient B6 mice were shown to behaviorally resemble controls despite being exposed to CSDS (Golden et al., 2011). Importantly, even though the detected patterns of gene expression were highly divergent, we observed a significant enrichment of oligodendrocyte-related genes in all the analyzed brain regions and both strains (see section 6.3.3).

Differences and similarities within the BNST and blood cells

We observed significant genetic background-dependent differences in gene and protein expression patterns in the BNST between all compared groups (stress-susceptible, stress-resilient, and control). In summary, contrary to the gene expression patterns in the B6 strain (see above), the greatest number of DE genes in the D2 mice was found in the resilient vs control comparison. This result mirrored the differences in behavior observed between the strains. Conversely, the relative proportion of the DE genes in the susceptible mice in comparison to the same-strain controls was similar in the two strains in both the BNST and the blood cells. Notably, a number of those genes differed in the directionality of expression between the B6 and D2 strains. Those genes were enriched for mitochondria and translation-related pathways (see section 6.3.3) and showed higher expression levels in the B6 susceptible and lower levels in the D2 susceptible mice in comparison to the same-strain controls. As in the case of the susceptible

vs control comparisons, we found significant enrichment of the same gene sets in the B6 and D2 susceptible mice in comparison to the same-strain resilient groups. Furthermore, we also observed differences in miRNA expression levels in blood cells of both strains for miR-181b and miR-148a. Notably, miR-181b has been previously implicated in the pathophysiology of Alzheimer's disease (Femminella et al., 2015) and mitochondrial oxidative stress (Migliore et al., 2005; Bhatnagar et al., 2014), while SNP rs735316 within the miR-148a region is associated with a subtype of PD (Muinos-Gimeno et al., 2011).

Taken together, these findings suggest that the transcriptomic response to chronic stress not only varies between the analyzed brain structures, but that this difference is also strongly dependent on the genetic background (Mozhui et al., 2010; Malki et al., 2015) and may reflect the distinct coping strategies observed in both strains.

6.3.3 BNST myelin and mitochondria-related differences in normal and pathological anxiety

The role of oligodendrocyte-related genes and myelination in anxiety-like behavior

Consistent with the detected differences in the expression of oligodendrocyte-related genes, we observed thicker myelin in B6 mice susceptible to chronic stress in comparison to both the stress-resilient and same-strain control groups. Myelin is produced by oligodendrocytes and insulates axons, thus promoting rapid nerve conduction in the central nervous system and thereby influencing the speed of communication between and within the brain structures implicated in normal and pathological anxiety (Aggarwal et al., 2011). Although the biogenesis of myelin has been mostly described in relation to brain development (McDougall et al., 2018) and has been largely considered static, recent studies have shown that deposition of myelin (Gibson et al., 2014; McKenzie et al., 2014; Chang et al., 2016; Xiao et al., 2016) and the mature myelin structure are in fact dynamic, driven by changes in neuronal activity (Fields, 2014) and regulated by astrocytes at the nodes of Ranvier (Dutta et al., 2018). Additionally, early life stressors have been shown to induce myelination in the amygdala, an upstream and downstream target of the BNST (Lebow and Chen, 2016). Furthermore, although we observed lower levels of oligodendrocyte-related genes in the D2 strain, we did not observe differences in myelin thickness. Taken together, our findings suggest that while chronic stress affects myelin plasticity, its influence is dependent on the genetic background.

The role of mitochondria in anxiety-related behavior

Our study implicated system-wide involvement of mitochondria-related pathways in anxiety-related behavior in both mice and humans. Importantly, the mitochondria-related oxidative phosphorylation pathway, involved in both the production of ATP and apoptosis, showed opposite patterns of expression between the B6 and D2 strains. Interestingly, the pathway was downregulated in both the susceptible D2 mice and PD patients following a panic attack but was upregulated in B6 susceptible mice. Consistent with our results, previous gene expression studies have shown widespread mitochondria-related changes after stress, with their directionality strongly dependent on the duration of the stressor (i.e., acute or chronic stress) and the genetic background, among other factors (Gray et al., 2014; Picard et al., 2015; Larrieu et al., 2017). Furthermore, it has been suggested that the cumulative effect of stress over a lifetime contributes to mitochondria allostatic load and overload, thus promoting changes in mitochondrial functional adaptation (e.g., activation of hormonal receptors and structure, among others) (Picard and McEwen, 2018b; Picard and McEwen, 2018a; Picard et al., 2018).

This opposite directionality of the transcriptomic response was consistent with the differences in the BNST mitochondrial morphology, where we observed a larger number of mitochondrial cross-sections in the B6 stress-susceptible mice than in the B6 stress-resilient mice after CSDS. The observed difference is likely connected to the unique property of mitochondria to undergo dynamic changes in shape, possibly in connection with a simultaneous shift in their function (Picard et al., 2013). Additionally, changes in mitochondrial shape, which are triggered by a disruption of Ca^{2+} mediated by cross-talk between the endoplasmic reticulum (ER) and the mitochondria, have been previously shown in response to stress. The known changes include fragmentation in response to cytochrome c release, hyperelongation, or donut formation (Eisner et al., 2018).

The converging story: Are differences in brain neuroenergetics the answer?

The body mobilizes energy stores in response to a threatening situation. This process is especially prominent in the brain, which accounts for more than 20% of the body's energy consumption. Different cell types in the brain have various metabolic profiles. While much is known about neurons and astrocytes, less is known about oligodendrocytes and microglia (Magistretti and Allaman, 2015). As research by the Barres group on genes expressed in acutely isolated (not cultured prior to their experimental use) neurons and astrocytes has shown (Zhang et al., 2016),

neurons and astrocytes share metabolic complementarity. However, while neurons are predominantly oxidative, glycolysis is dominant in astrocytes. Axons represent a particular burden, namely a significant amount of ATP is required to maintain the activity of Na+/K+ channels to ensure action potential on limited energy storage and supply of neurons (Almeida et al., 2001; Saez-Atienzar et al., 2014) and are therefore vulnerable to situations where increased electrical activity is required (e.g., response to a threat). Past studies have shown that not only astrocytes, but also oligodendrocytes, participate in supporting metabolism in neurons and maintaining ATP homeostasis (Funfschilling et al., 2012) in addition to their role in myelin production, and that these two processes might be independent from each other (Philips and Rothstein, 2017). It is hypothesized that OXPHOS molecules are transferred from the mitochondria to oligodendrocytes by a fusion between mitochondria and the ER (Ravera and Panfoli, 2015). It is therefore possible that the observed higher number of mitochondria and upregulation of oxidative phosphorylation pathways support higher axon energy demand in stressed B6 mice. However, the mechanism behind this process is not yet clear and requires additional studies.

6.3.4 Translational -omics approach to anxiety disorders: implications for future studies

Comparison of gene expression profiles in brain and blood

One of the main challenges in studying anxiety disorders in humans is access to human brain tissue from the regions implicated in the development and maintenance of pathological anxiety. Obtaining large and homogenous sample sets is especially difficult. Therefore, researchers have used peripheral tissues (e.g., blood) as a proxy (Erhardt and Spoormaker, 2013). Consistent with previous studies (Sullivan et al., 2006), our results demonstrated that the average gene expression between blood cells and brain tissue (i.e., BNST) was moderately correlated (r = 0.410, $P = 2.93E^{-33}$), suggesting that although not perfectly linked to gene expression in the brain, gene expression in peripheral tissues might be useful in studying pathological anxiety.

Genetic biomarkers for anxiety disorders

Much effort is currently focused on the discovery of treatment-related and pathogenic biomarkers for anxiety disorders (Nikolova et al., 2014; Maron and Nutt, 2017). The main strength of our study was that the gene expression in the BNST and blood cells was studied in

parallel, allowing us to examine the system-wide response associated with chronic stress. Interestingly, we identified two miRNAs, miR-3076 and miR-34c, present in both blood cells and the BNST of the B6 mice subjected to CSDS. Members of the miRNA-34 family, and miR-34c in particular, have been previously reported as critical modulators in many psychiatric diseases, including schizophrenia (Lai et al., 2011), major depressive disorder (Sun et al., 2016), and bipolar disorder (Bavamian et al., 2015). Additionally, dynamic changes of miR-34c were shown in the central nucleus of the amygdala in mice (Haramati et al., 2011) and in the hypothalamus in rats (Li et al., 2016) after either, or both, chronic and acute exposure to stress (Andolina et al., 2017). Our finding further validates miR-34c as a possible biomarker for anxiety disorders.

The relevance of genetic background in mouse models of anxiety disorders

Lastly, our study was performed in two mouse strains (B6 and D2) that have been shown to differ in their innate anxiety levels and in their response to stress (Hovatta et al., 2005; Miller et al., 2010; Mozhui et al., 2010). Our study further confirms these findings. Moreover, although similar molecular pathways are involved in the regulation of anxiety-like behavior in both strains, they show opposite directionality in some gene expression profiles. Importantly, the converging analyses between mouse and human gene expression data showed a similar pattern between the D2 mice exposed to CSDS and the PD patients after exposure-induced panic attack. This might be important for future translational research as currently most of the animal models in anxiety disorders use the B6 and not the D2 strain (Bryant et al., 2008).

6.3.5 The multiple comparison problem in genome-wide studies

Due to rapid advances in the fields of RNA-seq and mass spectrometry, we can now simultaneously measure the expression of thousands to tens of thousands of genes and proteins. This inevitably leads to statistical testing of more than one hypothesis at the same time (i.e., multiple comparisons) and therefore requires proper adjustment. Although much progress has been made in recent years, the selection of a proper method that considers the different experimental properties of the studies remains difficult (Hardcastle and Kelly, 2010; Li et al., 2012; Chen et al., 2017). As most of our study has an exploratory and relative character (i.e., relative comparison of the studied data sets), we reported genes and proteins to be DE as those with nominal $P < 0.05$. Although this inevitably led to a number of false-positive findings, the

possibility of a large number of identical false positives across a large number of data sets presented in this study is also highly unlikely. We rely on future studies to replicate our results.

7 Concluding remarks

Over 15 years have passed since the end of the Human Genome Project, arguably one of the largest human collaborations, which revolutionized the field of genetics and led to considerable innovations in molecular biology, biochemistry, and other fields. Today we can map a person's genome within a few days and at a fraction of the original cost. The progress in genomics has been quickly matched with technical developments in other -omics approaches (e.g., transcriptomics, epigenomics, proteomics, and metabolomics). This allows for integration of different layers of information by understanding the interactions between different molecules, such as genes, mRNAs, miRNAs, proteins and their interplay with the environment (Fig. 26a). With these developments, the promise of precision medicine (i.e., a customized healthcare plan tailored to each individual patient based on his or her intrinsic biology) (Radder et al., 2014) was made.

Even with integrative multi-omics approaches providing detailed information on where to look, we still do not understand which genetic variants are responsible for susceptibility to pathological fear and anxiety nor the precise molecular mechanisms behind these phenotypes. The problem might partially lie within the heterogeneity of the anxiety disorder subtypes, the historical approach to their categorization (Fig. 26b) within the DSM, and our currently developing view on anxiety disorders as involving symptoms that are a part of continuous normal state (see section 2.2.3) (Iacono, 2016). It is probably also related to the insufficient statistical power in the currently available GWAS studies of anxiety disorders (Otowa et al., 2016). However, the methodologies we use and how we approach a given scientific problem may also play a role.

Studies of human neuroscience and genetics have traditionally followed a reductionist approach, namely an understanding of a complex system or phenomenon has been achieved by learning about its individual parts, such as studying sequence information from an individual cell (through single-cell sequencing) (Hwang et al., 2018), using model organisms (Hovatta et al., 2005), or genetic isolates with reduced genetic and environmental heterogeneity (Peltonen et al., 2000). Such approaches have been successful in the past and led to advances in tackling complex problems such as memory (Kandel and Spencer, 1968) or processing of visual sensory information (Hubel and Wiesel, 1962). However, the reductionist approach also has its limitations. Although the visual system constructs a complex representation of visual

information from simple stimulus, with rare exceptions (Quiroga et al., 2005), the model cannot explain the complexity of our visual system. This is because most complex systems are not only the sum of their parts (Fig. 26d) but are also their connections, both direct and indirect. Although learning about their components is meaningful, we cannot understand the whole, or modify it, by understanding or modifying its parts, as the process of forming connections is equal to the process of correcting the existing ones, thus leading to a Catch-22 (Fig. 26e). Such complex systems need a blueprint (e.g., our genome) to know what the outcome should be before they begin. However, they are not all created equal, e.g., monozygotic twins receive an unequal random number of mitochondria with the first cell division, nor are they all linear, e.g., the random motion of particles suspended in liquids, such as cytoplasm, known as Brownian movements (Fig. 26f-j). These unequal initial conditions result in diverging outcomes over a protracted time period, rendering long-term predictions of its approximate behavior difficult. The noise is an important part of this complex system, and by removing it we cannot answer the questions about the system as a whole (Fig. 26j) regardless of the degree of magnification we are using. Therefore, we need to embrace the chaos and develop new mathematical models instead (Macau, 2018). Because, unlike the answer in The Hitchhiker's Guide to the Galaxy, the answer to understanding complex diseases will not be simply *forty-two*, but please *Don't panic*.

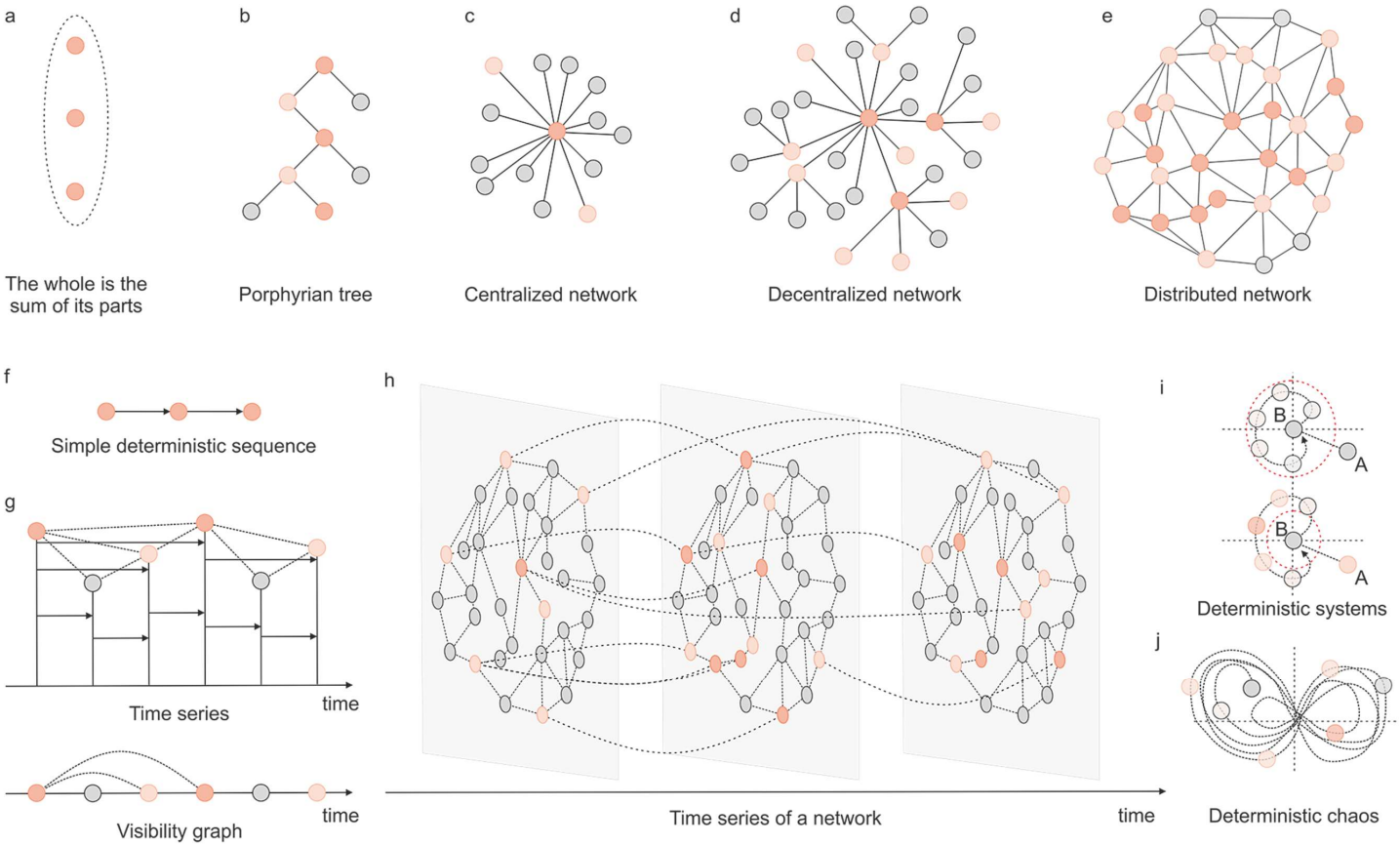

Figure 26. From a node to chaos. (a) *The whole is greater than the sum of its parts*, e.g., not only the molecules, but also the interactions between them are important to decipher complex diseases. **(b)** Tree-like diagram created by the logician Porphyry of multi-level dichotomous divisions that allow for a logical classification based on exclusion. **(c)** Centralized network (i.e., a network with a single central "hub" node). If the "hub" node collapses, the whole network disintegrates. **(d)** Decentralized network (i.e., a network with several "hub" nodes).

Figure 26. From a node to chaos (cont.). (e) Distributed network, which can also be understood as an example of a rhizome (Deleuze and Guattari, 1988). The network cannot be untangled as all its points are connected, and the process of forming connections is equal to the process of correcting the existing ones. Therefore, the description of a rhizome is always *local*, with each local description having the tendency of becoming a global hypothesis (see panels **c** and **d**) from an outsider's point of view (Eco and Oldcorn, 2014). **(f)** Simple deterministic sequence showing that a particular input will always produce the same output. **(g)** Time series, showing a single node of a network indexed in time order. Time series can be also mapped to a visibility graph (lower panel) (Lacasa et al., 2008). **(h)** Time series of a distributed network. **(i)** Examples of simple deterministic systems showing a dysregulation of a single node. The node *aims* to return to its initial condition *(homeostasis),* while traveling across time along a predictable path. As the path is predictable, we can determine the state of the node at any given time and its interactions with other connected nods. The tolerability towards the deviation from the initial condition can differ across the connections between two nodes (i.e., nodes A and B) **(j)** A deterministic chaos, or simply chaos. In a chaotic system, small differences in the initial condition of a node result in diverging outcomes, rendering long-term predictions impossible. As in other deterministic systems, this system is sensitive to its initial condition. Importantly, chaotic systems are also characterized by topological mixing (i.e., nodes that are arbitrarily far apart will eventually look nearly the same) that give the illusion of being identical while they are in fact different.

8 Acknowledgments

The present study was carried out at the Faculty of Biological and Environmental Sciences, University of Helsinki, Finland, and the Max Planck Institute of Psychiatry, Munich, Germany, with generous financial support from the ERA-NET NEURON grant, the Sigrid Jusélius Foundation, the Doctoral Programme Brain & Mind, the Orion Research Foundation and the Max Planck Society.

First and foremost, I would like to warmly thank my supervisor Professor Iiris Hovatta for giving me the opportunity to work on many exciting projects during my years in her laboratory. Thank you for your contagious passion for science, critical thinking and teaching me about my strengths and weaknesses, which will be invaluable in my future as a scientist.

I am extremely grateful to Professor Christoph W. Turck for welcoming me to his group during my stay at the Max Planck Institute of Psychiatry. Thank you for your unlimited support and trust in me. It has been a pleasure to work with you. I would also like to thank Professor Alon Chen, Dr. Angelika Erhardt and the members of their groups for the collaboration on the ERA-NET NEURON project.

I would like to express my gratitude to my thesis committee group members, Professor Samuli Ripatti and Professor Eero Catsrén, for their intellectual support. Professor Mikko Hiltunen and Adjunct Professor Eleanor Coffey are greatly acknowledged for carefully reviewing my thesis. I value the insightful feedback and suggestions you have given me. I am honored and delighted to have Professor John F. Cryan as my Opponent and Professor Juha Partanen as my Custos. I also wish to thank Professor Aarno Palotie for his kindness and understanding during the process of writing this thesis.

I am truly appreciative of all my collaborators and co-authors without whom the work included in this thesis would not have been possible. I would especially like to thank Research Director and Docent Petri Auvinen and Laboratory engineer Lars Paulin from the DNA Sequencing and Genomics Laboratory, Institute of Biotechnology, Docent Vootele Voikar from the Mouse

Behavioral Phenotyping Facility and Dr. Tero Hiekkalinna for generously sharing with me their time and vast knowledge.

I wish to thank all the past and current members of both Hovatta and Turck groups for their important role during my PhD studies. I am extremely grateful to Laura Salminen for working alongside me all those years and for all the fun moments we had together. My gratitude extends to Assistant Professor Michaela Filiou, Dr. Helena Passarelli Giroud Joaquim, Dr. Dong Ik Park, Dr. Frederik Dethloff, Christiane Rewerts, Božidar Novak, Sanna Kängsep, Suvi Saarnio, Juho Väänänen, Jenni Lahtinen, Dr. Ari Rouhiainen, Dr. Natalia Kulesskaya, Dr. Ewa Sokolowska, Dr. Ingrid Balcells, Dr. Kalevi Trontti, Mikaela Laine, Luis Rodrigues, Dr. Giuseppina Maccarrone, Marie Mennesson, Saija Anita-Callan, Dr. Katherine Icay, Sini Kerminen, Judit Garcia, Lea Urpa, Dr. Barbara Liori, Karin Yeoh and Yan Yu.

Above all, I wish to thank my friends and family for their love and support. Thank you Mom, Dad, grandparents, Magdalena, Karolina, Margo, Cori, Marc, Josep M, Eva, Miquel, Enriqueta and William. More than anything, I am grateful to Marc for being by my side through all those years and always filling our home, wherever it has been, with music, warmth, laughter and unconditional love.

Helsinki, March 2019
Zuzanna Misiewicz

9 References

23andme. 2018. Available: https://medical.23andme.com/wp-content/uploads/2018/08/Fear-of-Heights.pdf [Accessed November 2, 2018].

Aggarwal, S., Yurlova, L. and Simons, M. 2011. Central nervous system myelin: structure, synthesis and assembly. *Trends Cell Biol,* 21, 585-93.

Albert, P. R., Vahid-Ansari, F. and Luckhart, C. 2014. Serotonin-prefrontal cortical circuitry in anxiety and depression phenotypes: pivotal role of pre- and post-synaptic 5-HT1A receptor expression. *Front Behav Neurosci,* 8, 199.

Alberts, B. 2015. Molecular biology of the cell, New York, NY, Garland Science, *Taylor and Francis Group*, pp. 198-201.

Alexa, A., Rahnenfuhrer, J. and Lengauer, T. 2006. Improved scoring of functional groups from gene expression data by decorrelating GO graph structure. *Bioinformatics,* 22, 1600-7.

Allsop, S. A., Vander Weele, C. M., Wichmann, R. and Tye, K. M. 2014. Optogenetic insights on the relationship between anxiety-related behaviors and social deficits. *Front Behav Neurosci,* 8, 241.

Almeida, A., Almeida, J., Bolanos, J. P. and Moncada, S. 2001. Different responses of astrocytes and neurons to nitric oxide: the role of glycolytically generated ATP in astrocyte protection. *Proc Natl Acad Sci U S A,* 98, 15294-9.

Alonso, J., Lepine, J. P. and Committee, E. S. M. S. 2007. Overview of key data from the European Study of the Epidemiology of Mental Disorders (ESEMeD). *J Clin Psychiatry,* 68 Suppl 2, 3-9.

American Psychiatric Association 2013. *Diagnostic and statistical manual of mental disorders (5th ed.)*, Arlington, VA: American Psychiatric Publishing.

Anders, S., Pyl, P. T. and Huber, W. 2015. HTSeq--a Python framework to work with high-throughput sequencing data. *Bioinformatics*, 31, 166-9.

Andolina, D., Di Segni, M. and Ventura, R. 2017. MiRNA-34 and stress response. *Oncotarget,* 8, 5658-5659.

Anyan, J. and Amir, S. 2018. Too Depressed to Swim or Too Afraid to Stop? A Reinterpretation of the Forced Swim Test as a Measure of Anxiety-Like Behavior. *Neuropsychopharmacology,* 43, 931-933.

Arai, I., Tsuyuki, Y., Shiomoto, H., Satoh, M. and Otomo, S. 2000. Decreased body temperature dependent appearance of behavioral despair in the forced swimming test in mice. *Pharmacol Res,* 42, 171-6.

Arajarvi, R., Ukkola, J., Haukka, J., Suvisaari, J., Hintikka, J., Partonen, T. and Lonnqvist, J. 2006. Psychosis among "healthy" siblings of schizophrenia patients. *BMC Psychiatry,* 6, 6.

Ashbrook, D. G., Gini, B. and Hager, R. 2015. Genetic variation in offspring indirectly influences the quality of maternal behaviour in mice. *Elife,* 4.

Avramopoulos, D., Willour, V. L., Zandi, P. P., Huo, Y., Mackinnon, D. F., Potash, J. B., Depaulo, J. R., Jr. and Mcinnis, M. G. 2004. Linkage of bipolar affective disorder on chromosome 8q24: follow-up and parametric analysis. *Mol Psychiatry,* 9, 191-6.

Bagot, R. C., Cates, H. M., Purushothaman, I., Lorsch, Z. S., Walker, D. M., Wang, J., Huang, X., Schluter, O. M., Maze, I., Pena, C. J., Heller, E. A., Issler, O., Wang, M., Song, W. M., Stein, J. L., Liu, X., Doyle, M. A., Scobie, K. N., Sun, H. S., Neve, R. L., Geschwind, D., Dong, Y., Shen, L., Zhang, B. and Nestler, E. J. 2016. Circuit-wide Transcriptional Profiling Reveals Brain Region-Specific Gene Networks Regulating Depression Susceptibility. Neuron, 90, 969-83.

Bandelow, B. and Michaelis, S. 2015. Epidemiology of anxiety disorders in the 21st century. *Dialogues Clin Neurosci,* 17, 327-35.

Baron, R. V., Kollar, C., Mukhopadhyay, N. and Weeks, D. E. 2014. Mega2: validated data-reformatting for linkage and association analyses. *Source Code Biol Med*, 9, 26.

Bartel, D. P. 2004. MicroRNAs: genomics, biogenesis, mechanism, and function. *Cell,* 116, 281-97.

Bauernfeind, A. L. and Babbitt, C. C. 2017. The predictive nature of transcript expression levels on protein expression in adult human brain. *BMC Genomics,* 18, 322.

Bavamian, S., Mellios, N., Lalonde, J., Fass, D. M., Wang, J., Sheridan, S. D., Madison, J. M., Zhou, F., Rueckert, E. H., Barker, D., Perlis, R. H., Sur, M. and Haggarty, S. J. 2015. Dysregulation of miR-34a links neuronal development to genetic risk factors for bipolar disorder. *Mol Psychiatry,* 20, 573-84.

Belevich, I., Joensuu, M., Kumar, D., Vihinen, H. and Jokitalo, E. 2016. Microscopy Image Browser: A Platform for Segmentation and Analysis of Multidimensional Datasets. *PLoS Biol,* 14, e1002340.

Benchek, P. H. and Morris, N. J. 2013. How meaningful are heritability estimates of liability? *Hum Genet,* 132, 1351-60.

Berkowitz, R. L., Coplan, J. D., Reddy, D. P. and Gorman, J. M. 2007. The human dimension: how the prefrontal cortex modulates the subcortical fear response. *Rev Neurosci,* 18, 191-207.

Berton, O., Mcclung, C. A., Dileone, R. J., Krishnan, V., Renthal, W., Russo, S. J., Graham, D., Tsankova, N. M., Bolanos, C. A., Rios, M., Monteggia, L. M., Self, D. W. and Nestler, E. J. 2006. Essential role of BDNF in the mesolimbic dopamine pathway in social defeat stress. *Science,* 311, 864-8.

Bhat, A., Heath, S. C. and Ott, J. 1999. Heterogeneity for multiple disease loci in linkage analysis. *Hum Hered,* 49, 229-31.

Bhatnagar, S., Chertkow, H., Schipper, H. M., Yuan, Z., Shetty, V., Jenkins, S., Jones, T. and Wang, E. 2014. Increased microRNA-34c abundance in Alzheimer's disease circulating blood plasma. *Front Mol Neurosci,* 7, 2.

Bibb, M. J., Van Etten, R. A., Wright, C. T., Walberg, M. W. and Clayton, D. A. 1981. Sequence and gene organization of mouse mitochondrial DNA. *Cell,* 26, 167-80.

Bodmer, W. and Bonilla, C. 2008. Common and rare variants in multifactorial susceptibility to common diseases. *Nat Genet,* 40, 695-701.

Bouton, M. E. 2002. Context, ambiguity, and unlearning: sources of relapse after behavioral extinction. *Biol Psychiatry,* 52, 976-86.

Brandt, T., Kugler, G., Schniepp, R., Wuehr, M. and Huppert, D. 2015. Acrophobia impairs visual exploration and balance during standing and walking. *Ann N Y Acad Sci,* 1343, 37-48.

Bryant, C. D., Zhang, N. N., Sokoloff, G., Fanselow, M. S., Ennes, H. S., Palmer, A. A. and Mcroberts, J. A. 2008. Behavioral differences among C57BL/6 substrains: implications for transgenic and knockout studies. *J Neurogenet,* 22, 315-31.

Brydges, N. M., Jin, R., Seckl, J., Holmes, M. C., Drake, A. J. and Hall, J. 2014. Juvenile stress enhances anxiety and alters corticosteroid receptor expression in adulthood. *Brain Behav,* 4, 4-13.

Buchanan, A. V., Weiss, K. M. and Fullerton, S. M. 2006. Dissecting complex disease: the quest for the Philosopher's Stone? *Int J Epidemiol,* 35, 562-71.

Bumgarner, R. 2013. Overview of DNA microarrays: types, applications, and their future. *Curr Protoc Mol Biol,* Chapter 22, Unit 22 1.

Bushel, P. 2018. PVCA: Principal Variance Component Analysis (PVCA). R package version 1.22.0. https://bioconductor.org/packages/release/bioc/manuals/pvca/man/pvca.pdf [Accessed November 1, 2018]

Campos, A. C., Fogaca, M. V., Aguiar, D. C. and Guimaraes, F. S. 2013. Animal models of anxiety disorders and stress. *Braz J Psychiatr,* 35 Suppl 2, S101-11.

Can, A., Dao, D. T., Arad, M., Terrillion, C. E., Piantadosi, S. C. and Gould, T. D. 2012. The mouse forced swim test. *J Vis Exp*, e3638

Carlen, M. 2017. What constitutes the prefrontal cortex? *Science,* 358, 478-482.

Carlyle, B. C., Kitchen, R. R., Kanyo, J. E., Voss, E. Z., Pletikos, M., Sousa, A. M. M., Lam, T. T., Gerstein, M. B., Sestan, N. and Nairn, A. C. 2017. A multiregional proteomic survey of the postnatal human brain. *Nat Neurosci,* 20, 1787-1795.

Catalanotto, C., Cogoni, C. and Zardo, G. 2016. MicroRNA in Control of Gene Expression: An Overview of Nuclear Functions. *Int J Mol Sci,* 17.

Chadick, J. Z., Zanto, T. P. and Gazzaley, A. 2014. Structural and functional differences in medial prefrontal cortex underlie distractibility and suppression deficits in ageing. *Nat Commun,* 5, 4223.

Chamrad, D. C., Koerting, G., Gobom, J., Thiele, H., Klose, J., Meyer, H. E. and Blueggel, M. 2003. Interpretation of mass spectrometry data for high-throughput proteomics. *Anal Bioanal Chem*, 376, 1014-22.

Chang, K. J., Redmond, S. A. and Chan, J. R. 2016. Remodeling myelination: implications for mechanisms of neural plasticity. *Nat Neurosci,* 19, 190-7.

Chen, L., Heikkinen, L., Wang, C., Yang, Y., Sun, H. and Wong, G. 2018. Trends in the development of miRNA bioinformatics tools. *Brief Bioinform*.

Chen, S. Y., Feng, Z. and Yi, X. 2017. A general introduction to adjustment for multiple comparisons. *J Thorac Dis,* 9, 1725-1729.

Choi, W. S., Lee, B. H., Yang, J. C. and Kim, Y. K. 2010. Association Study between 5-HT1A Receptor Gene C(-1019)G Polymorphism and Panic Disorder in a Korean Population. *Psychiatry Investig,* 7, 141-6.

Coelho, C. M. and Wallis, G. 2010. Deconstructing acrophobia: physiological and psychological precursors to developing a fear of heights. *Depress Anxiety,* 27, 864-70.

Commons, K. G., Cholanians, A. B., Babb, J. A. and Ehlinger, D. G. 2017. The Rodent Forced Swim Test Measures Stress-Coping Strategy, Not Depression-like Behavior. *ACS Chem Neurosci,* 8, 955-960.

Conway, J. R., Lex, A. and Gehlenborg, N. 2017. UpSetR: an R package for the visualization of intersecting sets and their properties. *Bioinformatics,* 33, 2938-2940.

Cottingham, R. W., Jr., Idury, R. M. and Schaffer, A. A. 1993. Faster sequential genetic linkage computations. *Am J Hum Genet,* 53, 252-63.

Cox, J. and Mann, M. 2012. 1D and 2D annotation enrichment: a statistical method integrating quantitative proteomics with complementary high-throughput data. *BMC Bioinformatics*, 13 Suppl 16, S12.

Craske, M. G., Stein, M. B., Eley, T. C., Milad, M. R., Holmes, A., Rapee, R. M. and Wittchen, H. U. 2017. Anxiety disorders. *Nat Rev Dis Primers,* 3, 17024.

Cryan, J. F. and Holmes, A. 2005. The ascent of mouse: advances in modelling human depression and anxiety. *Nat Rev Drug Discov,* 4, 775-90.

David, D. J., Renard, C. E., Jolliet, P., Hascoet, M. and Bourin, M. 2003. Antidepressant-like effects in various mice strains in the forced swimming test. *Psychopharmacology (Berl),* 166, 373-82.

Davis, M. M., Olausson, P., Greengard, P., Taylor, J. R. and Nairn, A. C. 2012. Regulator of calmodulin signaling knockout mice display anxiety-like behavior and motivational deficits. Eur J Neurosci, 35, 300-8.

Deacon, R. M., Bannerman, D. M. and Rawlins, J. N. 2002. Anxiolytic effects of cytotoxic hippocampal lesions in rats. *Behav Neurosci,* 116, 494-7.

De Kloet, E. R. and Molendijk, M. L. 2016. Coping with the Forced Swim Stressor: Towards Understanding an Adaptive Mechanism. *Neural Plast,* 2016, 6503162.

Deckert, J., Catalano, M., Syagailo, Y. V., Bosi, M., Okladnova, O., Di Bella, D., Nothen, M. M., Maffei, P., Franke, P., Fritze, J., Maier, W., Propping, P., Beckmann, H., Bellodi, L. and Lesch, K. P. 1999. Excess of high activity monoamine oxidase A gene promoter alleles in female patients with panic disorder. *Hum Mol Genet,* 8, 621-4.

Deckert, J., Nothen, M. M., Franke, P., Delmo, C., Fritze, J., Knapp, M., Maier, W., Beckmann, H. and Propping, P. 1998. Systematic mutation screening and association study of the A1 and A2a adenosine receptor genes in panic disorder suggest a contribution of the A2a gene to the development of disease. *Mol Psychiatry,* 3, 81-5.

Deleuze, G. and Guattari, F. 1988. *A thousand plateaus: capitalism and schizophrenia,* London, Athlone Press.

Dermitzakis, E. T., Reymond, A. and Antonarakis, S. E. 2005. Conserved non-genic sequences - an unexpected feature of mammalian genomes. *Nat Rev Genet,* 6, 151-7.

Diz, A. P., Carvajal-Rodriguez, A. and Skibinski, D. O. 2011. Multiple hypothesis testing in proteomics: a strategy for experimental work. *Mol Cell Proteomics,* 10, M110 004374.

Dobin, A., Davis, C. A., Schlesinger, F., Drenkow, J., Zaleski, C., Jha, S., Batut, P., Chaisson, M. and Gingeras, T. R. 2013. STAR: ultrafast universal RNA-seq aligner. *Bioinformatics*, 29, 15-21.

Domschke, K. and Maron, E. 2013. Genetic factors in anxiety disorders. *Mod Trends Pharmacopsychiatry,* 29, 24-46.

Donner, J., Haapakoski, R., Ezer, S., Melen, E., Pirkola, S., Gratacos, M., Zucchelli, M., Anedda, F., Johansson, L. E., Soderhall, C., Orsmark-Pietras, C., Suvisaari, J., Martin-Santos, R., Torrens, M., Silander, K., Terwilliger, J. D., Wickman, M., Pershagen, G., Lonnqvist, J., Peltonen, L., Estivill, X., D'amato, M., Kere, J., Alenius, H. and Hovatta, I. 2010. Assessment of the neuropeptide S system in anxiety disorders. *Biol Psychiatry,* 68, 474-83.

Dudbridge, F. 2003. A survey of current software for linkage analysis. *Hum Genomics,* 1, 63-5.

Dulawa, S. C. and Hen, R. 2005. Recent advances in animal models of chronic antidepressant effects: the novelty-induced hypophagia test. *Neurosci Biobehav Rev*, 29, 771-83.

Dutta, D. J., Woo, D. H., Lee, P. R., Pajevic, S., Bukalo, O., Huffman, W. C., Wake, H., Basser, P. J., Sheikhbahaei, S., Lazarevic, V., Smith, J. C. and Fields, R. D. 2018. Regulation of myelin structure and conduction velocity by perinodal astrocytes. *Proc Natl Acad Sci U S A,* 115, 11832-11837.

Eco, U. and Oldcorn, A. 2014. *From the tree to the labyrinth: historical studies on the sign and interpretation,* Cambridge, Massachusetts, Harvard University Press.

Eddelbuettel, D. and Balamuta, J. 2018. Extending R with C++: A Brief Introduction to Rcpp. The Amer Stat, 1, 28-36.

Eisner, V., Picard, M. and Hajnoczky, G. 2018. Mitochondrial dynamics in adaptive and maladaptive cellular stress responses. *Nat Cell Biol,* 20, 755-765.

Emes, R. D., Riley, M. C., Laukaitis, C. M., Goodstadt, L., Karn, R. C. and Ponting, C. P. 2004. Comparative evolutionary genomics of androgen-binding protein genes. *Genome Res,* 14, 1516-29.

Encode Project Consortium 2012. An integrated encyclopedia of DNA elements in the human genome. *Nature,* 489, 57-74.

Erhardt, A. and Spoormaker, V. I. 2013. Translational approaches to anxiety: focus on genetics, fear extinction and brain imaging. *Curr Psychiatry Rep,* 15, 417.

Faravelli, C., Lo Sauro, C., Lelli, L., Pietrini, F., Lazzeretti, L., Godini, L., Benni, L., Fioravanti, G., Talamba, G. A., Castellini, G. and Ricca, V. 2012. The role of life events and HPA axis in anxiety disorders: a review. *Curr Pharm Des,* 18, 5663-74.

Femminella, G. D., Ferrara, N. and Rengo, G. 2015. The emerging role of microRNAs in Alzheimer's disease. *Front Physiol,* 6, 40.

Fields, R. D. 2014. Myelin formation and remodeling. *Cell,* 156, 15-7.

Filiou, M. D., Turck, C. W. and Martins-De-Souza, D. 2011. Quantitative proteomics for investigating psychiatric disorders. *Proteomics Clin Appl,* 5, 38-49.

Fisher, R. 1918. The correlation between relatives on the supposition of Mendelian inheritance. *Trans R Soc Edinb*, 399–433.

Francis, J. L., Moitra, E., Dyck, I. and Keller, M. B. 2012. The impact of stressful life events on relapse of generalized anxiety disorder. *Depress Anxiety,* 29, 386-91.

Freimer, N. and Sabatti, C. 2004. The use of pedigree, sib-pair and association studies of common diseases for genetic mapping and epidemiology. *Nat Genet,* 36, 1045-51.

Friedman, A. K., Juarez, B., Ku, S. M., Zhang, H., Calizo, R. C., Walsh, J. J., Chaudhury, D., Zhang, S., Hawkins, A., Dietz, D. M., Murrough, J. W., Ribadeneira, M., Wong, E. H., Neve, R. L. and Han, M. H. 2016. KCNQ channel openers reverse depressive symptoms via an active resilience mechanism. *Nat Commun,* 7, 11671.

Funfschilling, U., Supplie, L. M., Mahad, D., Boretius, S., Saab, A. S., Edgar, J., Brinkmann, B. G., Kassmann, C. M., Tzvetanova, I. D., Mobius, W., Diaz, F., Meijer, D., Suter, U., Hamprecht, B., Sereda, M. W., Moraes, C. T., Frahm, J., Goebbels, S. and Nave, K. A. 2012. Glycolytic oligodendrocytes maintain myelin and long-term axonal integrity. *Nature,* 485, 517-21.

Gabriel, S. B., Schaffner, S. F., Nguyen, H., Moore, J. M., Roy, J., Blumenstiel, B., Higgins, J., Defelice, M., Lochner, A., Faggart, M., Liu-Cordero, S. N., Rotimi, C., Adeyemo, A., Cooper, R., Ward, R., Lander, E. S., Daly, M. J. and Altshuler, D. 2002. The structure of haplotype blocks in the human genome. *Science,* 296, 2225-9.

Gantier, M. P., Mccoy, C. E., Rusinova, I., Saulep, D., Wang, D., Xu, D., Irving, A. T., Behlke, M. A., Hertzog, P. J., Mackay, F. and Williams, B. R. 2011. Analysis of microRNA turnover in mammalian cells following Dicer1 ablation. *Nucleic Acids Res,* 39, 5692-703.

Garakani, A., Martinez, J. M., Aaronson, C. J., Voustianiouk, A., Kaufmann, H. and Gorman, J. M. 2009. Effect of medication and psychotherapy on heart rate variability in panic disorder. *Depress Anxiety,* 26, 251-8.

GENCODE. 2018. Available: https://www.gencodegenes.org/ [Accessed November 2, 2018].

Gerra, G., Zaimovic, A., Zambelli, U., Timpano, M., Reali, N., Bernasconi, S. and Brambilla, F. 2000. Neuroendocrine responses to psychological stress in adolescents with anxiety disorder. *Neuropsychobiology,* 42, 82-92.

Gertz, E. M. et al. 2014. PSEUDOMARKER 2.0: efficient computation of likelihoods using NOMAD. *BMC Bioinformatics* 15, 47.

Gibson, E. M., Purger, D., Mount, C. W., Goldstein, A. K., Lin, G. L., Wood, L. S., Inema, I., Miller, S. E., Bieri, G., Zuchero, J. B., Barres, B. A., Woo, P. J., Vogel, H. and Monje, M. 2014. Neuronal activity promotes oligodendrogenesis and adaptive myelination in the mammalian brain. *Science,* 344, 1252304.

Gleick, J. 2008. *Chaos: making a new science,* New York, N.Y., Penguin Books.

Glish, G. L. and Vachet, R. W. 2003. The basics of mass spectrometry in the twenty-first century. *Nat Rev Drug Discov,* 2, 140-50.

Golden, S. A., Covington, H. E., 3rd, Berton, O. and Russo, S. J. 2011. A standardized protocol for repeated social defeat stress in mice. *Nat Protoc,* 6, 1183-91.

Gonzalez, S., Camarillo, C., Rodriguez, M., Ramirez, M., Zavala, J., Armas, R., Contreras, S. A., Contreras, J., Dassori, A., Almasy, L., Flores, D., Jerez, A., Raventos, H., Ontiveros, A., Nicolini, H. and Escamilla, M. 2014. A genome-wide linkage scan of bipolar disorder in Latino families identifies susceptibility loci at 8q24 and 14q32. *Am J Med Genet B Neuropsychiatr Genet,* 165B, 479-91.

Goode, E. L., Badzioch, M. D. and Jarvik, G. P. 2005. Bias of allele-sharing linkage statistics in the presence of intermarker linkage disequilibrium. *BMC Genet,* 6 Suppl 1, S82.

Goodwin, R. D., Faravelli, C., Rosi, S., Cosci, F., Truglia, E., De Graaf, R. and Wittchen, H. U. 2005. The epidemiology of panic disorder and agoraphobia in Europe. *Eur Neuropsychopharmacol,* 15, 435-43.

Gordon, A. and Hannon. G.J. 2010. FASTX-Toolkit. FASTQ/A short-reads pre-processing tools. http://hannonlab.cshl.edu/fastx_toolkit/ [Accessed November 1, 2018].

Gordon, J. A. and Hen, R. 2004. The serotonergic system and anxiety. *Neuromolecular Med,* 5, 27-40.

Goto, T., Kubota, Y., Tanaka, Y., Iio, W., Moriya, N. and Toyoda, A. 2014. Subchronic and mild social defeat stress accelerates food intake and body weight gain with polydipsia-like features in mice. *Behav Brain Res*, 270, 339-48.

Gottschalk, M. G. and Domschke, K. 2018. Oxytocin and Anxiety Disorders. *Curr Top Behav Neurosci,* 35, 467-498.

Gray, J. D., Rubin, T. G., Hunter, R. G. and Mcewen, B. S. 2014. Hippocampal gene expression changes underlying stress sensitization and recovery. *Mol Psychiatry,* 19, 1171-8.

Grupe, D. W. and Nitschke, J. B. 2013. Uncertainty and anticipation in anxiety: an integrated neurobiological and psychological perspective. *Nat Rev Neurosci,* 14, 488-501.

Hall C., Ballachey E. L. 1932. A Study of the rat's behavior in a field. A contribution to method in comparative psychology. *Univ. Calif. Publ. Psychol*. 6, 1–12

Hanley, J. A., Negassa, A., Edwardes, M. D. and Forrester, J. E. 2003. Statistical analysis of correlated data using generalized estimating equations: an orientation. *Am J Epidemiol,* 157, 364-75.

Haramati, S., Navon, I., Issler, O., Ezra-Nevo, G., Gil, S., Zwang, R., Hornstein, E. and Chen, A. 2011. MicroRNA as repressors of stress-induced anxiety: the case of amygdalar miR-34. *J Neurosci,* 31, 14191-203.

Hardcastle, T. J. and Kelly, K. A. 2010. baySeq: empirical Bayesian methods for identifying differential expression in sequence count data. *BMC Bioinformatics,* 11, 422.

Hartley, C. A., Gorun, A., Reddan, M. C., Ramirez, F. and Phelps, E. A. 2014. Stressor controllability modulates fear extinction in humans. *Neurobiol Learn Mem,* 113, 149-56.

Hasin, Y., Seldin, M. and Lusis, A. 2017. Multi-omics approaches to disease. *Genome Biol,* 18, 83.

Hettema, J. M., Neale, M. C. and Kendler, K. S. 2001. A review and meta-analysis of the genetic epidemiology of anxiety disorders. *Am J Psychiatry,* 158, 1568-78.

Hiekkalinna, T. 2012. *On the superior power of likelihoodbased linkage disequilibrium mapping in large multiplex families compared to population based case-control designs*. Available: https://helda.helsinki.fi/bitstream/handle/10138/36771/onthesup.pdf?sequence=1 [Accessed November 2, 2018].

Hiekkalinna, T., Schaffer, A. A., Lambert, B., Norrgrann, P., Goring, H. H. and Terwilliger, J. D. 2011. PSEUDOMARKER: a powerful program for joint linkage and/or linkage disequilibrium analysis on mixtures of singletons and related individuals. *Hum Hered,* 71, 256-66.

Hindorff, L. A., Gillanders, E. M. and Manolio, T. A. 2011. Genetic architecture of cancer and other complex diseases: lessons learned and future directions. *Carcinogenesis,* 32, 945-54.

Hohoff, C., Mullings, E. L., Heatherley, S. V., Freitag, C. M., Neumann, L. C., Domschke, K., Krakowitzky, P., Rothermundt, M., Keck, M. E., Erhardt, A., Unschuld, P. G., Jacob, C., Fritze, J., Bandelow, B., Maier, W., Holsboer, F., Rogers, P. J. and Deckert, J. 2010. Adenosine A(2A) receptor gene: evidence for association of risk variants with panic disorder and anxious personality. *J Psychiatr Res,* 44, 930-7.

Holmans, P. A., Riley, B., Pulver, A. E., Owen, M. J., Wildenauer, D. B., Gejman, P. V., Mowry, B. J., Laurent, C., Kendler, K. S., Nestadt, G., Williams, N. M., Schwab, S. G., Sanders, A. R., Nertney, D., Mallet, J., Wormley, B., Lasseter, V. K., O'donovan, M. C., Duan, J., Albus, M., Alexander, M., Godard, S., Ribble, R., Liang, K. Y., Norton, N., Maier, W., Papadimitriou, G., Walsh, D., Jay, M., O'neill, A., Lerer, F. B., Dikeos, D., Crowe, R. R., Silverman, J. M. and Levinson, D. F. 2009. Genomewide linkage scan of schizophrenia in a large multicenter pedigree sample using single nucleotide polymorphisms. *Mol Psychiatry,* 14, 786-95.

Holmes, T. H. and Rahe, R. H. 1967. The Social Readjustment Rating Scale. *J Psychosom Res,* 11, 213-8.

Hovatta, I., Tennant, R. S., Helton, R., Marr, R. A., Singer, O., Redwine, J. M., Ellison, J. A., Schadt, E. E., Verma, I. M., Lockhart, D. J. and Barlow, C. 2005. Glyoxalase 1 and glutathione reductase 1 regulate anxiety in mice. *Nature,* 438, 662-6.

Hovatta, I., Varilo, T., Suvisaari, J., Terwilliger, J. D., Ollikainen, V., Arajarvi, R., Juvonen, H., Kokko-Sahin, M. L., Vaisanen, L., Mannila, H., Lonnqvist, J. and Peltonen, L. 1999. A genomewide screen for schizophrenia genes in an isolated Finnish subpopulation, suggesting multiple susceptibility loci. *Am J Hum Genet,* 65, 1114-24.

Hroudova, J. and Fisar, Z. 2011. Connectivity between mitochondrial functions and psychiatric disorders. *Psychiatry Clin Neurosci,* 65, 130-41.

Hu, J., Sathanoori, M., Kochmar, S., Azage, M., Mann, S., Madan-Khetarpal, S., Goldstein, A. and Surti, U. 2015. A novel maternally inherited 8q24.3 and a rare paternally inherited 14q23.3 CNVs in a family with neurodevelopmental disorders. *Am J Med Genet A,* 167A, 1921-6.

Hubel, D. H. and Wiesel, T. N. 1962. Receptive fields, binocular interaction and functional architecture in the cat's visual cortex. *J Physiol,* 160, 106-54.

Hunsberger, J. G., Austin, D. R., Chen, G. and Manji, H. K. 2009. MicroRNAs in mental health: from biological underpinnings to potential therapies. *Neuromolecular Med,* 11, 173-82.

Hwang, B., Lee, J. H. and Bang, D. 2018. Single-cell RNA sequencing technologies and bioinformatics pipelines. *Exp Mol Med,* 50, 96.

Iacono, W. G. 2016. Achieving success with the Research Domain Criteria (RDoC): Going beyond the matrix. *Psychophysiology,* 53, 308-11.

Innocenti, G. M. and Caminiti, R. 2017. Axon diameter relates to synaptic bouton size: structural properties define computationally different types of cortical connections in primates. *Brain Struct Funct,* 222, 1169-1177.

International Human Genome Sequencing, C. 2004. Finishing the euchromatic sequence of the human genome. *Nature,* 431, 931-45.

Issler, O. and Chen, A. 2015. Determining the role of microRNAs in psychiatric disorders. *Nat Rev Neurosci,* 16, 201-12.

Jacobson, L. H. and Cryan, J. F. 2007. Feeling strained? Influence of genetic background on depression-related behavior in mice: a review. *Behav Genet,* 37, 171-213.

Jin, H. M., Shrestha Muna, S., Bagalkot, T. R., Cui, Y., Yadav, B. K. and Chung, Y. C. 2015. The effects of social defeat on behavior and dopaminergic markers in mice. *Neuroscience,* 288, 167-77.

Johnson, W. E., Li, C. and Rabinovic, A. 2007. Adjusting batch effects in microarray expression data using empirical Bayes methods. *Biostatistics*, 8, 118-27.

Jung, E. J., Im, D. H., Park, Y. H., Byun, J. M., Kim, Y. N., Jeong, D. H., Sung, M. S., Kim, K. T., An, H. J., Jung, S. J. and Lee, K. B. 2017. Female with 46, XY karyotype. *Obstet Gynecol Sci,* 60, 378-382.

Kaminsky, Z., Jones, I., Verma, R., Saleh, L., Trivedi, H., Guintivano, J., Akman, R., Zandi, P., Lee, R. S. and Potash, J. B. 2015. DNA methylation and expression of KCNQ3 in bipolar disorder. *Bipolar Disord,* 17, 150-9.

Kandel, E. R. and Spencer, W. A. 1968. Cellular neurophysiological approaches in the study of learning. *Physiol Rev,* 48, 65-134.

Kapfhammer, H. P., Fitz, W., Huppert, D., Grill, E. and Brandt, T. 2016. Visual height intolerance and acrophobia: distressing partners for life. *J Neurol,* 263, 1946-53.

Karagkouni, D., Paraskevopoulou, M. D., Chatzopoulos, S., Vlachos, I. S., Tastsoglou, S., Kanellos, I., Papadimitriou, D., Kavakiotis, I., Maniou, S., Skoufos, G., Vergoulis, T., Dalamagas, T. and Hatzigeorgiou, A. G. 2018. DIANA-TarBase v8: a decade-long collection of experimentally supported miRNA-gene interactions. *Nucleic Acids Res,* 46, D239-D245.

Karnkowska, A., Vacek, V., Zubacova, Z., Treitli, S. C., Petrzelkova, R., Eme, L., Novak, L., Zarsky, V., Barlow, L. D., Herman, E. K., Soukal, P., Hroudova, M., Dolezal, P., Stairs, C. W., Roger, A. J., Elias, M., Dacks, J. B., Vlcek, C. and Hampl, V. 2016. A Eukaryote without a Mitochondrial Organelle. *Curr Biol,* 26, 1274-84.

Karpievitch, Y., Stanley, J., Taverner, T., Huang, J., Adkins, J. N., Ansong, C., Heffron, F., Metz, T. O., Qian, W. J., Yoon, H., Smith, R. D. and Dabney, A. R. 2009. A statistical framework for protein quantitation in bottom-up MS-based proteomics. *Bioinformatics*, 25, 2028-34.

Kessler, R. C., Aguilar-Gaxiola, S., Alonso, J., Chatterji, S., Lee, S., Ormel, J., Ustun, T. B. and Wang, P. S. 2009. The global burden of mental disorders: an update from the WHO World Mental Health (WMH) surveys. *Epidemiol Psichiatr Soc,* 18, 23-33.

Kessler, R. C., Angermeyer, M., Anthony, J. C., R, D. E. G., Demyttenaere, K., Gasquet, I., G, D. E. G., Gluzman, S., Gureje, O., Haro, J. M., Kawakami, N., Karam, A., Levinson, D., Medina Mora, M. E., Oakley Browne, M. A., Posada-Villa, J., Stein, D. J., Adley Tsang, C. H., Aguilar-Gaxiola, S., Alonso, J., Lee, S., Heeringa, S., Pennell, B. E., Berglund, P., Gruber, M. J., Petukhova, M., Chatterji, S. and Ustun, T. B. 2007. Lifetime prevalence and age-of-onset distributions of mental disorders in the World Health Organization's World Mental Health Survey Initiative. *World Psychiatry,* 6, 168-76.

Kessler, R. C., Chiu, W. T., Demler, O., Merikangas, K. R. and Walters, E. E. 2005. Prevalence, severity, and comorbidity of 12-month DSM-IV disorders in the National Comorbidity Survey Replication. *Arch Gen Psychiatry,* 62, 617-27.

Kessler, R. C., Petukhova, M., Sampson, N. A., Zaslavsky, A. M. and Wittchen, H. U. 2012. Twelve-month and lifetime prevalence and lifetime morbid risk of anxiety and mood disorders in the United States. *Int J Methods Psychiatr Res,* 21, 169-84.

Khatri, P., Sirota, M. and Butte, A. J. 2012. Ten years of pathway analysis: current approaches and outstanding challenges. *PLoS Comput Biol,* 8, e1002375.

Kheirallah, A. K., Miller, S., Hall, I. P. and Sayers, I. 2016. Translating Lung Function Genome-Wide Association Study (GWAS) Findings: New Insights for Lung Biology. *Adv Genet,* 93, 57-145.

Kim, S. Y., Adhikari, A., Lee, S. Y., Marshel, J. H., Kim, C. K., Mallory, C. S., Lo, M., Pak, S., Mattis, J., Lim, B. K., Malenka, R. C., Warden, M. R., Neve, R., Tye, K. M. and Deisseroth, K. 2013. Diverging neural pathways assemble a behavioural state from separable features in anxiety. *Nature,* 496, 219-23.

Kolata, G. 2013. Human Genome, Then and Now. *The New Your Times*, April 15, 2013.

Koopman, W. J., Willems, P. H. and Smeitink, J. A. 2012. Monogenic mitochondrial disorders. *N Engl J Med,* 366, 1132-41.

Kopylova, E., Noe, L. and Touzet, H. 2012. SortMeRNA: fast and accurate filtering of ribosomal RNAs in metatranscriptomic data. *Bioinformatics*, 28, 3211-7.

Kovalenko, I. L., Galyamina, A. G., Smagin, D. A., Michurina, T. V., Kudryavtseva, N. N. and Enikolopov, G. 2014. Extended effect of chronic social defeat stress in childhood on behaviors in adulthood. *PLoS One,* 9, e91762.

Kovalenko, I. L., Smagin, D. A., Galyamina, A. G., Orlov, Y. L. and Kudryavtseva, N. N. 2016. [Changes in the Expression of Dopaminergic Genes in Brain Structures of Male Mice Exposed to Chronic Social Defeat Stress: An RNA-seq Study]. *Mol Biol (Mosk),* 50, 184-7.

Krishnan, V., Han, M. H., Graham, D. L., Berton, O., Renthal, W., Russo, S. J., Laplant, Q., Graham, A., Lutter, M., Lagace, D. C., Ghose, S., Reister, R., Tannous, P., Green, T. A., Neve, R. L., Chakravarty, S., Kumar, A., Eisch, A. J., Self, D. W., Lee, F. S., Tamminga, C. A., Cooper, D. C., Gershenfeld, H. K. and Nestler, E. J. 2007. Molecular adaptations underlying susceptibility and resistance to social defeat in brain reward regions. *Cell,* 131, 391-404.

Kulesskaya, N., Karpova, N. N., Ma, L., Tian, L. and Voikar, V. 2014. Mixed housing with DBA/2 mice induces stress in C57BL/6 mice: implications for interventions based on social enrichment. *Front Behav Neurosci,* 8, 257.

Kumar, B., Kuhad, A. and Chopra, K. 2011. Neuropsychopharmacological effect of sesamol in unpredictable chronic mild stress model of depression: behavioral and biochemical evidences. *Psychopharmacology (Berl)*, 214, 819-28.

Kvetnansky, R. and Mikulaj, L. 1970. Adrenal and urinary catecholamines in rats during adaptation to repeated immobilization stress. *Endocrinology*, 87, 738-43.

Lacasa, L., Luque, B., Ballesteros, F., Luque, J. and Nuno, J. C. 2008. From time series to complex networks: the visibility graph. *Proc Natl Acad Sci U S A,* 105, 4972-5.

Lai, C. Y., Yu, S. L., Hsieh, M. H., Chen, C. H., Chen, H. Y., Wen, C. C., Huang, Y. H., Hsiao, P. C., Hsiao, C. K., Liu, C. M., Yang, P. C., Hwu, H. G. and Chen, W. J. 2011. MicroRNA expression aberration as potential peripheral blood biomarkers for schizophrenia. *PLoS One,* 6, e21635.

Laine, M. A., Sokolowska, E., Dudek, M., Callan, S. A., Hyytia, P. and Hovatta, I. 2017. Brain activation induced by chronic psychosocial stress in mice. *Sci Rep,* 7, 15061.

Lam, P., Hong, C. J. and Tsai, S. J. 2005. Association study of A2a adenosine receptor genetic polymorphism in panic disorder. *Neurosci Lett,* 378, 98-101.

Lamers, F., Van Oppen, P., Comijs, H. C., Smit, J. H., Spinhoven, P., Van Balkom, A. J., Nolen, W. A., Zitman, F. G., Beekman, A. T. and Penninx, B. W. 2011. Comorbidity patterns of anxiety and depressive disorders in a large cohort study: the Netherlands Study of Depression and Anxiety (NESDA). *J Clin Psychiatry,* 72, 341-8.

Lander, E. and Kruglyak, L. 1995. Genetic dissection of complex traits: guidelines for interpreting and reporting linkage results. *Nat Genet,* 11, 241-7.

Lander, E. S., Linton, L. M., Birren, B., et al. 2001. Initial sequencing and analysis of the human genome. *Nature,* 409, 860-921.

Landgraf, R. 2005. Neuropeptides in anxiety modulation. *Handb Exp Pharmacol*, 335-69.

Lange, E. M. and Lange, K. 2004. Powerful allele sharing statistics for nonparametric linkage analysis. *Hum. Hered*. 57, 49–58.

Larner, A. J. 2008. Monogenic Mendelian disorders in general neurological practice. *Int J Clin Pract,* 62, 744-6.

Larrieu, T., Cherix, A., Duque, A., Rodrigues, J., Lei, H., Gruetter, R. and Sandi, C. 2017. Hierarchical Status Predicts Behavioral Vulnerability and Nucleus Accumbens Metabolic Profile Following Chronic Social Defeat Stress. *Curr Biol,* 27, 2202-2210 e4.

Lebow, M. A. and Chen, A. 2016. Overshadowed by the amygdala: the bed nucleus of the stria terminalis emerges as key to psychiatric disorders. *Mol Psychiatry,* 21, 450-63.

Ledoux, J. E. 2015. *Anxious: using the brain to understand and treat fear and anxiety,* New York, New York, Viking.

Lee, L. O. and Prescott, C. A. 2014. Association of the catechol-O-methyltransferase val158met polymorphism and anxiety-related traits: a meta-analysis. *Psychiatr Genet,* 24, 52-69.

Lee, Y., Kim, M., Han, J., Yeom, K. H., Lee, S., Baek, S. H. and Kim, V. N. 2004. MicroRNA genes are transcribed by RNA polymerase II. *EMBO J,* 23, 4051-60.

Leek, J. T., Johnson, W. E., Parker, H. S., Jaffe, A. E. and Storey, J. D. 2012. The sva package for removing batch effects and other unwanted variation in high-throughput experiments. *Bioinformatics*, 28, 882-3.

Leung, A. K. and Sharp, P. A. 2010. MicroRNA functions in stress responses. *Mol Cell,* 40, 205-15.

Levy, S., Sutton, G., Ng, P. C., Feuk, L., Halpern, A. L., Walenz, B. P., Axelrod, N., Huang, J., Kirkness, E. F., Denisov, G., Lin, Y., Macdonald, J. R., Pang, A. W., Shago, M., Stockwell, T. B., Tsiamouri, A., Bafna, V., Bansal, V., Kravitz, S. A., Busam, D. A., Beeson, K. Y., Mcintosh, T. C., Remington, K. A., Abril, J. F., Gill, J., Borman, J., Rogers, Y. H., Frazier, M. E., Scherer, S. W., Strausberg, R. L. and Venter, J. C. 2007. The diploid genome sequence of an individual human. *PLoS Biol,* 5, e254.

Lewontin, R. C. 1964. The Interaction of Selection and Linkage. I. General Considerations; Heterotic Models. *Genetics,* 49, 49-67.

Lezak, K. R., Missig, G. and Carlezon, W. A., Jr. 2017. Behavioral methods to study anxiety in rodents. *Dialogues Clin Neurosci,* 19, 181-191.

Li, H., Ruan, Y., Zhang, K., Jian, F., Hu, C., Miao, L., Gong, L., Sun, L., Zhang, X., Chen, S., Chen, H., Liu, D. and Song, Z. 2016. Mic60/Mitofilin determines MICOS assembly essential for mitochondrial dynamics and mtDNA nucleoid organization. *Cell Death Differ,* 23, 380-92.

Li, J., Witten, D. M., Johnstone, I. M. and Tibshirani, R. 2012. Normalization, testing, and false discovery rate estimation for RNA-sequencing data. *Biostatistics,* 13, 523-38.

Lucas, M., Ilin, Y., Anunu, R., Kehat, O., Xu, L., Desmedt, A. and Richter-Levin, G. 2014. Long-term effects of controllability or the lack of it on coping abilities and stress resilience in the rat. *Stress,* 17, 423-30.

Lorenzini, C., Bucherelli, C. and Giachetti, A. 1984. Passive and active avoidance behavior in the light-dark box test. *Physiol Behav*, 32, 687-9.

Macarthur, D. G., Manolio, T. A., Dimmock, D. P., Rehm, H. L., Shendure, J., Abecasis, G. R., Adams, D. R., Altman, R. B., Antonarakis, S. E., Ashley, E. A., Barrett, J. C., Biesecker, L. G., Conrad, D. F., Cooper, G. M., Cox, N. J., Daly, M. J., Gerstein, M. B., Goldstein, D. B., Hirschhorn, J. N., Leal, S. M., Pennacchio, L. A., Stamatoyannopoulos, J. A., Sunyaev, S. R., Valle, D., Voight, B. F., Winckler, W. and Gunter, C. 2014. Guidelines for investigating causality of sequence variants in human disease. *Nature,* 508, 469-76.

Macau, E. 2018. *A mathematical modeling approach from nonlinear dynamics to complex systems,* New York, NY, Springer Science+Business Media.

Maclean, P. 1949. Psychosomatic disease and the visceral brain; recent developments bearing on the Papez theory of emotion. *Psychosom Med,* 11, 338-53.

Magistretti, P. J. and Allaman, I. 2015. A cellular perspective on brain energy metabolism and functional imaging. *Neuron,* 86, 883-901.

Maier, S. U., Makwana, A. B. and Hare, T. A. 2015. Acute Stress Impairs Self-Control in Goal-Directed Choice by Altering Multiple Functional Connections within the Brain's Decision Circuits. *Neuron,* 87, 621-31.

Malki, K., Mineur, Y. S., Tosto, M. G., Campbell, J., Karia, P., Jumabhoy, I., Sluyter, F., Crusio, W. E. and Schalkwyk, L. C. 2015. Pervasive and opposing effects of Unpredictable Chronic Mild Stress (UCMS) on hippocampal gene expression in BALB/cJ and C57BL/6J mouse strains. *BMC Genomics,* 16, 262.

Manolio, T. A., Collins, F. S., Cox, N. J., Goldstein, D. B., Hindorff, L. A., Hunter, D. J., Mccarthy, M. I., Ramos, E. M., Cardon, L. R., Chakravarti, A., Cho, J. H., Guttmacher, A. E., Kong, A., Kruglyak, L., Mardis, E., Rotimi, C. N., Slatkin, M., Valle, D., Whittemore, A. S., Boehnke, M., Clark, A. G., Eichler, E. E., Gibson, G., Haines, J. L., Mackay, T. F., Mccarroll, S. A. and Visscher, P. M. 2009. Finding the missing heritability of complex diseases. *Nature,* 461, 747-53.

Maron, E. and Nutt, D. 2017. Biological markers of generalized anxiety disorder. *Dialogues Clin Neurosci,* 19, 147-158.

Martin M. 2011. Cutadapt removes adapter sequences from high-throughput sequencing reads. *EMBnet Journal*, 17, 10-12

Martins-De-Souza, D. 2014. Proteomics, metabolomics, and protein interactomics in the characterization of the molecular features of major depressive disorder. *Dialogues Clin Neurosci,* 16, 63-73.

Mau Kai, C., Juul, A., Mcelreavey, K., Ottesen, A. M., Garn, I. D., Main, K. M., Loft, A., Jorgensen, N., Skakkebaek, N. E., Andersen, A. N. and Rajpert-De Meyts, E. 2008. Sons conceived by assisted reproduction techniques inherit deletions in the azoospermia factor (AZF) region of the Y chromosome and the DAZ gene copy number. *Hum Reprod,* 23, 1669-78.

McCarthy, D. J., and Smyth, G. K. 2009. Testing significance relative to a fold-change threshold is a TREAT. Bioinformatics 25:765–71.

Mcdougall, S., Vargas Riad, W., Silva-Gotay, A., Tavares, E. R., Harpalani, D., Li, G. L. and Richardson, H. N. 2018. Myelination of Axons Corresponds with Faster Transmission Speed in the Prefrontal Cortex of Developing Male Rats. *eNeuro,* 5.

Mckenzie, I. A., Ohayon, D., Li, H., De Faria, J. P., Emery, B., Tohyama, K. and Richardson, W. D. 2014. Motor skill learning requires active central myelination. *Science,* 346, 318-22.

Merikangas, K. R. and Kalaydjian, A. 2007. Magnitude and impact of comorbidity of mental disorders from epidemiologic surveys. *Curr Opin Psychiatry,* 20, 353-8.

Migliore, L., Fontana, I., Trippi, F., Colognato, R., Coppede, F., Tognoni, G., Nucciarone, B. and Siciliano, G. 2005. Oxidative DNA damage in peripheral leukocytes of mild cognitive impairment and AD patients. *Neurobiol Aging,* 26, 567-73.

Miller, B. H., Schultz, L. E., Gulati, A., Su, A. I. and Pletcher, M. T. 2010. Phenotypic characterization of a genetically diverse panel of mice for behavioral despair and anxiety. *PLoS One,* 5, e14458.

Millstein, R. A. and Holmes, A. 2007. Effects of repeated maternal separation on anxiety- and depression-related phenotypes in different mouse strains. *Neurosci Biobehav Rev,* 31, 3-17.

Miloyan, B., Joseph Bienvenu, O., Brilot, B. and Eaton, W. W. 2018. Adverse life events and the onset of anxiety disorders. *Psychiatry Res,* 259, 488-492.

Mineur, Y. S., Belzung, C. and Crusio, W. E. 2006. Effects of unpredictable chronic mild stress on anxiety and depression-like behavior in mice. *Behav Brain Res,* 175, 43-50.

Moffitt, T. E., Caspi, A., Harrington, H., Milne, B. J., Melchior, M., Goldberg, D. and Poulton, R. 2007. Generalized anxiety disorder and depression: childhood risk factors in a birth cohort followed to age 32. *Psychol Med,* 37, 441-52.

Monteiro, S., Roque, S., De Sa-Calcada, D., Sousa, N., Correia-Neves, M. and Cerqueira, J. J. 2015. An efficient chronic unpredictable stress protocol to induce stress-related responses in C57BL/6 mice. *Front Psychiatry*, 6, 6.

Montoya, A., Bruins, R., Katzman, M. A. and Blier, P. 2016. The noradrenergic paradox: implications in the management of depression and anxiety. *Neuropsychiatr Dis Treat,* 12, 541-57.

Mootha, V. K., Lindgren, C. M., Eriksson, K. F., Subramanian, A., Sihag, S., Lehar, J., Puigserver, P., Carlsson, E., Ridderstrale, M., Laurila, E., Houstis, N., Daly, M. J., Patterson, N., Mesirov, J. P., Golub, T. R., Tamayo, P., Spiegelman, B., Lander, E. S., Hirschhorn, J. N., Altshuler, D. and Groop, L. C. 2003. PGC-1alpha-responsive genes involved in oxidative phosphorylation are coordinately downregulated in human diabetes. *Nat Genet,* 34, 267-73.

Mouse Genome Sequencing, C., Waterston, R. H., Lindblad-Toh, K., et al. 2002. Initial sequencing and comparative analysis of the mouse genome. *Nature,* 420, 520-62.

Mozhui, K., Karlsson, R. M., Kash, T. L., Ihne, J., Norcross, M., Patel, S., Farrell, M. R., Hill, E. E., Graybeal, C., Martin, K. P., Camp, M., Fitzgerald, P. J., Ciobanu, D. C., Sprengel, R., Mishina, M., Wellman, C. L., Winder, D. G., Williams, R. W. and Holmes, A. 2010. Strain differences in stress responsivity are associated with divergent amygdala gene expression and glutamate-mediated neuronal excitability. *J Neurosci,* 30, 5357-67.

Muinos-Gimeno, M., Espinosa-Parrilla, Y., Guidi, M., Kagerbauer, B., Sipila, T., Maron, E., Pettai, K., Kananen, L., Navines, R., Martin-Santos, R., Gratacos, M., Metspalu, A., Hovatta, I. and Estivill, X. 2011. Human microRNAs miR-22, miR-138-2, miR-148a, and miR-488 are associated with panic disorder and regulate several anxiety candidate genes and related pathways. *Biol Psychiatry,* 69, 526-33.

Myers, B., Mark Dolgas, C., Kasckow, J., Cullinan, W. E. and Herman, J. P. 2014. Central stress-integrative circuits: forebrain glutamatergic and GABAergic projections to the dorsomedial hypothalamus, medial preoptic area, and bed nucleus of the stria terminalis. *Brain Struct Funct,* 219, 1287-303.

National Human Genome Research Institute 2003. Beyond Genes: Scientists Venture Deeper Into the Human Genome.

Nestler, E. J. and Hyman, S. E. 2010. Animal models of neuropsychiatric disorders. *Nat Neurosci,* 13, 1161-9.

Nikolova, Y. S., Koenen, K. C., Galea, S., Wang, C. M., Seney, M. L., Sibille, E., Williamson, D. E. and Hariri, A. R. 2014. Beyond genotype: serotonin transporter epigenetic modification predicts human brain function. *Nat Neurosci,* 17, 1153-5.

Nuss, P. 2015. Anxiety disorders and GABA neurotransmission: a disturbance of modulation. *Neuropsychiatr Dis Treat,* 11, 165-75.

O'Connell, J., and Weeks, D. 1998. PedCheck: a program for identification of genotype incompatibilities in linkage analysis. *Am. J. Hum. Genet*. 63, 259–266.

Oler, J. A., Fox, A. S., Shelton, S. E., Rogers, J., Dyer, T. D., Davidson, R. J., Shelledy, W., Oakes, T. R., Blangero, J. and Kalin, N. H. 2010. Amygdalar and hippocampal substrates of anxious temperament differ in their heritability. *Nature,* 466, 864-8.

Otowa, T., Hek, K., Lee, M., Byrne, E. M., Mirza, S. S., Nivard, M. G., Bigdeli, T., Aggen, S. H., Adkins, D., Wolen, A., Fanous, A., Keller, M. C., Castelao, E., Kutalik, Z., Van Der Auwera, S., Homuth, G., Nauck, M., Teumer, A., Milaneschi, Y., Hottenga, J. J., Direk, N., Hofman, A., Uitterlinden, A., Mulder, C. L., Henders, A. K., Medland, S. E., Gordon, S., Heath, A. C., Madden, P. A., Pergadia, M. L., Van Der Most, P. J., Nolte, I. M., Van Oort, F. V., Hartman, C. A., Oldehinkel, A. J., Preisig, M., Grabe, H. J., Middeldorp, C. M., Penninx, B. W., Boomsma, D., Martin, N. G., Montgomery, G., Maher, B. S., Van Den Oord, E. J., Wray, N. R., Tiemeier, H. and Hettema, J. M. 2016. Meta-analysis of genome-wide association studies of anxiety disorders. *Mol Psychiatry,* 21, 1391-9.

Ott, J. 1989. Computer-simulation methods in human linkage analysis. *Proc Natl Acad Sci U S A,* 86, 4175-8.

Ott, J. 1999. Methods of analysis and resources available for genetic trait mapping. *J Hered,* 90, 68-70.

Ott, J., Wang, J. and Leal, S. M. 2015. Genetic linkage analysis in the age of whole-genome sequencing. *Nat Rev Genet,* 16, 275-84.

Padilla-Coreano, N., Bolkan, S. S., Pierce, G. M., Blackman, D. R., Hardin, W. D., Garcia-Garcia, A. L., Spellman, T. J. and Gordon, J. A. 2016. Direct Ventral Hippocampal-Prefrontal Input Is Required for Anxiety-Related Neural Activity and Behavior. *Neuron,* 89, 857-66.

Parasuraman, S., Raveendran, R. and Kesavan, R. 2010. Blood sample collection in small laboratory animals. *J Pharmacol Pharmacother*, 1, 87-93

Paunio, T., Arajarvi, R., Terwilliger, J. D., Hiekkalinna, T., Haimi, P., Partonen, T., Lonnqvist, J., Peltonen, L. and Varilo, T. 2009. Linkage analysis of schizophrenia controlling for population substructure. *Am J Med Genet B Neuropsychiatr Genet,* 150B, 827-35.

Paunio, T., Ekelund, J., Varilo, T., Parker, A., Hovatta, I., Turunen, J. A., Rinard, K., Foti, A., Terwilliger, J. D., Juvonen, H., Suvisaari, J., Arajarvi, R., Suokas, J., Partonen, T., Lonnqvist, J., Meyer, J. and Peltonen, L. 2001. Genome-wide scan in a nationwide study sample of schizophrenia families in Finland reveals susceptibility loci on chromosomes 2q and 5q. *Hum Mol Genet,* 10, 3037-48.

Pellow, S., Chopin, P., File, S. E. and Briley, M. 1985. Validation of open:closed arm entries in an elevated plus-maze as a measure of anxiety in the rat. *J Neurosci Methods*, 14, 149-67.

Peltonen, L., Palotie, A. and Lange, K. 2000. Use of population isolates for mapping complex traits. *Nat Rev Genet,* 1, 182-90.

Perusini, J. N. and Fanselow, M. S. 2015. Neurobehavioral perspectives on the distinction between fear and anxiety. *Learn Mem,* 22, 417-25.

Petit-Demouliere, B., Chenu, F. and Bourin, M. 2005. Forced swimming test in mice: a review of antidepressant activity. *Psychopharmacology (Berl),* 177, 245-55.

Pfeffer, S., Zavolan, M., Grasser, F. A., Chien, M., Russo, J. J., Ju, J., John, B., Enright, A. J., Marks, D., Sander, C. and Tuschl, T. 2004. Identification of virus-encoded microRNAs. *Science,* 304, 734-6.

Philips, T. and Rothstein, J. D. 2017. Oligodendroglia: metabolic supporters of neurons. *J Clin Invest,* 127, 3271-3280.

Phipson, B., Lee, S., Majewski, I. J., Alexander, W. S. and Smyth, G. K. 2016. Robust Hyperparameter Estimation Protects against Hypervariable Genes and Improves Power to Detect Differential Expression. Ann Appl Stat, 10, 946-963.

Picard, M., Gentil, B. J., Mcmanus, M. J., White, K., St Louis, K., Gartside, S. E., Wallace, D. C. and Turnbull, D. M. 2013. Acute exercise remodels mitochondrial membrane interactions in mouse skeletal muscle. *J Appl Physiol (1985),* 115, 1562-71.

Picard, M. and Mcewen, B. S. 2018a. Psychological Stress and Mitochondria: A Conceptual Framework. *Psychosom Med,* 80, 126-140.

Picard, M. and Mcewen, B. S. 2018b. Psychological Stress and Mitochondria: A Systematic Review. *Psychosom Med,* 80, 141-153.

Picard, M., Mcewen, B. S., Epel, E. S. and Sandi, C. 2018. An energetic view of stress: Focus on mitochondria. *Front Neuroendocrinol*.

Picard, M., Mcmanus, M. J., Gray, J. D., Nasca, C., Moffat, C., Kopinski, P. K., Seifert, E. L., Mcewen, B. S. and Wallace, D. C. 2015. Mitochondrial functions modulate neuroendocrine, metabolic, inflammatory, and transcriptional responses to acute psychological stress. *Proc Natl Acad Sci U S A,* 112, E6614-23.

Pirkola, S. P., Isometsa, E., Suvisaari, J., Aro, H., Joukamaa, M., Poikolainen, K., Koskinen, S., Aromaa, A. and Lonnqvist, J. K. 2005. DSM-IV mood-, anxiety- and alcohol use disorders and their comorbidity in the Finnish general population--results from the Health 2000 Study. *Soc Psychiatry Psychiatr Epidemiol,* 40, 1-10.

Ritchie, M. E., Phipson, B., Wu, D., Hu, Y., Law, C. W., Shi, W. and Smyth, G. K. 2015. limma powers differential expression analyses for RNA-sequencing and microarray studies. *Nucleic Acids Res*, 43, e47.

Pooley, E. C., Fineberg, N. and Harrison, P. J. 2007. The met(158) allele of catechol-O-methyltransferase (COMT) is associated with obsessive-compulsive disorder in men: case-control study and meta-analysis. *Mol Psychiatry,* 12, 556-61.

Porsolt, R. D., Le Pichon, M. and Jalfre, M. 1977. Depression: a new animal model sensitive to antidepressant treatments. *Nature,* 266, 730-2.

Pothion, S., Bizot, J. C., Trovero, F. and Belzung, C. 2004. Strain differences in sucrose preference and in the consequences of unpredictable chronic mild stress. *Behav Brain Res,* 155, 135-46.

Provencal, N. and Binder, E. B. 2015. The effects of early life stress on the epigenome: From the womb to adulthood and even before. *Exp Neurol,* 268, 10-20.

Puglisi-Allegra, S. and Ventura, R. 2012. Prefrontal/accumbal catecholamine system processes high motivational salience. *Front Behav Neurosci,* 6, 31.

Purves, D. 2018. *Neuroscience,* New York, Oxford University Press, pp. 99-102.

Qiagen Inc. 2018. *Ingenuity Pathway Analysis* [Online]. Available: https://www.qiagenbioinformatics.com/products/ingenuity-pathway-analysis/ [Accessed 17 October 2018].

Quiroga, R. Q., Reddy, L., Kreiman, G., Koch, C. and Fried, I. 2005. Invariant visual representation by single neurons in the human brain. *Nature,* 435, 1102-7.

Radder, J. E., Shapiro, S. D. and Berndt, A. 2014. Personalized medicine for chronic, complex diseases: chronic obstructive pulmonary disease as an example. *Per Med,* 11, 669-679.

Ravera, S. and Panfoli, I. 2015. Role of myelin sheath energy metabolism in neurodegenerative diseases. *Neural Regen Res,* 10, 1570-1.

Razzoli, M., Domenici, E., Carboni, L., Rantamaki, T., Lindholm, J., Castren, E. and Arban, R. 2011. A role for BDNF/TrkB signaling in behavioral and physiological consequences of social defeat stress. *Genes Brain Behav,* 10, 424-33.

Reul, J. M. and Holsboer, F. 2002. On the role of corticotropin-releasing hormone receptors in anxiety and depression. *Dialogues Clin Neurosci,* 4, 31-46.

Ritchie, M. E., Phipson, B., Wu, D., Hu, Y., Law, C. W., Shi, W. and Smyth, G. K. 2015. limma powers differential expression analyses for RNA-sequencing and microarray studies. *Nucleic Acids Res*, 43, e47.

Roadmap Epigenomics Consortium, Kundaje, A., Meuleman, W., Ernst, J., Bilenky, M., Yen, A., Heravi-Moussavi, A., Kheradpour, P., Zhang, Z., Wang, J., Ziller, M. J., Amin, V., Whitaker, J. W., Schultz, M. D., Ward, L. D., Sarkar, A., Quon, G., Sandstrom, R. S., Eaton, M. L., Wu, Y. C., Pfenning, A. R., Wang, X., Claussnitzer, M., Liu, Y., Coarfa, C., Harris, R. A., Shoresh, N., Epstein, C. B., Gjoneska, E., Leung, D., Xie, W., Hawkins, R. D., Lister, R., Hong, C., Gascard, P., Mungall, A. J., Moore, R., Chuah, E., Tam, A., Canfield, T. K., Hansen, R. S., Kaul, R., Sabo, P. J., Bansal, M. S., Carles, A., Dixon, J. R., Farh, K. H., Feizi, S., Karlic, R., Kim, A. R., Kulkarni, A., Li, D., Lowdon, R., Elliott, G., Mercer, T. R., Neph, S. J., Onuchic, V., Polak, P., Rajagopal, N., Ray, P., Sallari, R. C., Siebenthall, K. T., Sinnott-Armstrong, N. A., Stevens, M., Thurman, R. E., Wu, J., Zhang, B., Zhou, X., Beaudet, A. E., Boyer, L. A., De Jager, P. L., Farnham, P. J., Fisher, S. J., Haussler, D., Jones, S. J., Li, W., Marra, M. A., Mcmanus, M. T., Sunyaev, S., Thomson, J. A., Tlsty, T. D., Tsai, L. H., Wang, W., Waterland, R. A., Zhang, M. Q., Chadwick, L. H., Bernstein, B. E., Costello, J. F., Ecker, J. R., Hirst, M., Meissner, A., Milosavljevic, A., Ren, B., Stamatoyannopoulos, J. A., Wang, T. and Kellis, M. 2015. Integrative analysis of 111 reference human epigenomes. *Nature,* 518, 317-30.

Robinson, O. J., Krimsky, M., Lieberman, L., Allen, P., Vytal, K. and Grillon, C. 2014. Towards a mechanistic understanding of pathological anxiety: the dorsal medial prefrontal-amygdala 'aversive amplification' circuit in unmedicated generalized and social anxiety disorders. *Lancet Psychiatry,* 1, 294-302.

Roelofs, K. 2017. Freeze for action: neurobiological mechanisms in animal and human freezing. *Philos Trans R Soc Lond B Biol Sci,* 372.

Rothe, C., Gutknecht, L., Freitag, C., Tauber, R., Mossner, R., Franke, P., Fritze, J., Wagner, G., Peikert, G., Wenda, B., Sand, P., Jacob, C., Rietschel, M., Nothen, M. M., Garritsen, H., Fimmers, R., Deckert, J. and Lesch, K. P. 2004. Association of a functional 1019C>G 5-HT1A receptor gene polymorphism with panic disorder with agoraphobia. *Int J Neuropsychopharmacol,* 7, 189-92.

Rothe, C., Koszycki, D., Bradwejn, J., King, N., Deluca, V., Tharmalingam, S., Macciardi, F., Deckert, J. and Kennedy, J. L. 2006. Association of the Val158Met catechol O-methyltransferase genetic polymorphism with panic disorder. *Neuropsychopharmacology,* 31, 2237-42.

Roxo, M. R., Franceschini, P. R., Zubaran, C., Kleber, F. D. and Sander, J. W. 2011. The limbic system conception and its historical evolution. *ScientificWorldJournal,* 11, 2428-41.

Russo, S. J. and Nestler, E. J. 2013. The brain reward circuitry in mood disorders. *Nat Rev Neurosci,* 14, 609-25.

Saez-Atienzar, S., Bonet-Ponce, L., Blesa, J. R., Romero, F. J., Murphy, M. P., Jordan, J. and Galindo, M. F. 2014. The LRRK2 inhibitor GSK2578215A induces protective autophagy in SH-SY5Y cells: involvement of Drp-1-mediated mitochondrial fission and mitochondrial-derived ROS signaling. *Cell Death Dis,* 5, e1368.

Sapolsky, R. M. 2015. Stress and the brain: individual variability and the inverted-U. *Nat Neurosci,* 18, 1344-6.

Sato, M. and Sato, K. 2013. Maternal inheritance of mitochondrial DNA by diverse mechanisms to eliminate paternal mitochondrial DNA. *Biochim Biophys Acta,* 1833, 1979-84.

Savarese, A. and Lasek, A. W. 2018. Regulation of anxiety-like behavior and Crhr1 expression in the basolateral amygdala by LMO3. *Psychoneuroendocrinology,* 92, 13-20.

Savignac, H. M., Dinan, T. G. and Cryan, J. F. 2011. Resistance to early-life stress in mice: effects of genetic background and stress duration. *Front Behav Neurosci,* 5, 13.

Scaini, G., Fries, G. R., Valvassori, S. S., Zeni, C. P., Zunta-Soares, G., Berk, M., Soares, J. C. and Quevedo, J. 2017. Perturbations in the apoptotic pathway and mitochondrial network dynamics in peripheral blood mononuclear cells from bipolar disorder patients. *Transl Psychiatry,* 7, e1111.

Schartner, C., Ziegler, C., Schiele, M. A., Kollert, L., Weber, H., Zwanzger, P., Arolt, V., Pauli, P., Deckert, J., Reif, A. and Domschke, K. 2017. CRHR1 promoter hypomethylation: An epigenetic readout of panic disorder? *Eur Neuropsychopharmacol,* 27, 360-371.

Schipper, H. M., Maes, O. C., Chertkow, H. M. and Wang, E. 2007. MicroRNA expression in Alzheimer blood mononuclear cells. *Gene Regul Syst Bio,* 1, 263-74.

Schmieder, R. and Edwards, R. 2011. Quality control and preprocessing of metagenomic datasets. *Bioinformatics*, 27, 863-4.

Schneider, C. A., Rasband, W. S. and Eliceiri, K. W. 2012. NIH Image to ImageJ: 25 years of image analysis. *Nat Methods,* 9, 671-5.

Schmieder, R. and Edwards, R. 2011. Quality control and preprocessing of metagenomic datasets. *Bioinformatics*, 27, 863-4.

Schwarze, K., Buchanan, J., Taylor, J. C. and Wordsworth, S. 2018. Are whole-exome and whole-genome sequencing approaches cost-effective? A systematic review of the literature. *Genet Med*.

Shackman, A. J. and Fox, A. S. 2016. Contributions of the Central Extended Amygdala to Fear and Anxiety. *J Neurosci,* 36, 8050-63.

Sham, P. C. 1998. Statistical methods in psychiatric genetics. *Stat Methods Med Res,* 7, 279-300.

Sham, P. C., Cherny, S. S., Purcell, S. and Hewitt, J. K. 2000. Power of linkage versus association analysis of quantitative traits, by use of variance-components models, for sibship data. *Am J Hum Genet,* 66, 1616-30.

Sharma, K., Schmitt, S., Bergner, C. G., Tyanova, S., Kannaiyan, N., Manrique-Hoyos, N., Kongi, K., Cantuti, L., Hanisch, U. K., Philips, M. A., Rossner, M. J., Mann, M. and Simons, M. 2015. Cell type- and brain region-resolved mouse brain proteome. *Nat Neurosci,* 18, 1819-31.

Shepherd, J. K., Grewal, S. S., Fletcher, A., Bill, D. J. and Dourish, C. T. 1994. Behavioural and pharmacological characterisation of the elevated "zero-maze" as an animal model of anxiety. Psychopharmacology (Berl), 116, 56-64.

Shimada-Sugimoto, M., Otowa, T. and Hettema, J. M. 2015. Genetics of anxiety disorders: Genetic epidemiological and molecular studies in humans. *Psychiatry Clin Neurosci,* 69, 388-401.

Shushan, B. 2010. A review of clinical diagnostic applications of liquid chromatography-tandem mass spectrometry. *Mass Spectrom Rev,* 29, 930-44.

Sial, O. K., Warren, B. L., Alcantara, L. F., Parise, E. M. and Bolanos-Guzman, C. A. 2016. Vicarious social defeat stress: Bridging the gap between physical and emotional stress. *J Neurosci Methods*, 258, 94-103.

Smoller, J. W., Acierno, J. S., Jr., Rosenbaum, J. F., Biederman, J., Pollack, M. H., Meminger, S., Pava, J. A., Chadwick, L. H., White, C., Bulzacchelli, M. and Slaugenhaupt, S. A. 2001. Targeted genome screen of panic disorder and anxiety disorder proneness using homology to murine QTL regions. *Am J Med Genet,* 105, 195-206.

Smoller, J. W., Block, S. R. and Young, M. M. 2009. Genetics of anxiety disorders: the complex road from DSM to DNA. *Depress Anxiety,* 26, 965-75.

Sobel, E., and Lange, K. 1996. Descent graphs in pedigree analysis: applications to haplotyping, location scores, and marker-sharing statistics. *Am. J. Hum. Genet*. 58, 1323–1337.

Sobel, E., Sengul, H. and Weeks, D. E. 2001. Multipoint estimation of identity-by-descent probabilities at arbitrary positions among marker loci on general pedigrees. *Hum. Hered*. 52, 121–131.

Sokolowska, E. and Hovatta, I. 2013. Anxiety genetics - findings from cross-species genome-wide approaches. *Biol Mood Anxiety Disord,* 3, 9.

Soliman, F., Glatt, C. E., Bath, K. G., Levita, L., Jones, R. M., Pattwell, S. S., Jing, D., Tottenham, N., Amso, D., Somerville, L. H., Voss, H. U., Glover, G., Ballon, D. J., Liston, C., Teslovich, T., Van Kempen, T., Lee, F. S. and Casey, B. J. 2010. A genetic variant BDNF polymorphism alters extinction learning in both mouse and human. *Science,* 327, 863-6.

Somers, J. M., Goldner, E. M., Waraich, P. and Hsu, L. 2006. Prevalence and incidence studies of anxiety disorders: a systematic review of the literature. *Can J Psychiatry,* 51, 100-13.

Somerville, L. H., Whalen, P. J. and Kelley, W. M. 2010. Human bed nucleus of the stria terminalis indexes hypervigilant threat monitoring. *Biol Psychiatry,* 68, 416-24.

Sonawane, A. R., Platig, J., Fagny, M., Chen, C. Y., Paulson, J. N., Lopes-Ramos, C. M., Demeo, D. L., Quackenbush, J., Glass, K. and Kuijjer, M. L. 2017. Understanding Tissue-Specific Gene Regulation. *Cell Rep,* 21, 1077-1088.

Sousa, N. 2016. The dynamics of the stress neuromatrix. *Mol Psychiatry,* 21, 302-12.

Steimer, T. 2011. Animal models of anxiety disorders in rats and mice: some conceptual issues. *Dialogues Clin Neurosci,* 13, 495-506.

Steinman, S. A. and Teachman, B. A. 2011. Cognitive processing and acrophobia: validating the Heights Interpretation Questionnaire. *J Anxiety Disord,* 25, 896-902.

Stephens, M. A. and Wand, G. 2012. Stress and the HPA axis: role of glucocorticoids in alcohol dependence. *Alcohol Res,* 34, 468-83.

Stoll, G., Pietilainen, O. P. H., Linder, B., Suvisaari, J., Brosi, C., Hennah, W., Leppa, V., Torniainen, M., Ripatti, S., Ala-Mello, S., Plottner, O., Rehnstrom, K., Tuulio-Henriksson, A., Varilo, T., Tallila, J., Kristiansson, K., Isohanni, M., Kaprio, J., Eriksson, J. G., Raitakari, O. T., Lehtimaki, T., Jarvelin, M. R., Salomaa, V., Hurles, M., Stefansson, H., Peltonen, L., Sullivan, P. F., Paunio, T., Lonnqvist, J., Daly, M. J., Fischer, U., Freimer, N. B. and Palotie, A. 2013. Deletion of TOP3beta, a component of FMRP-containing mRNPs, contributes to neurodevelopmental disorders. *Nat Neurosci,* 16, 1228-1237.

Strand, A. D., Aragaki, A. K., Baquet, Z. C., Hodges, A., Cunningham, P., Holmans, P., Jones, K. R., Jones, L., Kooperberg, C. and Olson, J. M. 2007. Conservation of regional gene expression in mouse and human brain. *PLoS Genet,* 3, e59.

Subramanian, A., Tamayo, P., Mootha, V. K., Mukherjee, S., Ebert, B. L., Gillette, M. A., Paulovich, A., Pomeroy, S. L., Golub, T. R., Lander, E. S. and Mesirov, J. P. 2005. Gene set enrichment analysis: a knowledge-based approach for interpreting genome-wide expression profiles. *Proc Natl Acad Sci U S A,* 102, 15545-50.

Sullivan, P. F., Daly, M. J. and O'donovan, M. 2012. Genetic architectures of psychiatric disorders: the emerging picture and its implications. *Nat Rev Genet,* 13, 537-51.

Sullivan, P. F., Fan, C. and Perou, C. M. 2006. Evaluating the comparability of gene expression in blood and brain. *Am J Med Genet B Neuropsychiatr Genet,* 141B, 261-8.

Sun, N., Lei, L., Wang, Y., Yang, C., Liu, Z., Li, X. and Zhang, K. 2016. Preliminary comparison of plasma notch-associated microRNA-34b and -34c levels in drug naive, first episode depressed patients and healthy controls. *J Affect Disord,* 194, 109-14.

Szymczak, S., Simpson, C. L., Cropp, C. D. and Bailey-Wilson, J. E. 2014. False-positive rates in two-point parametric linkage analysis. *BMC Proc,* 8, S110.

Tadic, A., Rujescu, D., Szegedi, A., Giegling, I., Singer, P., Moller, H. J. and Dahmen, N. 2003. Association of a MAOA gene variant with generalized anxiety disorder, but not with panic disorder or major depression. *Am J Med Genet B Neuropsychiatr Genet,* 117B, 1-6.

Tanoue, A., Ito, S., Honda, K., Oshikawa, S., Kitagawa, Y., Koshimizu, T. A., Mori, T. and Tsujimoto, G. 2004. The vasopressin V1b receptor critically regulates hypothalamic-pituitary-adrenal axis activity under both stress and resting conditions. *J Clin Invest,* 113, 302-9.

Taverner, T., Karpievitch, Y. V., Polpitiya, A. D., Brown, J. N., Dabney, A. R., Anderson, G. A. and Smith, R. D. 2012. DanteR: an extensible R-based tool for quantitative analysis of -omics data. *Bioinformatics*, 28, 2404-6.

Tenesa, A. and Haley, C. S. 2013. The heritability of human disease: estimation, uses and abuses. *Nat Rev Genet,* 14, 139-49.

Terwilliger, J. D. and Goring, H. H. 2000. Gene mapping in the 20th and 21st centuries: statistical methods, data analysis, and experimental design. *Hum Biol,* 72, 63-132.

The Genome Reference Consortium. 2017. Available: https://www.ncbi.nlm.nih.gov/grc [Accessed November 1, 2018].

Tiwari, A. K., Souza, R. P. and Muller, D. J. 2009. Pharmacogenetics of anxiolytic drugs. *J Neural Transm (Vienna),* 116, 667-77.

Toyoda, A. 2017. Social defeat models in animal science: What we have learned from rodent models. *Anim Sci J,* 88, 944-952.

Tsai, C. A., Chen, Y. J. and Chen, J. J. 2003. Testing for differentially expressed genes with microarray data. *Nucleic Acids Res,* 31, e52.

Tsigos, C. and Chrousos, G. P. 2002. Hypothalamic-pituitary-adrenal axis, neuroendocrine factors and stress. *J Psychosom Res,* 53, 865-71.

Tyanova, S., Temu, T., Sinitcyn, P., Carlson, A., Hein, M. Y., Geiger, T., Mann, M. and Cox, J. 2016. The Perseus computational platform for comprehensive analysis of (prote)omics data. *Nat Methods*, 13, 731-40.

Tye, K. M., Mirzabekov, J. J., Warden, M. R., Ferenczi, E. A., Tsai, H. C., Finkelstein, J., Kim, S. Y., Adhikari, A., Thompson, K. R., Andalman, A. S., Gunaydin, L. A., Witten, I. B. and Deisseroth, K. 2013. Dopamine neurons modulate neural encoding and expression of depression-related behaviour. *Nature,* 493, 537-541.

Uszczynska-Ratajczak, B., Lagarde, J., Frankish, A., Guigo, R. and Johnson, R. 2018. Towards a complete map of the human long non-coding RNA transcriptome. *Nat Rev Genet,* 19, 535-548.

Valencia-Sanchez, M. A., Liu, J., Hannon, G. J. and Parker, R. 2006. Control of translation and mRNA degradation by miRNAs and siRNAs. *Genes Dev,* 20, 515-24.

Varghese, F. P. and Brown, E. S. 2001. The Hypothalamic-Pituitary-Adrenal Axis in Major Depressive Disorder: A Brief Primer for Primary Care Physicians. *Prim Care Companion J Clin Psychiatry,* 3, 151-155.

Varilo, T., Savukoski, M., Norio, R., Santavuori, P., Peltonen, L. and Jarvela, I. 1996. The age of human mutation: genealogical and linkage disequilibrium analysis of the CLN5 mutation in the Finnish population. *Am J Hum Genet,* 58, 506-12.

Veenstra-Vanderweele, J., Christian, S. L. and Cook, E. H., Jr. 2004. Autism as a paradigmatic complex genetic disorder. *Annu Rev Genomics Hum Genet,* 5, 379-405.

Venter, J. C., Adams, M. D., Myers, E. W., et al. 2001. The sequence of the human genome. *Science,* 291, 1304-51.

Vogel, C. and Marcotte, E. M. 2012. Insights into the regulation of protein abundance from proteomic and transcriptomic analyses. *Nat Rev Genet,* 13, 227-32.

Volk, N., Pape, J. C., Engel, M., Zannas, A. S., Cattane, N., Cattaneo, A., Binder, E. B. and Chen, A. 2016. Amygdalar MicroRNA-15a Is Essential for Coping with Chronic Stress. *Cell Rep,* 17, 1882-1891.

Volk, N., Paul, E. D., Haramati, S., Eitan, C., Fields, B. K., Zwang, R., Gil, S., Lowry, C. A. and Chen, A. 2014. MicroRNA-19b associates with Ago2 in the amygdala following chronic stress and regulates the adrenergic receptor beta 1. *J Neurosci,* 34, 15070-82.

Wang, H. S., Pan, Z., Shi, W., Brown, B. S., Wymore, R. S., Cohen, I. S., Dixon, J. E. and Mckinnon, D. 1998. KCNQ2 and KCNQ3 potassium channel subunits: molecular correlates of the M-channel. *Science,* 282, 1890-3.

Wang, Z., Gerstein, M. and Snyder, M. 2009. RNA-Seq: a revolutionary tool for transcriptomics. *Nat Rev Genet,* 10, 57-63.

Warnefors, M., Liechti, A., Halbert, J., Valloton, D. and Kaessmann, H. 2014. Conserved microRNA editing in mammalian evolution, development and disease. *Genome Biol,* 15, R83.

Wedenoja, J., Loukola, A., Tuulio-Henriksson, A., Paunio, T., Ekelund, J., Silander, K., Varilo, T., Heikkila, K., Suvisaari, J., Partonen, T., Lonnqvist, J. and Peltonen, L. 2008. Replication of linkage on chromosome 7q22 and association of the regional Reelin gene with working memory in schizophrenia families. *Mol Psychiatry,* 13, 673-84.

Winn, M. E., Zapala, M. A., Hovatta, I., Risbrough, V. B., Lillie, E. and Schork, N. J. 2010. The effects of globin on microarray-based gene expression analysis of mouse blood. *Mamm Genome*, 21, 268-75.

Wittchen, H. U. and Jacobi, F. 2005. Size and burden of mental disorders in Europe--a critical review and appraisal of 27 studies. *Eur Neuropsychopharmacol,* 15, 357-76.

Wittchen, H. U., Jacobi, F., Rehm, J., Gustavsson, A., Svensson, M., Jonsson, B., Olesen, J., Allgulander, C., Alonso, J., Faravelli, C., Fratiglioni, L., Jennum, P., Lieb, R., Maercker, A., Van Os, J., Preisig, M., Salvador-Carulla, L., Simon, R. and Steinhausen, H. C. 2011. The size and burden of mental disorders and other disorders of the brain in Europe 2010. *Eur Neuropsychopharmacol,* 21, 655-79.

Wolf, E. J., Rasmusson, A. M., Mitchell, K. S., Logue, M. W., Baldwin, C. T. and Miller, M. W. 2014. A genome-wide association study of clinical symptoms of dissociation in a trauma-exposed sample. *Depress Anxiety,* 31, 352-60.

Wood, S. K. and Bhatnagar, S. 2015. Resilience to the effects of social stress: evidence from clinical and preclinical studies on the role of coping strategies. *Neurobiol Stress,* 1, 164-173.

Wright, J. E., Jr., Johnson, K., Hollister, A. and May, B. 1983. Meiotic models to explain classical linkage, pseudolinkage, and chromosome pairing in tetraploid derivative salmonid genomes. *Isozymes Curr Top Biol Med Res,* 10, 239-60.

Wu, Z. and Fang, Y. 2014. Comorbidity of depressive and anxiety disorders: challenges in diagnosis and assessment. *Shanghai Arch Psychiatry,* 26, 227-31.

Xiao, F., Zuo, Z., Cai, G., Kang, S., Gao, X. and Li, T. 2009. miRecords: an integrated resource for microRNA-target interactions. *Nucleic Acids Res,* 37, D105-10.

Xiao, L., Ohayon, D., Mckenzie, I. A., Sinclair-Wilson, A., Wright, J. L., Fudge, A. D., Emery, B., Li, H. and Richardson, W. D. 2016. Rapid production of new oligodendrocytes is required in the earliest stages of motor-skill learning. *Nat Neurosci,* 19, 1210-1217.

Ye, J., Gillespie, K. M. and Rodriguez, S. 2018. Unravelling the Roles of Susceptibility Loci for Autoimmune Diseases in the Post-GWAS Era. *Genes (Basel),* 9.

Yue, F., Cheng, Y., Breschi, A., et al. 2014. A comparative encyclopedia of DNA elements in the mouse genome. *Nature,* 515, 355-64.

Yugi, K., Kubota, H., Hatano, A. and Kuroda, S. 2016. Trans-Omics: How To Reconstruct Biochemical Networks Across Multiple 'Omic' Layers. *Trends Biotechnol,* 34, 276-290.

Zhang, Y., Sloan, S. A., Clarke, L. E., Caneda, C., Plaza, C. A., Blumenthal, P. D., Vogel, H., Steinberg, G. K., Edwards, M. S., Li, G., Duncan, J. A., 3rd, Cheshier, S. H., Shuer, L. M., Chang, E. F., Grant, G. A., Gephart, M. G. and Barres, B. A. 2016. Purification and Characterization of Progenitor and Mature Human Astrocytes Reveals Transcriptional and Functional Differences with Mouse. *Neuron,* 89, 37-53.

Zhou, W., Wang, Y., Fujino, M., Shi, L., Jin, L., Li, X. K. and Wang, J. 2018. A standardized fold change method for microarray differential expression analysis used to reveal genes involved in acute rejection in murine allograft models. *FEBS Open Bio,* 8, 481-490.

Ziegler, C., Richter, J., Mahr, M., Gajewska, A., Schiele, M. A., Gehrmann, A., Schmidt, B., Lesch, K. P., Lang, T., Helbig-Lang, S., Pauli, P., Kircher, T., Reif, A., Rief, W., Vossbeck-Elsebusch, A. N., Arolt, V., Wittchen, H. U., Hamm, A. O., Deckert, J. and Domschke, K. 2016. MAOA gene hypomethylation in panic disorder-reversibility of an epigenetic risk pattern by psychotherapy. *Transl Psychiatry,* 6, e773.